University of Alberta

Statistical Design Approach for Improving the Electrodeposition of Au-Sn Alloys

by

Nasim Morawej ©

A thesis submitted to the Faculty of Graduate Studies and Research
in partial fulfillment of the requirements for the degree of

Master of Science
in
Materials Engineering

Department of Chemical and Materials Engineering

Edmonton, Alberta
Spring 2007

Library and
Archives Canada

Published Heritage
Branch

395 Wellington Street
Ottawa ON K1A 0N4
Canada

Bibliothèque et
Archives Canada

Direction du
Patrimoine de l'édition

395, rue Wellington
Ottawa ON K1A 0N4
Canada

Your file Votre référence
ISBN: 978-0-494-29998-2
Our file Notre référence
ISBN: 978-0-494-29998-2

NOTICE:
The author has granted a non-exclusive license allowing Library and Archives Canada to reproduce, publish, archive, preserve, conserve, communicate to the public by telecommunication or on the Internet, loan, distribute and sell theses worldwide, for commercial or non-commercial purposes, in microform, paper, electronic and/or any other formats.

The author retains copyright ownership and moral rights in this thesis. Neither the thesis nor substantial extracts from it may be printed or otherwise reproduced without the author's permission.

AVIS:
L'auteur a accordé une licence non exclusive permettant à la Bibliothèque et Archives Canada de reproduire, publier, archiver, sauvegarder, conserver, transmettre au public par télécommunication ou par l'Internet, prêter, distribuer et vendre des thèses partout dans le monde, à des fins commerciales ou autres, sur support microforme, papier, électronique et/ou autres formats.

L'auteur conserve la propriété du droit d'auteur et des droits moraux qui protège cette thèse. Ni la thèse ni des extraits substantiels de celle-ci ne doivent être imprimés ou autrement reproduits sans son autorisation.

In compliance with the Canadian Privacy Act some supporting forms may have been removed from this thesis.

While these forms may be included in the document page count, their removal does not represent any loss of content from the thesis.

Conformément à la loi canadienne sur la protection de la vie privée, quelques formulaires secondaires ont été enlevés de cette thèse.

Bien que ces formulaires aient inclus dans la pagination, il n'y aura aucun contenu manquant.

Canada

Abstract

An electroplating process has been developed to deposit gold rich, Au-Sn eutectic alloys onto metallized semiconductor substrates. Commercial exploitation is, however, limited by plating bath lifetime and plating rates. The most effective factors influencing these limitations were determined to be the concentrations of ammonium citrate, potassium tetrachloroaurate, and tin (II) chloride in the electroplating bath. A statistical design of experiments for the gold tin electrodeposition process was performed, and an inverse relationship between shelf life and plating rate were readily apparent from the data analysis. From the obtained process model, two altered optimized solutions were obtained to maximize the shelf life and plating rates. The altered optimized solutions were characterized and plating rates of double and four times that of the standard process were attainable. The shelf life was not improved significantly since turbidity behaviour, which was chosen as a measure of shelf life, and shelf life did not correlate as expected.

Acknowledgements

I would like to express my sincere gratitude to Dr. Douglas Ivey for his supervision, encouragement, and guidance during my stay at University of Alberta. His availability and continuous support throughout my studies, which provided a great learning experience, were very much appreciated.

I would like to thank Dr. Siamak Akhlaghi for his supervision at Micralyne. I would also like to acknowledge Micralyne Inc. and Natural Sciences and Engineering Research Council of Canada (NSERC) for funding this work. My experience was further enriched by my interactions with many people at Micralyne.

I wish to thank Tina Barker for her time and flexibility through the SEM training. Dr. Amos Ben-Zvi also provided me with helpful information on topics pertaining to statistics, which was highly appreciated. I would also like to thank Heather Kaminsky for TEM analysis, and Clinton Windhorst and Laura Gill for helping with turbidity measurements. I also would like to thank the many people who made my experience at University of Alberta memorable.

Special thanks to my husband Reza, for his endless energy and support in the highs and lows of my graduate experience. Further thanks to my family for being a great encouragement throughout the course of my studies.

Table of Contents

Chapter 1: Introduction and Outline 1
  1.1. Introduction 1
  1.2. Outline of the Thesis 2
Chapter 2: Literature Review 4
  2.1. Solders 4
    2.1.1. Introduction to Solders 4
    2.1.2. Lead-Free Solders 6
    2.1.3. Gold-Tin Solders 7
  2.2. Electrodeposition 13
    2.2.1. Introduction 13
    2.2.2. Variables in Electrochemical Cells 16
    2.2.3. Factors Affecting Electrode Reaction Rate and Current 26
    2.2.4. Pulse Plating 28
  2.3. Electroplating of Gold-Tin Solders 30
    2.3.1. Introduction 30
    2.3.2. Sequential Electroplating of Gold-Tin Alloys 30
    2.3.3. Co-deposition of Gold-Tin Alloy from a Single Solution 36
    2.3.4. Electroless Plating of Gold-Tin 40
  2.4. Ivey Group's Method of Electroplating Gold-Tin 40
    2.4.1. Bath Solution 43
    2.4.2. Problems with Electroplating 43
  2.5. Bath Additives and Stability 44
  2.6. Improvements in Plating Rate 45
  2.7. Summary 46
Chapter 3: Statistical Design of Experiments 48
    3.1.1. Introduction to Experimental Design 49
    3.1.2. Design Selection 50
    3.1.3. Data Analysis 53
  3.2. Summary 59

Chapter 4: Long Term Stability Study 60

4.1. Overview of the Study 60

4.1.1. Scanning Electron Microscopy 60

4.1.2. Turbidity 63

4.1.3. Atomic Absorption Spectroscopy 66

4.2. Experimental Procedure 68

4.2.1. Solution Preparation 68

4.2.2. Long Term Plating 69

4.2.3. Scanning Electron Microscope Analysis 73

4.2.4. Turbidity 75

4.2.5. Atomic Absorption Spectroscopy 75

4.3. Results and Discussions 77

4.4. Conclusions 82

Chapter 5: Screening Tests 84

5.1. Overview 84

5.1.1. Transmission Electron Microscopy 85

5.2. Experimental Procedure 86

5.2.1. TEM Sample Preparation 86

5.2.2. Concentration of Solution Constituents 86

5.2.3. Modified Mixing Procedure and Additives 88

5.3. Results and Discussions 91

5.3.1. TEM Results 91

5.3.2. Concentration of Solution Constituents 94

5.3.3. Modified Mixing Procedure and Additives 110

5.4. Conclusions 115

Chapter 6: Statistical Design of Experiments for Gold Tin Electrodeposition Process 117

6.1. Overview 117

6.2. Experimental Design Procedure 117

6.2.1. Black Box Model 117

6.2.2. Design Selection 119

6.2.3. Box-Behnken Design 119
6.3. Experimental Procedure 122
6.3.1. Profilometry 125
6.4. Results and Discussions 125
6.4.1. Composition and Plating Rate 125
6.4.2. Shelf Life 129
6.5. Data Analysis 130
6.5.1. Regression Tables 130
6.5.2. Surface, Contour, and Interaction Plots 137
6.5.3. Optimization 142
6.6. Conclusions 150
Chapter 7: Characterization of Optimized Solutions 151
7.1. Overview 151
7.2. Experimental Procedure 151
7.3. Results and Discussions 152
7.3.1. OP1 155
7.3.2. Opt3 158
7.4. Conclusions 161
Chapter 8: Conclusions and Recommendations 164
8.1. Conclusions 164
8.2. Recommendations and Comments 167
References 170
Appendix A: Additives and Techniques Used to Improve Bath Stability and Plating Rate 179
Appendix B: Turbidity Curves 194
Appendix C: Design Sheets 203

List of Tables

Table 2-1: Electrical responses to selected electrical inputs [summarized from Bard and Faulkner 2001]. 19
Table 2-2: Possible constituents in plating baths [Zhang 2001]. 22
Table 2-3: Acidic electrolytes for electrodeposition of pure gold (cyanide based) [Reid and Goldie 1974] 31
Table 2-4: Sodium Gold sulfite electrolyte [Reid and Goldie 1974]. 32
Table 2-5: Typical bath composition and operating parameters of fluoborate chemistry [Schlesinger and Paunovic 2000] 33
Table 2-6: Typical bath composition and operating parameters for a sulfate/sulfuric acid based electroplating chemistry [Schlesinger and Paunovic 2000]. 34
Table 2-7: Typical bath composition and operating parameters of phenolsulfonic acid based electroplating chemistry [Schlesinger and Paunovic 2000]. 34
Table 2-8: Typical bath composition and operating parameters of a halogen chemistry [Schlesinger and Paunovic 2000] 35
Table 2-9: Typical bath composition and operating parameters of a satin bright MSA based electroplating chemistry [Schlesinger and Paunovic 2000]. 35
Table 2-10: Acidic electrolytes for electrodeposition of alloy gold (cyanide based) [Reid and Goldie 1974] 36
Table 2-11: Composition and plating conditions of an acidic cyanide gold-tin system [Zhang 2001]. 38
Table 2-12: The bath composition and plating conditions of electroless gold-tin plating [Okinaka 1990]. 40
Table 2-13: Gold-tin plating bath constituents used by Ivey's group [Doesburg 2000]... 43
Table 3-1: Design selection guidelines [National Institute of Standards and Technology (NIST) and International Sematech 2005]. 51
Table 3-2: Factor settings for Box-Behnken design [National Institute of Standards and Technology (NIST) and International Sematech 2005]. 53
Table 4-1: Interferences associated with turbidity measurement [Sadar 2002]. 64

Table 4-2: Common standard turbidity units [McMillan and Considine 1999; Sadar 2002]. 65
Table 4-3: Turbidity applications [McMillan and Considine 1999]. 66
Table 4-4: Characteristic data for flame atomic absorptions [Perkin-Elmer]. 68
Table 4-5: Solutions used for long term stability study. 69
Table 4-6: Long term plating conditions and comments. 72
Table 4-7: Specifications of VWR 66120-200 turbidity meter. 75
Table 5-1: TEM Samples. 86
Table 5-2: Solutions with modified concentrations. 87
Table 6-1: Factor levels for Box-Behnken design. 120
Table 6-2: Box-Behnken design for gold-tin electroplating process. 122
Table 6-3: Compositions and plating rate results for the Box-Behnken design. 126
Table 6-4: SE plan view images of deposits for the Box-Behnken design. 127
Table 6-5: Shelf life results for the Box-Behnken design. 129
Table 6-6: Y-hat model regression table for shelf life response. 133
Table 6-7: Y-hat model regression tables for composition responses. 134
Table 6-8: Y-hat model regression tables for plating rate responses. 135
Table 6-9: An example of the prediction region. 137
Table 6-10: Interactions and contour plot types for ammonium citrate and $KAuCl_4$ at constant $SnCl_2.2H_2O$ concentrations. 140
Table 6-11: Interactions and contour plot types for ammonium citrate and $SnCl_2.2H_2O$ at constant $KAuCl_4$ concentrations. 140
Table 6-12: Interactions and contour plot types for $KAuCl_4$ and $SnCl_2.2H_2O$ at constant ammonium citrate concentrations. 140
Table 6-13: Examples of optimization constraints and results. 143
Table 6-14: Chosen optimal settings for characterization. 145
Table 7-1: Concentrations of the optimized solutions. 151
Table 7-2: SE plan view images of deposits for the optimized solutions. 152
Table 7-3: Measured and predicted response values for the optimized solutions. 153
Table A-1: Additives and techniques used to improve bath stability. 180
Table A-2: Additives and techniques used to improve plating rate. 190

Table C-1: Design sheet for composition at 0.8 mA/cm^2 204
Table C-2: Design sheet for composition at 2.4 mA/cm^2 204
Table C-3: Design sheet for composition at 3.5 mA/cm^2 205
Table C-4: Design sheet for plating rate at 0.8 mA/cm^2 205
Table C-5: Design sheet for plating rate at 2.4 mA/cm^2 206
Table C-6: Design sheet for plating rate at 3.5 mA/cm^2 206
Table C-7: Design sheet for shelf life 207

List of Figures

Figure 2-1: Time line demonstrating the history of use of solders [Schlesinger and Paunovic 2000]. 5

Figure 2-2: The gold-tin binary phase diagram [American Society for Metals 2005]. 8

Figure 2-3: Fractured solder bump after temperature cycling [Riley 2004]. 10

Figure 2-4: Flip chip packaging [Amkor 2006]. 12

Figure 2-5: (a) Flip chip, (b) Wire bonding [Amkor 2006]. 13

Figure 2-6: Variables in electrochemical cells, after [Bard and Faulkner 2001]. 16

Figure 2-7: Concentration profiles for several times after the start of a potential step experiment, $D_j=10^{-5}$ cm^2/s [Bard and Faulkner 2001]. 24

Figure 2-8: Schematic drawings of the diffusion layer thickness under three agitation modes [Menini 2005]. 25

Figure 2-9: Pathway of a general electrode reaction [after Bard and Faulkner 2001]...... 27

Figure 2-10: Some square-wave modulated current systems: (a) Pulse, (b) duplex pulse, (c) superimposed pulse, (d) pulse-on-pulse [after Knodler 1986]. 29

Figure 2-11: Deposit composition vs. current density [Djurfors and Ivey 2001]. 41

Figure 2-12: Scanning electron microscope (SEM) image of multilayer deposition of the two stoichiometric phases, AuSn and Au_5Sn [Djurfors and Ivey 2002] 41

Figure 3-1: Black-Box Model. 48

Figure 3-2: Box-Behnken design illustrations for 3 factors [Box, Hunter et al. 2005; National Institute of Standards and Technology (NIST) and International Sematech 2005]. 52

Figure 3-3: Contour plots: (a) peak, (b) hillside, (c) rising ridge, (d) saddle [National Institute of Standards and Technology (NIST) and International Sematech 2005]. 56

Figure 3-4: Interaction plots: (a) no interaction, (b) two-factor interaction 57

Figure 3-5: Three-factor interaction: (a) factor 1 & factor 2 interaction, ... 58

Figure 4-1: Schematic drawing of the electron and X-ray optics of a combined SEM-EPMA [Goldstein, Newbury et al. 2003] 61

Figure 4-2: Basic turbidity meter [McMillan and Considine 1999]. 64

Figure 4-3: Methods of light scatter measurement [McMillan and Considine 1999]....... 65

Figure 4-4: Schematic of an atomic absorption instrument [Ramachandran 1995]. 67
Figure 4-5: Experimental setup. 71
Figure 4-6: Schematic diagram of the electroplating circuit 72
Figure 4-7: SEM sample preparation: (a) plan view, (b) cross section 73
Figure 4-8: VWR 66120-200 turbidity meter. 75
Figure 4-9: Perkin-Elmer 4000 atomic absorption spectrometer. 76
Figure 4-10: SE images of deposit from a fresh standard solution: (a) plan view (b) cross section. 77
Figure 4-11: SE plan view and cross section images of deposits from an aged solution: (a) LTP2-1 day (b) LTP3-2 days old (c) LTP6b-5 days old (d) LTP6c-5 days old. 78
Figure 4-12: Tin content of the deposited film as a function of aging time. 79
Figure 4-13: Sample turbidity curve for the standard solution. 80
Figure 4-14: Atomic absorption spectroscopy results for tin 81
Figure 4-15: Atomic absorption spectroscopy results for gold. 82
Figure 5-1: BF imaging within the TEM [Goodhew, Humphreys et al. 2001]. 85
Figure 5-2: BF TEM images of sample TEM1 (ammonium citrate + $KAuCl_4$). 91
Figure 5-3: BF TEM image of sample TEM2 (ammonium citrate + $KAuCl_4$ + sodium sulfite (as mixed)). 92
Figure 5-4: BF TEM images of sample TEM3 (ammonium citrate + $KAuCl_4$ + sodium sulfite (after 30 minutes)) 92
Figure 5-5: BF TEM images of sample TEM4 (ammonium citrate + $KAuCl_4$ + sodium sulfite + ascorbic acid). 93
Figure 5-6: BF TEM images of TEM5 (ammonium citrate + $KAuCl_4$ + sodium sulfite + ascorbic acid + $SnCl_2.2H_2O$) 93
Figure 5-7: Tin content of the deposited films at various current densities using the 50Ci solution 95
Figure 5-8: SE image of deposit from 50Ci solution at $j = 2.4$ mA/cm^2. 96
Figure 5-9: Turbidity curve for 50Ci solution. 96
Figure 5-10: Tin content of the deposited films at 1.5 mA/cm^2 from 50Ci solution as a function of aging time. 97

Figure 5-11: Change in tin content of films deposited at 1.5 mA/cm^2 from the 50Ci solution as a function of ageing time. The addition of tin (II) chloride corresponds to abrupt increases in deposit tin composition. 98

Figure 5-12: Tin content of the deposited films at various current densities using the 50Ci10Au solution. 99

Figure 5-13: Tin content of the deposited films at various current densities using the 50Ci15Au solution. 99

Figure 5-14: Tin content of the deposited films from 50Ci15Au solution as a function of aging time. 100

Figure 5-15: SE plan view and cross section images of deposits: (a) from 50Ci10Au solution at 0.8 mA/cm^2 (b) from 50Ci10Au solution at 2.4 mA/cm^2 (c) from 50Ci15Au solution at 0.8 mA/cm^2. 101

Figure 5-16: Tin content of deposited films at various current densities using the 30Ci10Au10Sn solution. 102

Figure 5-17: Tin content of films deposited at 2.4 mA/cm^2 from the 30Ci10Au10Sn solution as a function of ageing time. 102

Figure 5-18: SE plan view and cross section images of deposit from 30Ci10Au10Sn solution at 2.4 mA/cm^2. 103

Figure 5-19: Tin content of the deposited films at various current densities using the 25Au solution. 104

Figure 5-20: Tin content of deposited films from the 25Au solution as a function of ageing time. 104

Figure 5-21: SE cross section images of deposits from the 25Au solution: (a) j = 2.4 mA/cm^2 (plating rate = 4.9 μm/hr) (b) j = 5.0 mA/cm^2 (plating rate = 7.0 μm/hr). 105

Figure 5-22: Tin content of films deposited at various current densities using the 7AA solution. 106

Figure 5-23: Turbidity curve for 5AA solution. 107

Figure 5-24: Tin content of films deposited at 1.6 mA/cm^2 from the 7AA solution as a function of ageing time. 107

Figure 5-25: Tin content of the films deposited at 1.6 mA/cm^2 from the 5AA solution as a function of ageing time. 108

Figure 5-26: SE plan view images of deposits from 7AA solution: (a) Fresh at 2.0 mA/cm^2 (b) Fresh at 1.6 mA/cm^2 (c) Fresh at 0.8 mA/cm^2 (d) 1 day old at 1.6 mA/cm^2. 109
Figure 5-27: Turbidity curve for 100SS solution. 110
Figure 5-28: Turbidity curve for A3 + L-ascorbic acid Solution + B3 solution. 111
Figure 5-29: Tin content of the deposited films from the A3 + L-ascorbic acid solution + B3 solution as a function of solution age. 111
Figure 5-30: SE plan view images of deposits from the A3 + L-ascorbic acid solution + B3 solution: (a) 2 days old at 2.3 mA/cm^2 (b) 2 days old at 1.6 mA/cm^2 (c) 3 days old at 1.6 mA/cm^2. 112
Figure 5-31: Tin content of the films deposited at various current densities from a solution containing cupferron. 113
Figure 5-32: Tin content of the films deposited at 2.4 mA/cm^2 from a solution containing cupferron after ageing for various times. 113
Figure 5-33: Tin content of the deposited films at various current densities from a solution containing tin sponge. 114
Figure 5-34: SE plan view and cross section images of deposits from a solution containing tin sponge: (a) at 0.8 mA/cm^2 (1.3 μm/hr) (b) at 2.4 mA/cm^2 (2.9 μm/hr)... 115
Figure 6-1: Black box model of the gold tin electroplating process. 119
Figure 6-2: Y-hat model surface plot of composition at 0.8 mA/cm^2 for ammonium citrate vs. $SnCl_2.2H_2O$ while keeping $KAuCl_4$ constant at 15 g/L (trough type). 138
Figure 6-3: Y-hat model contour plot of shelf life for ammonium citrate vs. $SnCl_2.2H_2O$ while keeping KAuCl4 constant at 5 g/L. 138
Figure 6-4: Y-hat model interaction plot of rate @ 2.4 mA/cm^2 as a function of ammonium citrate and $KAuCl_4$ concentration, keeping $SnCl_2.2H_2O$ constant at 5 g/L (interaction effect). 141
Figure 6-5: Y-hat model interaction plot of shelf life as a function of ammonium citrate & $KAuCl_4$ concentration, keeping $SnCl_2.2H_2O$ constant at 5 g/L (no interaction). 141
Figure 6-6: Y-hat model contour and surface plots of shelf life for ammonium citrate vs. $KAuCl_4$ while keeping $SnCl_2.2H_2O$ constant at 5 g/L. 147

Figure 6-7: Y-hat model contour and surface plots of rate at 3.5mA/cm^2 for ammonium citrate vs. $KAuCl_4$ while keeping $SnCl_2.2H_2O$ constant at 5 g/L. 148

Figure 6-8: Y-hat model contour and surface plots of composition at 3.5mA/cm^2 for ammonium citrate vs. $KAuCl_4$ while keeping $SnCl_2.2H_2O$ constant at 5 g/L. 148

Figure 6-9: Overlapped contour plots from Figure 6-6 to Figure 6-8. 149

Figure 7-1: Illustration of optimized solutions on Box-Behnken design process space. 154

Figure 7-2: Tin content of the deposited films from the Opt1 solution plated at various current densities. 156

Figure 7-3: Plating rate of the deposited films from the Opt1 solution plated at various current densities. 156

Figure 7-4: Tin content of films deposited at 2.4 mA/cm^2 from the Opt1 solution as a function of ageing time. 158

Figure 7-5: Tin content of the deposited films from the Opt3 solution at various current densities.. 159

Figure 7-6: Plating rate of the deposited films from the Opt3 solution at various current densities.. 160

Figure 7-7: Tin content of films deposited at 2.4 mA/cm^2 from the Opt3 solution as a function of ageing time. 161

Figure B-1: Turbidity curve for experimental run 1. 194

Figure B-2: Turbidity curve for experimental run2. 195

Figure B-3: Turbidity curve for experimental run 3. 195

Figure B-4: Turbidity curve for experimental run 4. 196

Figure B-5: Turbidity curve for experimental run 5. 196

Figure B-6: Turbidity curve for experimental run 6. 197

Figure B-7: Turbidity curve for experimental run 7. 197

Figure B-8: Turbidity curve for experimental run 8. 198

Figure B-9: Turbidity curve for experimental run 9. 198

Figure B-10: Turbidity curve for experimental run 10. 199

Figure B-11: Turbidity curve for experimental run 11. 199

Figure B-12: Turbidity curve for experimental run 12. 200

Figure B-13: Turbidity curve for experimental run 13. 200

Figure B-14: Turbidity curve for experimental run 14. 201
Figure B-15: Turbidity curve for experimental run 15. 201
Figure B-16: Turbidity curve for experimental run 16. 202

List of Symbols

A	surface area
C_d	double layer capacitance
C_j	concentration of species j
C_O	bulk concentration of oxidizing species
C_R	bulk concentration of reduced species
D_j	diffusion constant
E	potential
F	Faraday constant
i	current
J	current density
J_j	flux of species j in the solution
M	metal
N	number of moles
ŋ	number of electrons
O	oxidizing species
P	pressure
Q	quantity of electricity
R	reduced species, or molar gas constant (as stated in the text)
R_s	electrolyte resistance
T	temperature
t	time
v	velocity of solution flow
Z_{ct}	charge transfer impedance
z_j	charge of species j
Z_{mt}	mass transfer impedance
Z_{rxn}	preceding reaction impedance
δ	diffusion layer
η	overpotential
τ	turbidity

Φ	electrostatic potential
∇	gradient vector operator

List of Abbreviations

AA	atomic absorption
BSE	backscattered electrons
CRT	cathode ray tube
CSP	chip-scale package
DC	direct current
DCA	direct chip attach
DOE	statistical design of experiments
EDS	energy dispersive X-ray spectroscopy
FC	flip chip
FET	field emitting transistor
IPE	ideal polarized electrode
LED	light-emitting diodes
MEMS	micro-electro-mechanical systems
NHE	normal hydrogen electrode
NTU	Nephelometric turbidity unit
PC	pulse plating
RSM	response surface method
SCE	saturated calomel electrode
SE	secondary electrons
SEM	scanning electron microscopy
TAB	tape automated bonding
TEM	transmission electron microscopy
UA	ultrasonic agitation
WD	working distance

Chapter 1: Introduction and Outline

1.1. Introduction

Gold-tin eutectic solders have been widely used in the optoelectronics and microelectronics industry for packaging applications. An electroplating process has been developed to deposit Au-Sn alloys from a single, non-cyanide, slightly acidic bath onto metallized semiconductor substrates [Sun 1998; Sun and Ivey 1998; Sun and Ivey 1999; Sun and Ivey 2001]. This plating solution contains $KAuCl_4$ and $SnCl_2.2H_2O$ to provide gold and tin ions respectively. Ammonium citrate and sodium sulfite were initially added as the buffer and the complexing agent respectively. Also, this bath contains L-ascorbic acid to prevent Sn hydrolysis.

Two different current densities are used to create a combination of multi-layered phases Au_5Sn and AuSn. All compositions in the range of 14 to 50 atomic percent tin, including the eutectic, are producible by controlling the current densities and the thicknesses of the layers. This solder is well-known for its high thermal fatigue resistance in addition to excellent thermal properties. However, this plating bath needs improvements in terms of lifetime and plating rate. The lifetime of the bath solution is limited to two-three days due to gold precipitation, and plating rates are relatively low.

The objective of the work involved in this thesis is to select the key factors affecting the stability and the plating rate, and to find improved and optimal process settings.

One efficient procedure for planning experiments is the statistical design of experiments (DOE) which is used in this work. These experiments are designed so that the data obtained can be analyzed to yield valid and objective conclusions. For the objectives of this thesis, the experiment is designed to allow for estimation of interaction and quadratic effects, while presenting an idea of the (local) shape of the response surface being investigated. These types of experiments are called response surface method (RSM) designs. Moreover, multiple response optimizations are performed using commercial software to analyze the data and to determine the optimal combination of solution components to improve both the stability and the plating rate.

1.2. Outline of the Thesis

Chapter 2 starts by giving a brief introduction to solders, their fabrication methods and applications. This is followed by a background to electrodeposition process with a focus on the variables in electrochemical cells and factors affecting electrode reaction rate and current. The basics of pulse plating are discussed, since it is the plating method used in this work. Further, this chapter focuses on different techniques used for electroplating gold-tin solders including a literature review of previously developed plating baths for these techniques. Chapter 2 also discusses the gold-tin electroplating method developed by Ivey's group. Finally, this chapter reviews the literature on bath additives used to improve stability and methods used to improve electroplating rates.

Chapter 3 covers the background on the statistical design of experiments (DOE) which is the approach used to meet the objective of this thesis. After a brief introduction to experimental design, the design selection method is discussed. This chapter also gives background on data analysis techniques including response surface modeling, multiple response regression tables, process optimization, and different plotting techniques.

The long term stability of the standard electroplating bath developed by Ivey's group is studied in Chapter 4. This study was performed to obtain a better understanding of the solution aging behaviour before proceeding with improvements. This chapter covers the experimental procedure used for this study followed by the results, discussion, and conclusions.

Chapter 5 addresses the screening tests performed to determine the key factors affecting the stability and the plating rate. The term screening used here refers to a filtering process, in which a list of factors affecting the performance of a process are initially considered and a few of the most vital ones are chosen and studied thoroughly. This chapter covers the experimental procedure used for the screening tests followed by results, discussion, and conclusions.

Chapter 6 covers the statistical design of the experiment method. This chapter defines the experiment design and covers the experimental procedures to obtain data. Then, all the obtained data are presented and discussed followed by the data analysis. The data analysis section covers the regression table and the response surface models including the surface, contour and interaction plots. In addition, obtained improved and optimal process settings are presented. Finally, the data analysis and optimization results are summarized and concluded at the end of this chapter.

The solutions with the optimized process settings are studied further in Chapter 7. This study tests the new solutions for reproducibility and repeatability. The experimental procedures of this study are presented followed by results, discussion, and conclusions.

Finally, Chapter 8 presents the conclusions derived from this thesis work and provides recommendations for possible future work.

Chapter 2: Literature Review

2.1. Solders

2.1.1. Introduction to Solders

Soldering, today, is a critical component of microelectronics. At its most basic, "soldering" refers to the joining of two base materials using a third "filler" metal. The "filler" metal is called solder, which has a melting point well below those of the substrates. Solder alloys are categorized as soft or hard solders mainly depending on their melting temperature and mechanical properties. However, the defining melting temperature varies within literature. In some sources, solders with melting temperatures below or above approximately 350 or 450 °C are categorized as soft or hard solders respectively [Copper Development Association UK 2006]. But, typical soft solders are known to melt between 150 and 250 °C [Breviary Technical Ceramics 2006]. Nevertheless, soft solders often contain high amounts of soft metals such as tin and lead and sometimes indium, cadmium, and bismuth [Schlesinger and Paunovic 2000]. Hard solders contain high amounts of metals having a high melting temperature, such as silver, gold, zinc, aluminium, and silicon [Schlesinger and Paunovic 2000]. The hard solders usually contain a small amount of a soft metal to lower the melting temperature [Hnilica 2006].

The time line in Figure 2-1 illustrates the historical use of solders, which shows its application as early as 4000 BC. These applications included the manufacturing, construction, or repairing of metal tools, channels, jewellery, and crafts. Further, the usage was expanded by the industrial revolution to fabrication of larger structures (e.g., automobile radiators) and electronics (mainly for conductivity purposes). In the modern world, the solders have been adopted for micro-chip packaging and higher level assembly applications [Schlesinger and Paunovic 2000]. For example, optical devices have to be attached with precise alignment in optoelectronic packaging, (e.g., waveguides attached to photodetectors), and also higher melting temperature solders are needed to provide increased thermal stability and long term reliability for this application [Doesburg 2000].

The tin-lead solder is the most commonly used soft solder in most of the named applications. However, it suffers from a wide range of limitations including its strength, creep, and fatigue resistance when it comes to reduction of package size requirements [Schlesinger and Paunovic 2000].

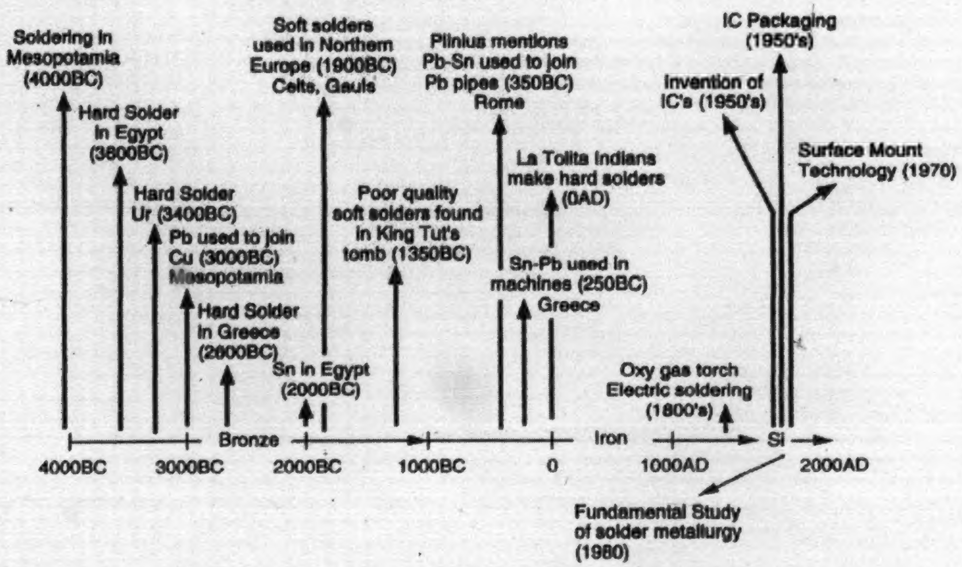
Soldering in Mesopotamia (4000BC)
Hard Solder in Egypt (3600BC)
Hard Solder Ur (3400BC)
Pb used to join Cu (3000BC) Mesopotamia
Hard Solder in Greece (2600BC)
Sn in Egypt (2000BC)
Soft solders used in Northern Europe (1900BC) Celts, Gauls
Poor quality soft solders found in King Tut's tomb (1350BC)
Plinius mentions Pb-Sn used to join Pb pipes (350BC) Rome
La Tolita Indians make hard solders (0AD)
Sn-Pb used in machines (250BC) Greece
Oxy gas torch Electric soldering (1800's)
IC Packaging (1950's)
Invention of IC's (1950's)
Surface Mount Technology (1970)
Fundamental Study of solder metallurgy (1980)
Bronze
Iron
Si
4000BC
3000BC
2000BC
1000BC
0
1000AD
2000AD

Figure 2-1: Time line demonstrating the history of use of solders [Schlesinger and Paunovic 2000].

2.1.2. Lead-Free Solders

As mentioned before, tin-lead solders are used prominently due to their low cost and material properties. However, environmental and health concerns are reasons for the introduction of alternative solder materials in addition to tin-lead material properties limitations. The main health concern is the toxicity of lead. Ingestion, inhalation, and absorption of lead can harm systems in the human body such as the brain, kidneys and reproductive systems [Environment Protection Authority 2003].

The role of lead in solders includes lowering the melting temperature of tin-rich solders, reducing the viscosity, and improving the wetting and mechanical strength of the solders [Schlesinger and Paunovic 2000]. Therefore, the material replacing lead should be able to perform in a similar manner. Only a few alternative alloys meet the specific criteria when considering material properties, toxicity, abundance of supply, and cost. These alloys include, but are not limited to, Sn-Cu, Sn-Bi, Sn-Ag, Sn-Bi-Ag, Sn-Bi-Ag-Cu and Sn-Ag-Sb-Bi [Schlesinger and Paunovic 2000]. However, other alternative solders have been introduced in the literature for each specific application requiring specific properties.

The high electrical conductivity of gold, the low contact resistance, and good solderability combined with its chemical inertness have made gold a perfect choice for the specific applications in electronics [compelete properties of gold are available in Reid and Goldie 1974]. For optoelectronic applications, higher melting point alloys can be used for packages that run hot (i.e., laser devices). Although gold is expensive, its material properties make gold eutectic alloys such as Au-Sn, Au-Ge, and Au-Si useful alternatives for optoelectronic applications [Doesburg 2000].

2.1.3. Gold-Tin Solders

The 20 wt. % tin composition is the gold-tin solder commonly used. It is classified in the hard solder category since its main component is the hard gold metal with a high melting temperature of 1064 °C. The melting temperature of this solder at the eutectic composition of 20 wt.% tin is 278 °C (phase diagram in Figure 2-2 [American Society for Metals 2005]).

There is another eutectic at 90 wt. % tin which has a lower melting temperature of 217 °C. The tin-rich solders are rarely studied. A fluxless bonding process that would form a gold-tin alloy joint with a high tin composition has been developed and has resulted in a uniform and nearly void free joint [Chin 1999]. However, this eutectic contains the $AuSn_4$ intermetallic phase which is reported to be a weak, brittle compound [Zribi, Chromik et al. 1999]. The presence of $AuSn_4$ degrades the thermal fatigue life of the solder joint when present in high concentrations. Mechanical failures have been observed because of $AuSn_4$ embrittling the solder joint [Fahong 2003].

The gold-rich eutectic composition has good creep behaviour and corrosion resistance [Sun and Ivey 2001]. Furthermore, this eutectic solder has superior high temperature performance, excellent electrical and thermal conductivity, and can be soldered without a flux [Smith and Akhlaghi 2004].

The drawback of the gold-rich eutectic solder is that accuracy is required to maintain the eutectic composition. The phase diagram in Figure 2-2 shows that the desired gold-tin eutectic point is defined by steep liquidus lines on both sides of the eutectic melting point meaning a small variation in composition can cause a large change in melting temperature, which can make the solder unusable.

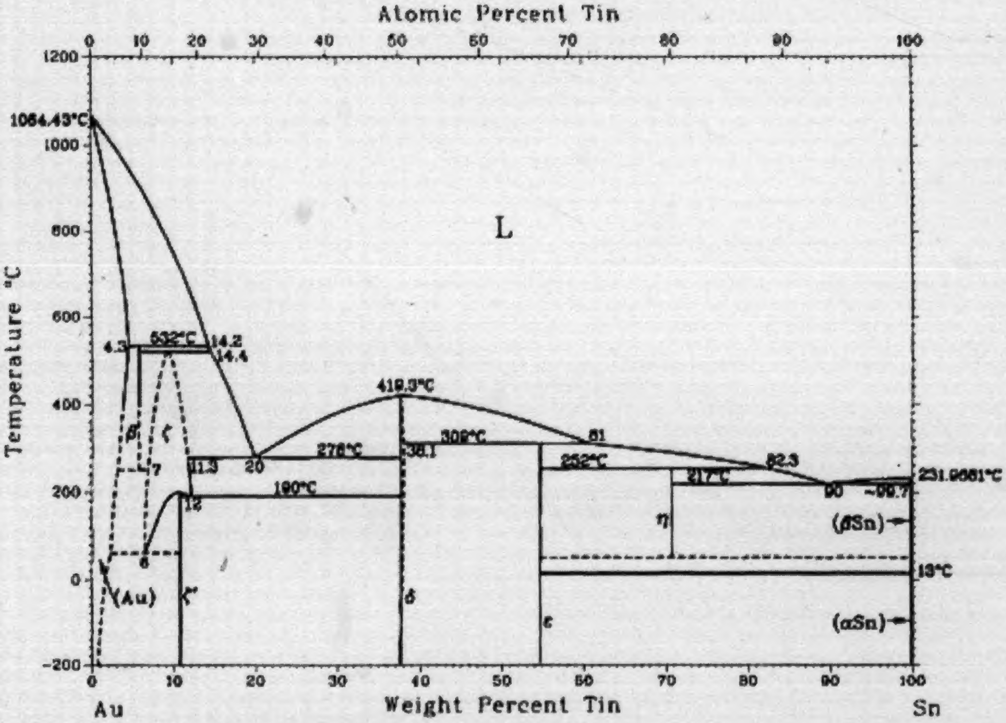

Figure 2-2: The gold-tin binary phase diagram [American Society for Metals 2005].

2.1.3.1. Fabrication Methods

Gold-tin solder can be applied using several methods: solder preforms, paste, sequential vacuum deposition and sequential electrodeposition [Sun and Ivey 1999]. In the solder preform method, molten gold and tin liquids are blended to the 80:20 ratio (by weight) and cast into ingots. After a series of rolling operations that flatten the ingots into strips, the finished thickness specifications range between 25 and 1500 μm. Preforms are stamped or machined from the rolled strip. The minimum preform size obtainable is 1mm x 1mm due to difficulties in preform stamping and handling [Forman and Minogue 2004, October]. Solder preforms are problematic for flip chip applications because of alignment problems and pre-application oxidation of the solder.

Solder pastes consist of eutectic alloy spheres and a thixotropic carrier material to support the spheres and fluxing agents. The composition is accurately controlled to within one percent of the design composition. However, the solder feature size, volume, and placement accuracy are limited to the capabilities of the selected screen printing process. The drawback of this method is elimination of fluxless reflow of the gold-tin solder. The use of flux introduces the possibility of out-gassing volatile compounds that may condense on the device surfaces or may be trapped inside the package [Forman and Minogue 2004, October]. Solder pastes may also be contaminated or oxidized prior to binding [Doesburg 2000].

In the sequential vacuum deposition method, alternating evaporated or sputtered layers of gold and tin are sequentially applied directly onto substrates to obtain the desired thickness and composition. These deposits are commonly less than 1 μm in thickness and are usually made up of gold and tin layers from 0.1-0.5 μm thick [Forman and Minogue 2004, October]. In this method, the top layer is typically gold to protect the tin layer from oxidation. The evaporation technique has the advantage of being cleaner (less oxide formation prior to bonding) over preforms and pastes. Also, the position and the thickness of the deposit can be controlled more precisely. However, the evaporation technique involves expensive vacuum systems and skilled operators, while the deposition rates are slow [Sun and Ivey 1999]. In vacuum deposition technology the solder coats the entire substrate and the chamber walls. The removal of the extraneous material makes the vacuum deposition technique inefficient since the area which needs solder is typically below 10% of the total substrate area.

In sequential electroplating, alternating gold and tin layers are deposited. The thickness ratio of gold to tin is controlled to achieve the desired eutectic composition. The outermost layer in this method is typically gold to insure proper wetting and reflow of the solder during assembly. This method is economical and efficient since the deposited material from solution goes only onto the desired area (using photoresist masks). It also does not need expensive vacuum systems or operators [Doesburg 2000]. However, the substrates are moved repeatedly between two separate gold and tin plating baths. The gold plating baths may contain hazardous materials (such as cyanide), or additives to control the deposit stress that may attack conventional photoresist. In addition, there are the risks of cross-contamination between the baths and exposure of the tin layers to oxidation during processing. Finally, diffusion between the sequential layers of gold and tin may create brittle gold-tin intermetallic compounds that increase the likelihood of joint cracking under mechanical stress. An example of fractured solder bump after temperature cycling is shown in Figure 2-3 below.

Figure 2-3: Fractured solder bump after temperature cycling [Riley 2004].

Co-electrodeposition of gold and tin from a single solution offers the same economical and efficiency advantages compared to vacuum deposition techniques as sequential plating. However, the co-electrodeposition offers the additional advantage of depositing the solder in a single step without oxidation of an outer tin layer [Sun and Ivey 1999] and eliminates the risk of cross-contamination and interdiffusion issues.

2.1.3.2. Applications

The challenges in optoelectronic and microelectronic packaging technology deal with the need for higher power, higher operating temperatures, higher connection density, and better geometric accuracy. Better heat transfer to the substrate is required for high power electronic and optical devices. However, moving towards smaller feature sizes makes heat transfer more difficult.

In optoelectronic applications, high-power light-emitting diodes (LED) and lasers operate at higher temperatures (beyond that of eutectic tin-lead) creating the need for solders with higher melting temperatures. Increasing application of high-power semiconductor lasers in industrial, military, commercial, and consumer products makes the thermal management of high-power lasers critical. The junction temperature rises due to large heat fluxes and strongly affects the device characteristics including wavelength, kink[1] power, threshold current and efficiency, and reliability [Liu, Song et al. 2005]. Furthermore, optical alignment precision plays a significant role in the device performance.

In Micro-Electro-Mechanical Systems (MEMS) fluxes and residues are intolerable. The MEMS devices for biomedical applications require corrosion resistance along with good electrical, thermal, and mechanical properties [Smith and Akhlaghi 2004].

Gold-tin solder is becoming the preferred choice to all of the above modern packaging challenges. Complete information on packaging concepts and design can be found in [Gilleo 2002]. However, since electrodeposited gold-tin solder bumps are used most commonly in the flip chip method in packaging, this technique is described in the following section.

2.1.3.2.1. Flip Chip

Flip chip (FC), which is also called direct chip attach (DCA), is one of the methods used to connect the die to the package carrier in optoelectronic and microelectronic packaging technology [Gilleo 2002].

In flip chip packaging, the conductive bumps are created directly on the die surface. The bumped surface on the die is then flipped over and placed face down on the carrier and then attached by a solder reflow process (see Figure 2-4). In this way the bumps create a direct connection between the die and the carrier. The dimensions of the conductive bumps are typically 70-100 μm in height, and 100-125 μm in diameter [Amkor 2006].

---

[1] Kink: non-linearity in the power-current characteristics of lasers.

These bumps can be formed by using either solder or conductive adhesive, but the most common packaging interconnect is solder.

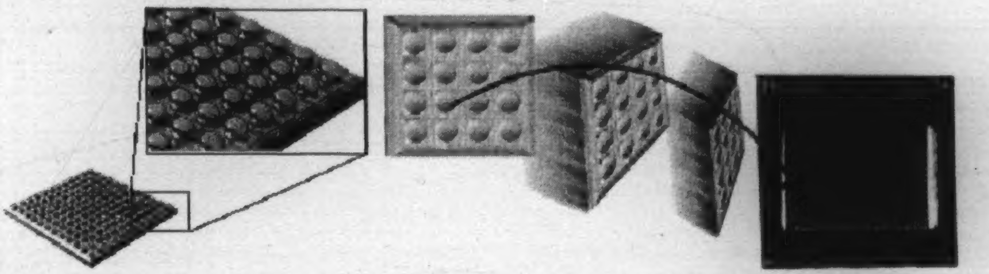

Figure 2-4: Flip chip packaging [Amkor 2006].

After die attachment using the reflow process, the space between the die and the substrate is filled with underfill material. The underfill is specially engineered epoxy designed to control the stress in the solder joints caused by the difference in thermal expansion between the silicon die and the carrier.

The method of connection in FC distinguishes this technology from all others. The interconnection in FC is a joint without any wires, while most chip-scale packages (CSPs) use wires between the chip pads and the substrate or package. Other connection schemes exist in which the chip is face down (flipped), such as tape automated bonding (TAB), but all such methods incorporate wires and never have a DCA connection.

The package carrier provides the connection from the die to the exterior of the package. Previously, wire bonding was used to create such connections. In wire bonding the die is attached to the carrier face up, and a wire is bonded first to the die and then looped and bonded to the carrier. The dimensions of such wires are typically 1-5 mm in length, and 25-35 μm in diameter [Amkor 2006].

Using the FC method offers a number of possible advantages to the wire bonding technique. The FC and wire bonding methods are illustrated in Figure 2-5. The flip chip method nearly eliminates the package. This feature both adds and subtracts attributes.

The total package size, thickness and weight can be reduced since extra space is not required for wires. However, FC lacks the protection, ease of handling, and standardization provided by packages [Gilleo 2002].

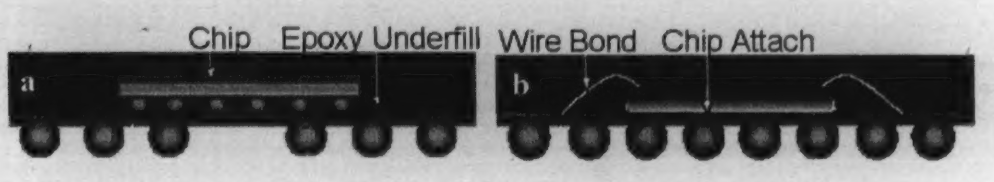

Figure 2-5: (a) Flip chip, (b) Wire bonding [Amkor 2006].

The flip chip method reduces signal inductance due to short length interconnection, and improves high speed communication and switching devices. The direct power connection allows for reduction in noise and improves the performance. In this method the entire surface of the die can be used for connection, rather than just the edges, allowing higher signal density in the design and larger numbers of interconnects on the same die size [Amkor 2006].

2.2. Electrodeposition

2.2.1. Introduction

Electroplating, which is often also called electrodeposition, is the process of producing a coating on a surface caused by chemical changes initiated by the passage of an electric current. This technology is one of the many technologies that encompass the science of electrochemistry, which is the branch of chemistry concerned with the interrelation of electrical and chemical effects [Bard and Faulkner 2001]. In other words, this field deals with the study of chemical changes caused by the passage of an electric current and production of electrical energy by chemical reactions. In order to understand the electroplating process and to be able to improve it and know its limitations, advantages, and disadvantages, it is necessary to have a comprehension of the science behind it.

In an electrochemical system, the main concerns are the processes and factors that affect the transport of charge across the interface between chemical phases. The two key phases in all systems are the electronic (electrodes) and ionic (electrolyte) conducting phases. Essentially, charge is transported through the electrodes (cathode[1] and anode[2]) and the electrolyte by the movement of electrons (or holes) and ions respectively. However, at the electrode-electrolyte interface, two types of processes are possible. In some systems charges (electrons) can transfer across the interface causing oxidation[3] or reduction[4] to occur. Such reactions are called Faradaic processes since they are governed by Faraday's Law. Under some conditions charge transfer reactions are not thermodynamically or kinetically favourable causing adsorption and desorption to occur. These processes are called non-Faradaic processes [Bard and Faulkner 2001].

An electrode that does not allow charge transfer across the electrode-electrolyte interface regardless of the amount of electrical energy imposed by an outside source is called an ideal polarized electrode (IPE). Although, no real electrode can behave as an IPE over all conditions, some materials such as mercury and gold approach this ideal behaviour over limited potential ranges. Therefore, the processes in a real system can appear Faradaic or non-Faradaic depending on what range of electrical energy is applied to the system [Bard and Faulkner 2001].

The most simplified electrochemical systems are defined as two electrodes separated by at least one electrolyte phase, which are called electrochemical cells. The electrochemical cells in which Faradaic processes take place are classified as either galvanic or electrolytic cells [Bard and Faulkner 2001]. In galvanic cells reactions occur spontaneously at electrodes (while connected externally by a conductor), whereas in electrolytic cells reactions are managed by imposition of an external power supply

---

[1] Cathode: electrode at which reduction occurs [Bard A. J. & Faulkner L. R. 2001].

[2] Anode: electrode at which oxidation occurs [Bard A. J. & Faulkner L. R. 2001].

[3] Oxidation: a reaction in which the reacting agent loses electron(s) [Electrochemical Science and Technology Information Resource (ESTIR) 2006].

[4] Reduction: a reaction in which the reacting agent gains electron(s) [Electrochemical Science and Technology Information Resource (ESTIR) 2006].

(applied voltage or current). The cathode is negative with respect to the anode in an electrolytic cell, while the cathode is positive with respect to the anode in a galvanic cell [Bard and Faulkner 2001].

The overall chemical reaction taking place in a cell is made up of two independent half cell reactions happening at the two electrodes. Usually, one of these half reactions is studied at a time. To do so, one of the electrodes is chosen to be a standardized material of known behaviour called the "reference electrode". Two examples of internationally accepted reference electrodes are the normal hydrogen electrode (NHE) and the saturated calomel electrode (SCE) [Bard and Faulkner 2001]. The behaviour of the desired reaction is then studied by constructing a cell consisting of a "working electrode" and a reference electrode. This method simplifies the characterization of the desired reaction at the working electrode, since one of the half reactions is already well known. The electrode potentials at standard conditions with respect to these reference electrodes are tabulated and are available in the literature. If the metal of interest has a greater tendency to give up electrons than the reference electrode, then its potential is more negative compared to that of the reference electrode. In each system, the metal with the highest standard potential is the least active metal (noble) and most probably will not be involved in any reaction.

For electroplating, an electrolytic cell is set up. The reaction of interest is the deposition of metal (M) through a reduction reaction at the cathode (which is connected to the negative output of the power supply). This reaction can be shown as [Doesburg 2000]:

$$M^{n+} + ne^- \rightarrow M. \qquad \textbf{(Equation 2-1)}$$

At the anode the following reactions can occur [Doesburg 2000]:

$$\textit{metal dissolution: } M \rightarrow M^{n+} + ne^-, \qquad \textbf{(Equation 2-2)}$$

$$\textit{oxygen evolution: } 2H_2O \rightarrow O_2 + 4H^+ + 4e^-, \qquad \textbf{(Equation 2-3)}$$

$$\textit{oxidation: } M^{2+} \rightarrow M^{3+} + e^-, \qquad \textbf{(Equation 2-4)}$$

$$\textit{passivation: } 2M^{2+} + O_2 \rightarrow 2MO + 4e^-. \qquad \textbf{(Equation 2-5)}$$

Engineers and scientists approach the design of a new system by considering a "black box". Certain inputs are applied to this "black box", and certain outputs are obtained. Then, a model can be created for the system knowing the design variables in the system and the factors affecting the output of the system. In the case of an electrochemical system, the design consists of knowing the variables in the cell and the factors affecting the rate of an electrode reaction.

2.2.2. Variables in Electrochemical Cells

Knowing the design variables of an electrochemical cell not only helps in designing a new system, but can also help in investigating any existing system. The investigation consists of holding certain variables constant and observing how other variables vary with changes in the controlled variables. It should be noted that in some cases the variables may not affect the output directly. The important parameters in electrochemical cells can be divided in five main categories summarized in Figure 2-6 [Bard and Faulkner 2001] and explained in the following subsections.

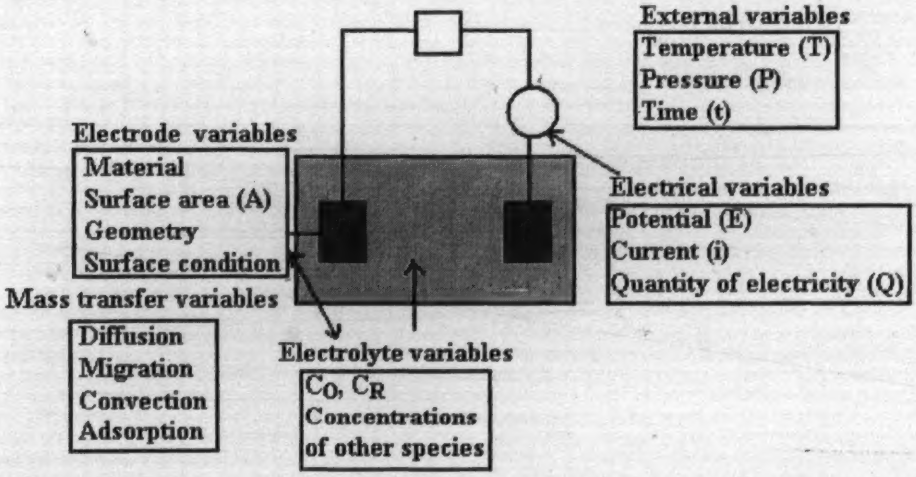
External variables
Temperature (T)
Pressure (P)
Time (t)
Electrode variables
Material
Surface area (A)
Geometry
Surface condition
Electrical variables
Potential (E)
Current (i)
Quantity of electricity (Q)
Mass transfer variables
Diffusion
Migration
Convection
Adsorption
Electrolyte variables
C_O, C_R
Concentrations
of other species

Figure 2-6: Variables in electrochemical cells, after [Bard and Faulkner 2001].

2.2.2.1. External Variables

The temperature (T) and the pressure (P) both affect the rate of chemical reactions and the electrical properties of the materials. In addition, the duration of the experiment, time (t), controls the amount of the chemicals produced (used) and the amount of charge transferred in the system.

2.2.2.2. Electrical Variables

The applied electrical energy is one of the main control tools of an electrochemical system. The electrical variables can be in the form of applied potential (E) or current (i). In other words, the charge which is the quantity of electricity (Q) applied will control which species in the system undergo a reaction, the nature of the reaction (oxidation/ reduction), and the amount of the electrolyzed species. For example, dull deposits may result at too high (or too low) a current density. The unsuitable current density could cause a change in the normal chemical limits of the solution and therefore a loss in the plating quality [Knodler 1986]. Some of the important roles of the electrical variables in Faradaic and non-Faradaic systems are discussed briefly in the following sections.

2.2.2.2.1. Faradaic Systems

In a Faradaic system, the following relation demonstrates the direct proportionality between Faradaic current (I) and electrolysis rate [Bard and Faulkner 2001]:

$$N(moles) = \frac{Q(coulombs)}{nF(coulombs/mol)}$$

$$\Rightarrow Rate(mol/s) = \frac{dN}{dt} = \frac{I}{nF}, \qquad \textbf{(Equation 2-6)}$$

where N is the number of moles electrolyzed, n is the stoichiometric number of electrons involved in the electrode reaction, and F is Faraday constant of 96,485.3 coulombs per mole of electrons [Bard and Faulkner 2001].

2.2.2.2.2. Non-Faradaic Systems

As mentioned before if an electrical perturbation is applied to a system consisting of non-Faradaic processes, no charge can cross the electrode-electrolyte interface. In this case, the behaviour of the interface is analogous to that of a capacitor.

Electrical Double Layer Capacitance:

For an IPE, an array of specifically adsorbed ions, solvated charged species, and oriented dipoles develop at the interface forming an electrical double layer capacitance (C_d) [Bard and Faulkner 2001]. The structure of the electrical double layer can affect the rates of electrode processes. However, C_d has one difference in comparison with real capacitors. Specifically, the capacitances of real capacitors are independent of the voltage across them, but the double layer capacitance is a function of potential. Sometimes, the effect of C_d may be neglected when considering the electrode reaction kinetics [Bard and Faulkner 2001].

A simple non-Faradaic system can be modeled as an electrical circuit of two elements C_d and R_s in series [Bard and Faulkner 2001]. C_d is the double layer capacitance as explained and R_s represents the electrolyte resistance. Applying different electrical perturbations to the system result in changes in characteristics of the system. Electrical responses to a few selected electrical inputs along with the circuit schematic of the modeled system are shown in Table 2-1 [summarized from Bard and Faulkner 2001].

Table 2-1: Electrical responses to selected electrical inputs [summarized from Bard and Faulkner 2001].

Experiment	Potential Step	Current Step	Voltage Ramp
Circuit Schematic	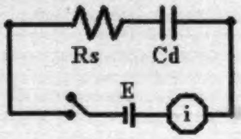	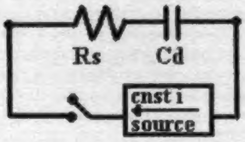	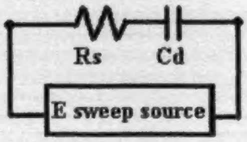
Input	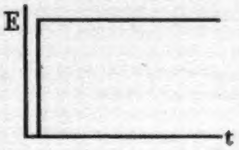	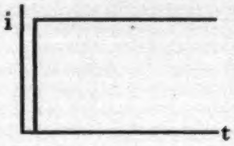	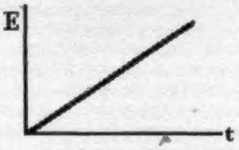
Output	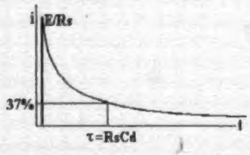	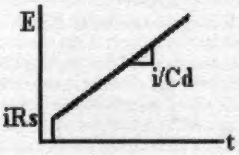	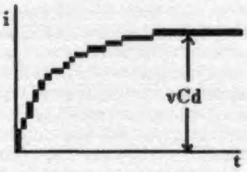
Output Equation	$i = \frac{E}{R_s} e^{-t/R_sC_d}$	$E = i(R_s + \frac{t}{C_d})$	$i = vC_d[1 - e^{-t/R_sC_d}]$

2.2.2.3. Electrode Variables

It is apparent that the material of the electrode used is an important design variable. An electrode may play a substantial role in the reaction of interest (working electrode), or it may be a "counter electrode" by having convenient electrochemical properties that do not affect the behaviour of the electrode of interest. In other words, the "counter electrode" does not produce substances by electrolysis that will reach and interfere with the "working electrode". One very common example of a "counter electrode" is platinum [Bard and Faulkner 2001]. As mentioned before, usually a "reference electrode" is also used in an electrochemical cell to provide a standard reference for monitoring the changes in potential of the "working electrode".

Plating technologies may be divided into two categories of electroplating and electroless plating.

The electroplating process, which is the focus of this thesis, is principally an electrolytic cell in which a chemical redox[1] process takes place resulting in formation of a layer of material on the substrate ("working electrode") and the generation of gas at the "counter electrode". For electroplating technology a conducting material is needed. In the case of an insulating substrate, a thin film of conducting material is deposited on the surface of the "working electrode".

The electroless plating process is principally a galvanic cell consisting of a complex chemical electrolyte in which a chemical redox process takes place spontaneously on any surface. Applications of this technology are now common in many industries including plastics, printing, mining, food processing machinery, optics, computer-related manufacturing processes, and automotive processes [TechSolve 2005]. One specific example would be the nickel electroless coating directly applied to zinc die cast for corrosion resistance and resistance to chipping and flaking [Sinorama 2002]. In comparison with electroplating technology, it is more difficult to control the film thickness and uniformity in electroless technology [Okinaka 1990].

The electrode involved in or providing a site for the reaction depends on the material of the electrode. Regardless of the electrodeposition process being used, there are other electrode variables that affect the result of the experiment. The surface area (A), geometry, and surface condition of the electrode play an important role in both cases [Bard and Faulkner 2001]. These variables influence the amount of charge transfer and electrolyzed material, the nature of the diffusion of ions around the electrode in the electrolyte, and the nature of adsorption and crystallization[2] of the thin film.

---

[1] Redox: the combination of reduction and oxidation half reactions [Electrochemical Science and Technology Information Resource (ESTIR) 2006].

[2] Crystallization: "the process by which adatoms or adions incorporate in the crystal lattice" [Knodler A. 1986].

2.2.2.4. Electrolyte Variables

The electrolyte can be in the form of a liquid solution (in electrolytic syntheses, electrorefining, and electroplating), a solid (in fuel cells), or a molten salt (in thermal batteries). Since, the focus of this paper is electroplating, the "solution variables" are considered here. Consider the overall reaction:

$$O + ne \leftrightarrow R. \qquad \textbf{(Equation 2-7)}$$

where O and R are the oxidizing species and the reduced form respectively, and n is the number of electrons. The bulk concentrations of the electroactive species (C_O, C_R) determine how much material is available for electrolysis. Furthermore, the characteristics and concentrations of other species in the solution affect the electrochemical properties of the solution and the kinetics of ions in the solution respectively. For example, the concentration of hydrogen ions controls the pH of the solution. The pH of the solution can favour or prevent the occurrence of certain acidic or basic reactions [Bard and Faulkner 2001].

Additional chemicals or metals often may accumulate in a bath. These additional materials may be harmful impurities or may function as beneficial agents. For example, copper contaminates zinc cyanide, cadmium cyanide, nickel, and tin baths [Mohler 1984]. However, in some systems the concentration of the secondary material could determine whether its existence is beneficial or harmful. For example, lead in a copper cyanide bath can act as a brightener at low concentrations, which is desired. However, at high concentrations it promotes brittleness and cracking [Mohler 1984].

Possible functions of constituents in typical plating baths are quoted by [Zhang 2001] from [Mathe 1992] and [Lowenheim 1974] and are shown in Table 2-2. Since a chemical may have more than one function in the bath, not all the components are needed for all baths [Zhang 2001].

Table 2-2: Possible constituents in plating baths [Zhang 2001].

Component	Function	Examples
Metal ion or complex ion	Supplies metals for deposition	$Au(CN)_2^-$, $AuCl_4^-$, $SnCl_4$
Chelating agent	Acts as buffer and prevents rapid decomposition of ions	citric acid, EDTA, cyanide
Stabilizer	Inhibits the bath decomposition, disperses active nuclei	non-ionic surfactants, fatty acids
Buffer	Maintains pH	alkali metal salts: borate, tartrate
Wetting agent	Promotes wetting of the solution parts to be plated	sulphated alcohols, fatty acids
Reducing agent	Regulates the bath potential	L-ascorbic acid, hydrazine, alkyl amine borane
Oxidizing agent	Regulates the bath potential	sodium perborate
Exaltant	Increases the rate of deposition	succinic acid
Brightener	Brightens the appearance of the deposit	metal additives
Conducting salt	Increases the electrical conductivity of electrolyte	phosphate, carbonate, sulphuric acid
Levelling agent	Smooths the surface of the deposit	pyridine, quinoline

2.2.2.5. Mass Transfer Variables

Mass transfer in an electrolyte solution is controlled by the transportation methods in different regions of the solution: the bulk solution, the electrode vicinity, and the surface of the electrodes. Transportation occurs by migration and convection methods in the bulk solution and by diffusion close to the electrodes. Moreover, mass transfer is affected by adsorption at the surface of the electrodes.

Diffusion, Migration and Convection:

Diffusion and migration result from a gradient in electrochemical potential (concentration gradient and/or electric potential gradient), and convection results from an imbalance of forces (stirring, stagnant solution, and density gradients). The flux of species j in the solution, J_j, is defined as the number of moles of species moving through a plane of unit area per unit time. In general the flux J_j relates to the mass transfer methods by the following equation [Bard and Faulkner 2001]:

$$J_j = -D_j \nabla C_j - \frac{z_j F}{RT} D_j C_j \nabla \phi + C_j v, \qquad \text{(Equation 2-8)}$$

where D_j is the diffusion constant, ∇ is the gradient vector operator, C_j is the concentration of species j, F is the Faraday constant, R is the molar gas constant, z_j is the charge of species j, T is the temperature, ϕ is the electrostatic potential, and v is the velocity of solution flow, usually a function of position.

Often for simplicity, a supporting electrolyte chemical (excess electrolyte) is added to the solution. The excess electrolyte does not participate in reactions and its addition eliminates the contribution of migration to the mass transfer of the electroactive species. It also has other advantages as it improves the accuracy of control of R_s measurements, stabilizes the pH of the solution, and decreases the thickness of the double layer capacitor. However, it has the disadvantages of bringing impurities, the possibility of adsorption of the excess chemical on the electrode, and changing the properties of the electrolyte [Bard and Faulkner 2001].

Diffusion Layer:

Upon the application of the current or voltage in the electrolytic cell, species are used (or produced) at an electrode causing the concentration at the surface to differ from the bulk concentration. Therefore, a gradient in concentration is created causing more of the species to diffuse to (or from) the electrode surface. The thin layer of solution in contact with the electrode controls the mass transfer by diffusion alone. The distance from the electrode where the ratio $(C - C_{interface})/(C_{bulk} - C_{interface})$ reaches a given value is called the thickness of diffusion layer (δ). At distances much greater than the diffusion thickness, the electrode has no effect on the concentration of the species. Similarly, the reactants in the solution have no access to the electrode at distances farther than the thickness of the diffusion layer. However, at much smaller distances, the electrode process is dominant [Bard and Faulkner 2001].

The thickness of diffusion layer, δ, is often defined as [Bard and Faulkner 2001]:

$$\sqrt{D_j t}, \sqrt{2D_j t}, \sqrt{\pi D_j t}, or 2\sqrt{D_j t}. \qquad \textbf{(Equation 2-9)}$$

It is obvious that the thickness of the diffusion layer depends on time and the diffusion constant (D) of the species. Concentration profiles for several times after the start of a potential step experiment are shown in Figure 2-7 [Bard and Faulkner 2001]. In the potential step experiment, an instantaneous change in potential from a value where no electrolysis occurs to a value in the mass-transfer-controlled region for reduction is conducted on a planar electrode in an unstirred solution [Bard and Faulkner 2001].

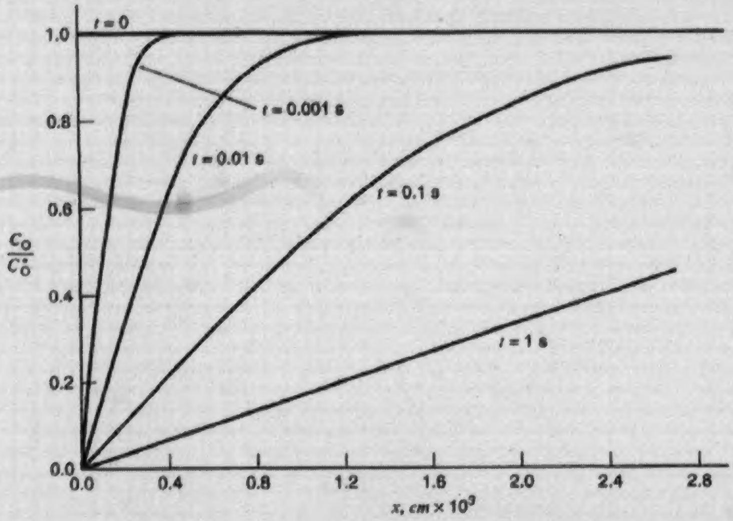

Figure 2-7: Concentration profiles for several times after the start of a potential step experiment, $D_j=10^{-5}$ cm²/s [Bard and Faulkner 2001].

Effect of Agitation:

Mass transfer is improved during electroplating using agitation. Agitation affects mass transfer both by increasing the velocity of solution flow in Equation 2-8 and by decreasing the thickness of the diffusion layer. Agitation can push the species closer to the electrode surface leaving a smaller region for migration through diffusion. Therefore, the species are more available closer to the electrode and the thickness of the diffusion layer is decreased. The electrode reaction rate can then be increased. Schematic drawings of the diffusion layer thickness under three agitation modes are shown in Figure 2-8, where the stirred solution refers to mechanical agitation and UA refers to ultrasonic agitation [Menini 2005]. Menini explains the effect of ultrasonic agitation on the thickness of diffusion layer by stating that bubble implosion created by negative and positive alternating pressures creates a tiny but intense area of pressure and temperature locally which reduces the thickness of diffusion layer locally [Menini 2005].

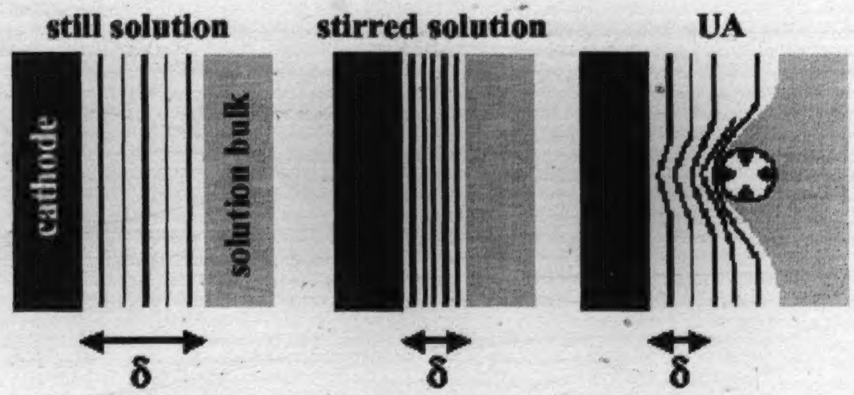

Figure 2-8: Schematic drawings of the diffusion layer thickness under three agitation modes [Menini 2005].

Adsorption:

There are two types of adsorption: non-specific or specific adsorption. Non-specific adsorption is when long range electrostatic forces alter the distribution of ions near the electrode surface (attraction of opposite charges). It affects the electrochemical response by affecting the concentration of the species and the potential distribution near the electrode. Specific adsorption is when a strong interaction between the adsorbate and the electrode material causes the formation of a layer on the electrode surface (formation of a bond), and it can have several effects. It can change the energetics of the reaction of the electroactive species (an adsorbed ion may have more difficultly reacting than a dissolved ion), or the adsorbed chemical may form a blocking layer on the electrode surface [Bard and Faulkner 2001].

Adsorption of atoms on the electrode surface has another importance. The adatoms may form stable nuclei and grow into crystals that form the desired thin film. Therefore, the rate of adsorption affects both the diffusion of the atoms near the electrodes and the rate of crystallization and growth [Bard and Faulkner 2001].

Now that all the variables in an electrochemical cell have been discussed, it is apparent that changing one variable may affect the result of the experiment both directly and indirectly (by changing other variables).

2.2.3. Factors Affecting Electrode Reaction Rate and Current

If Equation 2-7 is considered and it is assumed that both the O and R species exist in the solution (electrolyte phase), then Figure 2-9 shows the pathway of a general electrode reaction for such reactions [Bard and Faulkner 2001].

The rate of the reaction is governed by the rates of the following processes:

1. Mass transfer: This concept was explained in more detail in Section 2.2.2.5. An example would be the rate of the mass transfer of O from the bulk solution to the electrode surface.

2. Electron transfer at the electrode surface: The rate of electron transfer depends on the electrode and electrical and external variables. For example, application of different current densities will result in different electron transfer rates. In more complicated systems, electron transfer can happen in a multi-component or a multi-step manner. In a multi-component system, a set of half cell reactions happen independently and electron transfers proceed in parallel channels. In a multi-step system an intermediate substance (reduced form or oxidizing species) is formed, and the

electron transfer rate of each subsequent step depends on the rate of its preceding reaction [Bard and Faulkner 2001].

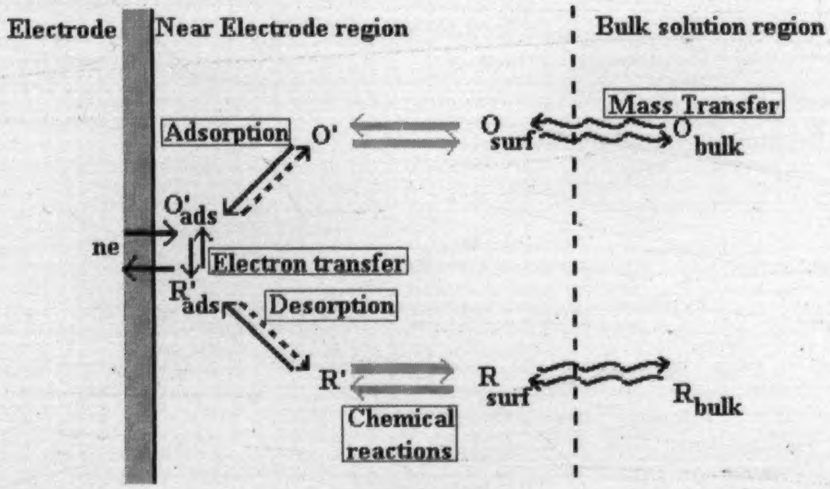
Electrode
Near Electrode region
Bulk solution region
Mass Transfer
Adsorption
O'
O_{surf}
O_{bulk}
O'_{ads}
ne
Electron transfer
R'_{ads}
Desorption
R'
R_{surf}
R_{bulk}
Chemical reactions

Figure 2-9: Pathway of a general electrode reaction [after Bard and Faulkner 2001].

3. Chemical reactions preceding or following electron transfer: These might be homogeneous (occur everywhere within the electrolyte) or heterogeneous reactions (occur only at the electrode-electrolyte interface) [Bard and Faulkner 2001].

4. Surface reactions such as adsorption, desorption, or crystallization: In contrast to adsorption, desorption can happen due to repulsion of similar charges or breakage of a bond. Furthermore, the rate of crystallization also affects the deposition rate and the current. Crystallization of an electroactive material is a very important step influencing the structure of the deposited thin film [Bard and Faulkner 2001].

The rate of the reaction is often limited by the rate-determining step, which is the slowest of one (or more) of these processes. Since, the value of the current density due to each factor depends on a certain overpotential, η, the electrode reaction can be modeled as an impedance Z. Then, Z is a series combination of three impedances; Z_{mt} (mass transfer impedance), Z_{ct} (charge transfer impedance), and Z_{rxn} (impedance associated with a preceding reaction) corresponding to overpotentials of η_{mt}, η_{ct}, and η_{rxn} respectively [Bard and Faulkner 2001]. Consequently, fast and slow steps are characterized by small and high impedances respectively. It should be noted that these impedances are functions of potential (or current) unlike the usual electrical elements.

2.2.4. Pulse Plating

As explained previously, plating technologies may be divided into two main categories of electroplating and electroless plating. Electroplating is the main focus of this thesis, and in the electrolytic cell, the applied electrical energy can be in the form of either potential or current. There are certain advantages and disadvantages if the controlled-current method is used over the controlled-potential method [Bard and Faulkner 2001]. For the controlled-current method:

- The instrumentation is simpler. In the electrochemical cell, it is the flow of electrons that supports the active electrochemical processes at a certain rate. Therefore, for controlling potential, a feedback system is needed to force the desired potential at any time.
- The mathematical treatments (i.e., solving diffusion equations) are much simpler.
- Correction for double layer charging effects is more complicated.
- Treating data from multi-component and multi-step systems is more complicated.

Currently, controlled-current methods are used more frequently in electrodeposition technologies, while controlled-potential methods are used more commonly in chemical synthesis and corrosion control technologies. One of the main controlled-current methods is pulse current plating. If the applied current is modified by applying the cathodic current as some function of time, pulse plating (PC) is achieved. The current is typically a square wave containing “on-times” and “off-times” of the cathodic[1] current.

---

[1] Cathodic current: a current in which electrons cross the interface from the electrode to a species in electrolyte [Electrochemical Science and Technology Information Resource (ESTIR) 2006].

Some schematic representations for some square-wave-modulated current systems are shown in Figure 2-10 [Knodler 1986]. Although square waveforms are currently popular, modified sine-wave pulses are used in some applications too [Knodler 1986].

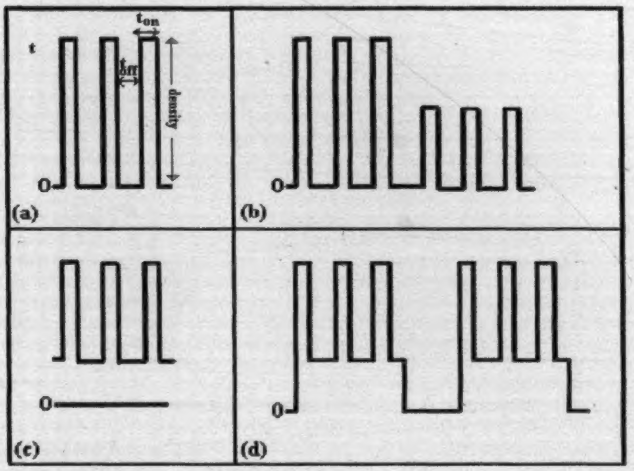

Figure 2-10: Some square-wave modulated current systems: (a) Pulse, (b) duplex pulse, (c) superimposed pulse, (d) pulse-on-pulse [after Knodler 1986].

The range of conditions of the modulated current is limited by two main factors. First, the charging time of the electrical double layer at the electrode-electrolyte interface should be much shorter than the pulse duration (limitation on pulse period). Second, mass transport considerations limit the peak and the average values of the pulse current density. This limitation is due to depletion of cations in the diffusion layer (close to electrode region) [Sun 1998].

Morphology and Pulse Plating:

The main purpose of PC plating rather than direct current (DC) plating is the improvement of deposit properties (i.e., porosity, ductility, hardness, electrical conductivity, wear resistance, and roughness) [Knodler 1986]. It should be noted that the properties of a deposit depend on its structure which, in turn, is influenced by the crystallization process. PC plating increases the nucleation rate leading to the formation of finer grains and a more homogeneous surface appearance [Ramanauskas, Gudaviciute et al. 2003]. In addition, plating thickness distribution is improved by periodic inversion of polarity. Furthermore, the desired composition and structure of some alloys are not obtainable with DC plating, and therefore pulse plating has to be used [Knodler 1986].

2.3. Electroplating of Gold-Tin Solders

2.3.1. Introduction

The gold alloys used for electronic packaging have to be electroplated in acidic plating baths, because the photoresists used to pattern the circuits are alkaline-developable. The electroplating of gold-tin eutectic solder can be done through both sequential plating and co-plating. In sequential plating gold and tin layers are plated consecutively, while in co-plating gold and tin are deposited together from a single bath. Careful attention to relative film thicknesses, film geometry, and grain sizes are important in sequential plating, because these factors influence the diffusion between gold and tin layers [Nakahara and McCoy 1980]. Tin over gold deposition results in a more homogeneous structure, because tin nucleates uniformly on Au [Nakahara and McCoy 1980]. Since the outer tin layer in sequential plating is exposed to air before heat treatment, an oxide layer can form and cause problems with soldering. However, co-plating can prevent oxidation and eliminates the post heat treatment of the film, which is needed to allow diffusion and mixing of gold and tin layers. In the following sections, the baths used for both sequential plating and co-plating are considered.

2.3.2. Sequential Electroplating of Gold-Tin Alloys

In sequential plating of gold-tin solders, commercial gold and tin baths have been used. gold/tin bumps can be fabricated on patterned silicon substrates with gold seed layers. Often, gold is deposited first followed by deposition of tin [Zhang 2001]. Common acidic baths used to plate gold and tin are discussed below.

2.3.2.1. Gold Electrodeposition

Gold needs a very small negative potential for reduction from the ionic to metallic state. In solutions containing free ions, non-adherent immersion deposits are formed rapidly. These deposits have large grain sizes and they grow forming dendrites. Thus, it is desired to plate gold from baths in which the metal ions are complexed [Reid and Goldie 1974].

Baths containing cyanoaurate (I) ions are generally used in electrodeposition of gold [Zhang 2001]. The gold-cyanide complexes have high stability constants. The stability coefficients for $[Au(CN)_2]^-$ and $[Au(CN)_4]^-$ are 2×10^{38} and 10^{56} respectively [Stanley 1987]. The stability of cyanide baths becomes apparent when these values are compared with the stability coefficients of some of the other possible complexes such as $[Au(SO_3)_2]^{3-}$ and $[Au(S_2O_3)_2]^{3-}$, which are 10^{10} and 10^{26} respectively [Sun and Ivey 1999]. Foulke summarized the types of acidic electrolytes from the patent literature which are shown in Table 2-3 [Reid and Goldie 1974].

Table 2-3: Acidic electrolytes for electrodeposition of pure gold (cyanide based) [Reid and Goldie 1974].

Constituents	Bath Composition (g/l) & Operating Conditions					
	Bath 1	**Bath 2**	**Bath 3**	**Bath 4**	**Bath 5**	**Bath 6**
Au (as $KAu(CN)_2$)	8	4-30	4	8	2.7	16
Potassium phosphate			45	100		
Citric acid	40	40				55
Sodium citrate	40					135
Ammonium citrate		40	7.5			
Potassium pyrophosphate					10	
Superphosphoric acid (42% pyrophosphoric)					10	
Arsenious oxide					0.2	
Thallium (as sulphate)				0.0025		
Hydrazine sulphate						6
pH	3-6	2.3-6.6	2.0	3-6	5.5-6.0	4.2
Temperature (°C)	Room	30-60		20-90	50-65	70
Current density (mA/cm^2)	5-10	1-8	10-20	1-10	5-10	10

Free cyanide ions (generated when gold deposits) attack the interface between the resist film and substrate and lift the resist. Therefore, extraneous gold can be deposited under the resist. Thus, non-cyanide baths are desired for electronic applications [Sun and Ivey 1999]. The need for non-cyanide baths is also due to the toxicity of cyanide systems [Reid and Goldie 1974].

Non-cyanide acidic gold complex ions are mainly sulfite, thiosulfate, halide or thiorea based [Zhang 2001]. The sulfite electrolytes used in five patents are summarized by Foulke and shown in Table 2-4 [Reid and Goldie 1974].

Table 2-4: Sodium Gold sulfite electrolyte [Reid and Goldie 1974].

Constituents	**Bath Composition (g/l) & Operating Conditions**				
	Bath 1	**Bath 2**	**Bath 3**	**Bath 4**	**Bath 5**
Au (as Sulphite complex)	3-4	10	10	6-8	1-8
Sodium EDTA	18	30	20		
Copper EDTA	.075		2.5		
Cu (as diethylene-triamine penta acetate)				0.5-3	
Diethylenetriamine penta Acetate				40-60	
Ethylenediamine (25%) (ml/l)			2.5*		40-120
As (as AsO_3)		0.004			
Sodium sulfite	NR	90	25	NR	NR
Temperature (°C)	40-60	50	60	40-50	40-50
pH	9-10	10	6.5	9.5-10	alkaline
Current density (mA/cm^2)	1.1-3.2	8.6	2.2	1.1-2.5	0.4-1.1

*Amine not characterized.
NR = Not revealed.

2.3.2.2. Tin Electrodeposition

Fluoboric acid, sulfuric acid, phenolsulfonic acid (PSA), hydrochloric/hydrofluoric acid, and methane sulfonic acid (MSA) are the most commonly encountered acidic electroplating chemicals used for plating pure tin [Schlesinger and Paunovic 2000].

Typical baths used for these chemicals are shown in Table 2-5 to Table 2-9 [Schlesinger and Paunovic 2000].

Fluoborate chemistry has the advantages of the ability to operate at high current densities, a high throwing power, and high current efficiencies. However, the high cost of waste treatment and the high corrosivity makes its use undesirable [Schlesinger and Paunovic 2000]. Typical bath composition and operating parameters of fluoborate chemistry are shown in Table 2-5 [Schlesinger and Paunovic 2000].

The sulfate/sulfuric acid electrolyte has high current efficiencies, but it has the disadvantages of anode passivation at high current densities and corrosivity of the plating equipment by the solution. It should be noted that its use is restricted to pure tin plating because of very limited solubility of $PbSO_4$ [Schlesinger and Paunovic 2000]. Typical bath composition and operating parameters of sulfate/sulfuric acid based electroplating chemistry are shown in Table 2-6 [Schlesinger and Paunovic 2000].

Table 2-5: Typical bath composition and operating parameters of fluoborate chemistry [Schlesinger and Paunovic 2000].

Parameters	Rack and Barrel	Reel to Reel
$Sn(BF_4)_2$ (g/l)	75-113	225-300
Sn (g/l)	30-45	45-60
HBF_4 (g/l)	188-263	225-300
H_3BO_3 (g/l)	22.5-37.5	22.5-37.5
Anode current density (mA/cm^2)	21.5-26.9	Do not exceed 27
Cathode current density (mA/cm^2)	1-86.1	Up to 323
Temperature (°C)	30-55	30-55
Typical additives	Pepton, β-naphthol, hydroquinone	
Anode	Pure tin, bagged with dynel or polypropylene	
Agitation	Mild, mechanical	
Filtration	Constant filtration using a nonsilicated filter aid is desirable, although not necessary; such treatment keeps the solution clean and affords agitation	

Table 2-6: Typical bath composition and operating parameters for a sulfate/sulfuric acid based electroplating chemistry [Schlesinger and Paunovic 2000].

Parameters	Range
$SnSO_4$ (g/l)	15-45
Sn (g/l)	7.5-22.5
Sulfuric acid (g/l)	135-210
Additives	Alkylphenol, imidazoline, heterocyclic aldehydes
Anodes	Pure tin
Anode current density (mA/cm^2)	27 max
Cathode current density (mA/cm^2)	1-27
Temperature	Room
Agitation	Mechanical, cathode rod

Phenolsulfonic acid (PSA) and halogen based electroplating electrolytes are mostly used to plate pure tin in the continuous steel strip plating industry. Typical bath compositions and operating parameters of these baths are shown in Table 2-7 and Table 2-8 respectively [Schlesinger and Paunovic 2000].

Both phenolsulfonic acid and halogen based electroplating baths have the ability to operate at very high current densities. However, slug formation and its waste treatment are major problems in the halogen system. The PSA system is very acidic and runs at a pH less than 1, while the halogen process runs at a pH around 3- 4 [Schlesinger and Paunovic 2000].

Table 2-7: Typical bath composition and operating parameters of phenolsulfonic acid based electroplating chemistry [Schlesinger and Paunovic 2000].

Parameters	Range
Sn (g/l)	20-35
Phenolsulfonic acid (g/l)	40-80
Additives	Ethoylated β-naphtholsulphonic acid
Antioxidant	Phenolsulfonic acid
Current density (mA/cm^2)	215-538
Temperature	30-40

Table 2-8: Typical bath composition and operating parameters of a halogen chemistry [Schlesinger and Paunovic 2000].

Parameters	Concentration or Condition
NaF (g/l)	30
$NaHF_2$ (g/l)	31
SnF_2 (g/l)	19
$SnCl_2.5H_2O$ (g/l)	22
$Na_4Fe(CN)_6.10H_2O$ (g/l)	2-4 (precipitates ferric ions)
Additives	Naphtholsulphonic acid and polyalkylene oxides
Antioxidant	$p\text{-}NH_2C_6H_4NHCOMe$
pH	3-4
Current density (mA/cm^2)	215-538
Temperature (°C)	55-65

Methane sulfonic acid (MSA) electrolyte is less corrosive and less costly than fluoborate and sulfate baths, and the anodic oxidation of tin (Sn(II) → Sn(IV)) is less of a problem. It is also less costly than PSA and halogen electrolytes for waste management and disposal. The conductivity of MSA is higher than PSA, which allows the usage of lower tin concentration. Most importantly, it is environmentally friendlier than the other baths [Schlesinger and Paunovic 2000]. Typical bath composition and operating parameters of a satin bright MSA based electroplating chemistry are shown in Table 2-9 [Schlesinger and Paunovic 2000]. In this table, PWB refers to printed wiring boards. In addition, reel to reel plating refers to unwinding the un-plated material from a feed coil and conveying through a series of processing stations and recoiling on a take-up reel [Graves 2005]. Finally, wire refers to plating of wires.

Table 2-9: Typical bath composition and operating parameters of a satin bright MSA based electroplating chemistry [Schlesinger and Paunovic 2000].

Parameters	PWB	Reel to Reel	Wire
Sn (g/l)	15-25	30-50	50-70
MSA (ml/l)	225-275	175-225	175-225
Surfactant (ml/l)	20-30	30-45	30-45
Grain refiner (ml/l)	10-20	20-30	20-30
Antioxidants (g/l)			0.75
Current density (mA/cm^2)	<107	27-270	54-753
Temperature (°C)	30-60	30-60	30-60

2.3.3. Co-deposition of Gold-Tin Alloy from a Single Solution

Gold-tin alloying co-electrodeposition baths can be designed using the baths for pure gold plating with that of pure tin plating. The system parameters can be adjusted to stabilize the new co-deposition system. Acidic and alkaline solutions have been developed both for gold alloy deposition and tin alloy deposition. The focus will be on acidic solutions in this section.

Typical formulations for cyanide based electrolytes for electroplating gold alloys are summarized by Foulke and are shown in Table 2-10 [Reid and Goldie 1974]. It should be noted that in these systems alloying refers to deposits produced from solutions to which base metals are deliberately added to improve the brightness and physical properties of the deposits. The amount of alloying element is small [Reid and Goldie 1974].

Table 2-10: Acidic electrolytes for electrodeposition of alloy gold (cyanide based) [Reid and Goldie 1974].

Constituents	Bath Composition (g/l) & Operating Conditions		
	Bath 1	Bath 2	Bath 3
Au (as $KAu(CN)_2$)	8	4	12
Citric acid	40	120	105
Sodium citrate	40		
Tetraethylene pentamine		20	
Phosphoric acid			12.6 ml
In (as $In_2(SO_4)_3$)	5		
Ni (as $Ni_3C_6H_5O_7$)		2.5	
Co (as CoK_2EDTA)			1
pH	3-5	4	3-4.5
Temperature (°C)	>Room	40	35
Current density (mA/cm^2)	5.4-21.5	21.5	5.4

One of the major challenges with electrodeposition of gold-tin alloys is the instability of the aqueous electroplating bath. One cause of instability is oxidation of the stannous ions to stannic ions when stannous ions provide the source of tin in the plating bath. This oxidation is either by atmospheric oxygen or anode oxidation [Schlesinger and Paunovic 2000]. Another challenge with electrodeposition of gold-tin alloys is maintaining the potential of the gold and tin compounds sufficiently close to allow for the co-deposition of both metals with the desired ratios.

A recent patent by Morrissey includes the invention of an electroplating solution for gold-tin alloys that is capable of operating over a wide and useful range of current densities [Morrissey 2005]. In this bath, gold and tin are contained in the form of soluble cyanide and stannous ion complexes respectively. Citric acid and 2,2'-dipyridyl are used as the complexing agent for stannous ions and the additive for alloy plating respectively. The gold-tin deposits obtained from this bath generally contain between 60 and 95 wt% gold. This plating solution, which is compatible with photoresists used to define circuit patterns, operates in the pH range of 3.5 to 4.

[Stevens, Deuber et al. 1977] describes a stable bath using a trivalent gold (auricyanide) complex and tin as a stannic halide complex. This acidic solution, with a pH less than 3, is claimed to be capable of depositing an 80-20 wt% gold-tin alloy. Phosphonics and EDTA analogs (i.e., Quadrol) are also included in this bath as complexing agents. Brightness of the deposit is enhanced by including 0.01 g/l of a surfactant such as alkylaryl polyethylene glycol, polyethylene oxide, isopropyl lanolate, alkylphenol polyglycol ether, ethoxylated fatty alcohol ether, ethoxylated fatty alcohol ether, octylphenoxy polyethoxy ethanol, octylphenoxy polyethoxy ethanol, and ethylene oxide ester condensate. Further brighteners that can be added to this bath include saccharin, butynediol, chloral hydrate, chloraniline, o-ethyl toluidine, aldol, and ascorbic acid.

Another example of acidic cyanide-based gold-tin systems is quoted by [Zhang 2001] from a German article by Kuhn. The bath composition and plating conditions of this system are shown in Table 2-11.

Table 2-11: Composition and plating conditions of an acidic cyanide gold-tin system [Zhang 2001].

Parameters	Concentration or Condition
Au (as $Au(CN)_2^-$) (g/l)	20
$SnCl_4.5H_2O$ (g/l)	30
KOH (g/l)	10
Potassium D-gluconate (g/l)	6
Citric acid (g/l)	10
Potassium citrate (g/l)	50
Piperazine (g/l)	4
As_2O_3 (g/l)	0.02
Anode	Platinized titanium
pH	4
Current density (mA/cm^2)	20
Temperature (°C)	45

Development of non-cyanide electrolytes for gold-tin alloy electrodeposition has been challenging. The challenge lies in obtaining a stable solution due to the lack of the strongest gold complexing agent (cyanide) in these solutions. Furthermore, new base metal complexes that ensure good compositional control of the alloy are needed [Sun 1998].

Chloride, sulfite, thiomalate complexes, thiocyanate, and thiosulphate baths have been developed for electroplating gold alloys.

[Uchida and Okada 2002] describe a non-cyanide bath that can include any water-soluble gold compound including any or combinations of potassium chloroaurate, sodium chloroaurate, ammonium chloroaurate, gold potassium sulfite, gold sodium sulfite, gold ammonium sulfite, gold potassium thiosulfate, gold sodium thiosulfate, and gold ammonium thiosulfate. Complexing agents for gold in this bath include any or combinations of sulfurous acid, sulfites (e.g., potassium sulfite, sodium sulfite, ammonium sulfite and alkaline earth metal sulfites), thiosulfuric acid, thiosulfates (e.g., potassium thiosulfate, sodium thiosulfate, ammonium thiosulfate and alkaline earth metal thiosulfates), pyrophosphoric acid, and pyrophosphates (e.g., potassium pyrophosphate, sodium pyrophosphate, ammonium pyrophosphate, and alkaline earth metal pyrophosphates). Water-soluble tin compounds contained in this bath include any or combinations of stannic and stannous salts of sulfonic acids, sulfosuccinates, chlorides, sulfates, oxides, and oxalates. A combination of tin compounds is preferred, since it improves the stability of the bath and the brightness and reflow properties of the deposit. Further, this bath includes 0.05 to 1 mole/l of tin complexing agent to stabilize the stannous ions. Specific examples of tin complexing agents include ethylenediamine, ethylenediamine tetraacetic acid (EDTA), diethylenetriamine pentaacetic acid (DTPA), nitrilotriacetic acid (NTA), iminodiacetic acid (IDA), iminodipropionic acid (IDP), hydroxyethylethylenediamine triacetic acid (HEDTA), triethylenetetramine hexaacetic acid (TTHA), ethylenedioxybis(ethylamine)-N,N,N',N'-tetraacetic acid, succinic acid, citric acid, tartaric acid, glycolic acid, glycine, mercaptosuccinic acid, gluconic acid, glucoheptonic acid, gluconolactone, glucoheptonolactone, and nitrilotrimethylphosphonic acid. Moreover, to prevent oxidation of Sn in the plating bath, an oxidation inhibitor (e.g., ascorbic acid, hydroquinone, catechol, resorcin, and phenolsulfonic acid) may be added. The deposit is brightened by a cationic macromolecular surfactant. Oxalate is listed among the possible buffer compounds.

Electrodeposition of a bright gold-tin alloy containing 15 to 40 wt% tin from a thiomalate complex bath is reported by [Sel Rex Corp. 1971]. The aqueous solution of this invention contains a soluble alkali metal gold thiomalate and a stannous compound or stannous ions. It also includes a weak organic acid such as thiomalic acid, citric acid or gluconic acid. However, this bath operates in the pH range of 10 to 12, and is not of interest here due to its incompatibility with the mask layer in electronic applications.

[Morrissey 1994] describes a non-cyanide bath that includes gold in the form of a soluble sulfite complex, a supporting electrolyte for conductivity and pH control (e.g., phosphoric, citric, succinic, or lactic acids), an organic polyamine (or mixture of polyamines of molecular weight from about 60 to 50,000), and an aromatic organic nitro compound (e.g., nitrobenzene and analogous). Suitable organic polyamines used in this bath include ethylenediamine, 1,2- and 1,3-propanediamines, 1,4-butanediamine, cis-1,2 diaminocyclohexane, trans-1,2 diaminocyclohexane, trans-1,4 diaminocyclohexane, diethylenetriamine, triethylenetetramine, and tetraethylenepentamine. Polyamines of higher molecular weight are reported to be more effective as stabilizing agents. This bath is claimed to be chemically stable indefinitely and operates under acidic pH conditions ($pH < 6$). Furthermore, this plating system can operate under relatively high current densities (more than 30 mA/cm^2). Specific examples of such baths are given by [Morrissey 1994].

2.3.4. Electroless Plating of Gold-Tin

Electroless plating baths for deposition of gold-tin alloys have been developed and are cyanide based. Table 4-10 below shows the components and conditions of one such bath [Okinaka 1990]. "This system employs stannous chloride as a reducing agent, and the deposition of tin proceeds via a disproportionation reaction of divalent tin from SnO and Sn (IV)" [Okinaka 1990]. At room temperature, a plating rate of 5 µm/hr is reached. The tin content of the deposit is reported to be variable between 5 and 60 percent.

Table 2-12: The bath composition and plating conditions of electroless gold-tin plating [Okinaka 1990].

Parameters	Concentration or Condition
Au (as $KAu(CN)_2$) (g/l)	4-10
KCN (g/l)	5-15
KOH (g/l)	60-100
$SnCl_2$ (g/l)	40-60
Toluene (g/l)	0.05-0.5
Temperature	Room
Plating rate, µm/hr	
with no toluene	1.8
with 0.5 g/l toluene	5.0

2.4. Ivey Group's Method of Electroplating Gold-Tin

A co-electroplating process for depositing gold-tin alloys, from a slightly acidic, chloride based solution using pulsed currents, onto unpatterned and patterned ceramic and semiconductor substrates has been developed recently by Ivey and his group [Sun 1998;

Sun and Ivey 1998; Sun and Ivey 1999; Ivey and Sun 2001]. Multiple current pulses and varying pulse cycles are used to deposit a composite solder structure (Figure 2-11 and Figure 2-12). The multilayer deposition of the two stoichiometric phases, AuSn and Au_5Sn, alternatively (see phase diagram in Figure 2-2) creates a film that acts like an eutectic composition [Ivey, Djurfors et al. 2003]. The plating of the two mentioned phases and their thicknesses can be accomplished by adjusting the pulse amplitude and duration respectively [Djurfors and Ivey 2002].

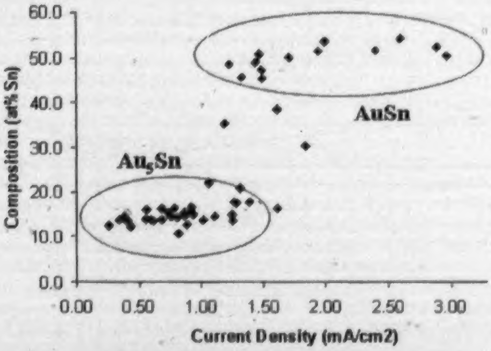

Figure 2-11: Deposit composition vs. current density [Djurfors and Ivey 2001].

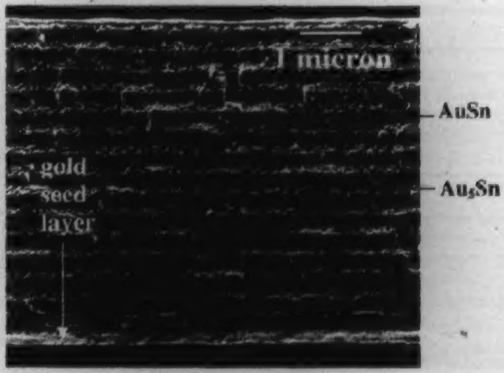

Figure 2-12: Scanning electron microscope (SEM) image of multilayer deposition of the two stoichiometric phases, AuSn and Au_5Sn [Djurfors and Ivey 2002].

Pulse current and direct current plating tests have been performed by [Sun and Ivey 2001], in which current density and duty cycle were varied to optimize the process. Pulse and direct currents were compared in the average current density range of 1.6 to 3.6

mA/cm^2. Application of pulse current resulted in higher tin content in the deposits. The microstructures at current densities lower than 2.4 mA/cm^2 were similar. However, pulse current resulted in finer and smoother deposits at higher current densities. When the average current density and cycle period of pulse current were kept constant at 2.4 mA/cm^2 and 10 ms respectively, the finest and smoothest microstructure was obtained when the duty cycle was at 20 percent [Sun and Ivey 2001].

Characterization of the microstructure of the electroplated eutectic Au-Sn phases by Djurfors, showed the formation of the AuSn phase is a growth-controlled process while that of the Au_5Sn phase is a nucleation controlled process [Djurfors and Ivey 2002]. These film growth mechanisms are typical of high and low current densities deposition mechanisms respectively. Formation of the AuSn phase begins with two-dimensional nucleation creating a layer of equiaxed grains, which later transform into a columnar structure due to the effect of preferred growth. A fine grain size is observed as a consequence of the relatively high deposition current density and consequent nucleation rate. Au_5Sn forms via a lateral growth mechanism, which results in a topographically smooth deposit. Unlike AuSn, the Au_5Sn grain size is significantly larger because of the lower current density used for deposition [Djurfors and Ivey 2002].

The effect of the concentration of ammonium citrate on deposit composition, deposit microstructure, and plating rate was studied by [Zhang and Ivey 2004]. A decrease in the concentration of ammonium citrate resulted in a shift of the AuSn and Au_5Sn plateaus to lower current densities. Moreover, smoother and denser deposits were obtained from a solution containing a lower ammonium citrate concentration. Zhang also increased the gold concentration in the solution. This increase resulted in a shift of the AuSn and Au_5Sn plateaus to higher current densities such that the AuSn phase was not obtainable separately [Zhang and Ivey 2004].

2.4.1. Bath Solution

The solution consists of chloride salts to provide gold and tin for plating. Originally, sodium sulfite was added as a complexing agent. Ammonium citrate is believed to function as the solution buffer, and L-ascorbic acid is added to prevent tin hydrolysis. All constituents are mixed at room temperature in de-ionized water [He, Djurfors et al. 2002]. These constituents and their functions are summarized in Table 2-13, after [Doesburg 2000].

Table 2-13: Gold-tin plating bath constituents used by Ivey's group [Doesburg 2000].

Chemical	Function	Concentration (g/l)
$KAuCl_4$	Au^{3+}	5
$SnCl_2.2H_2O$	Sn^{2+}	5
ammonium citrate	Buffer	200
sodium sulfite	Complexing agent	60
L-ascorbic acid	Prevents tin hydrolysis	15

2.4.2. Problems with Electroplating

The group's method has been relatively successful. However, improvements need to be made to the plating process in terms of bath stability and plating speed.

It has been challenging to obtain a stable solution, since cyanide is the strongest gold complexing agent and its usage is not desired here. It should be noted that the bath appears stable for about 15 days with no apparent change in the appearance of the solution [Doesburg and Ivey 2001]. After this time, black or yellow particles begin to precipitate settling to the container bottom or attaching to the container sides [Akhlaghi and Ivey 2003]. However, if the lifetime is defined based on useful plating time, the lifetime of the solution is much shorter, i.e., about 2 to 3 days. As the bath ages, the deposit composition becomes Au-rich and the morphology deteriorates. Therefore, the composition of the film is not consistent when depositing thick films or multiple samples after a two day period. Due to precipitation of gold from the solution and therefore a decrease in the amount of available gold for plating, the deposit from an aged solution would be expected to be gold-deficient. Deposits obtained from aged solutions (more than 2-3 days) are gold-rich, however. According to the paper by [He, Liu et al. 2005], the suspended nanosized particles of gold in the solution may have been physically incorporated during plating to give an overall deposit containing more gold than the deposit from the fresh solution. This incorporation of the gold particles also explains the increased surface roughness exhibited by deposits obtained from aged solutions.

The plating rate is about 2.0 μm/hour (for the AuSn phase) and 0.83 μm/hour (for the Au_5Sn phase) at current densities of 2.4 and 0.8 mA/cm^2 respectively. These rates are relatively low for mass production in industry and need to be improved. Furthermore, with a marked increase in the plating rate the stability of the bath would be of less concern, since thicker films could be plated with uniform composition and morphology [Doesburg 2000].

2.5. Bath Additives and Stability

As mentioned before, one of the major challenges with electrodeposition of gold-tin alloys is the instability of the aqueous electroplating bath. One cause of instability may be oxidation of the stannous ion to stannic ions, either by atmospheric oxygen or anode oxidation. Also, precipitation occurs in baths containing complexes with low stability constants.

It should be realized that bath instability can be triggered by the introduction of certain impurities. Some baths are extremely sensitive to contamination with certain ions or metals. Also, decomposition of the baths may occur when they are contaminated with certain organics. Contamination with trace amounts of organic materials from storage bottles and vessels as well as from the water used to prepare the solutions may also cause instability. An example of such a system is the decomposition of borohydride and DMAB baths used for electroless deposition of gold. These baths are contaminated with certain organics such as polyethylene, and they are extremely sensitive to contamination with Ni^{2+}, Co^{2+} or Fe^{2+}. For instance, 10^{-3} M of Ni^{2+} causes instability [Schlesinger and Paunovic 2000].

In tin plating baths, both soluble and insoluble anodes can be used. Soluble anodes are more commonly used in acidic solutions. Since oxygen is generated at the insoluble anode, the pH may become unstable in acidic solutions. Therefore, the continuous monitoring of the acid concentration is recommended if an insoluble anode is used [Schlesinger and Paunovic 2000].

Several electroplating systems, combined with additives or techniques used to improve or maintain bath stability, are summarized in Table A-1 (see Appendix A). It is apparent from the literature that bath stability, plating rate, deposit morphology, and composition are interrelated, and addition of a secondary ingredient to the bath usually affects more than one of these. Also, in some systems the concentration of the secondary material could determine whether its existence is beneficial or harmful.

2.6. Improvements in Plating Rate

Increasing the agitation speed of the bath, raising the bath temperature, and increasing the reducing agent concentration are some of the ways that can be used to obtain a plating rate as large as possible by adjusting basic bath composition and operating conditions without resorting to special methods [Schlesinger and Paunovic 2000].

It is well known that the addition of a small amount of Pb^{2+} or Tl^{+} depolarizes the gold electrode in an electrolytic soft gold plating bath and acts as a catalyst for the reduction of the gold species [Schlesinger and Paunovic 2000]. In general, adding depolarizers to electrodeposition baths may improve the plating rate.

In electroless plating of gold, Okinaka emphasizes that these systems are sensitive to traces of organic contaminants that may be present in the water used to prepare the bath.

Specifically, to avoid suppression of plating due to impurities in water, water or distilled water should be treated with active charcoal [Okinaka 1990].

Plating rates could be improved by adding a stabilizer. A trace amount of organic compound is added to the solution while increasing the concentration of the reducing agent or raising the plating temperature. For example, a trace amount of compounds such as ethylene glycol monoethylether, diethyleneglycol, monoethylether, and polyethyleneimine served as effective stabilizers for increasing the plating rate of electroless gold plating from a borohydride bath [Schlesinger and Paunovic 2000].

In general, optimum current distribution can be obtained by proper fixturing, good anode-cathode spacing and anode shielding. As a result higher overall current densities and plating rates can be achieved [Reid and Goldie 1974].

Several electroplating systems combined with additives or techniques used to improve or maintain high plating rate are summarized in Table A-2 (see Appendix A).

2.7. Summary

In this chapter, the fundamental concepts behind this thesis work were covered.

Solders, their fabrication methods, and applications were introduced. The background to the electrodeposition process, with a focus on the variables in electrochemical cells and factors affecting electrode reaction rate and current, was explained. The basics of pulse plating were also discussed.

Further, this chapter focused on different techniques used for electroplating gold-tin solders including a literature review of previously developed plating baths for these techniques. The gold-tin electroplating method developed by Ivey's group was also discussed.

Finally, this chapter reviewed the literature on bath additives used to improve stability and methods used to improve electroplating rates.

The next chapter will cover the background on the statistical design of experiments (DOE) which is the approach used to meet the objective of this thesis.

Chapter 3: Statistical Design of Experiments

Unless otherwise stated, this chapter is a summary of work presented by [Diamond 1919; Mason, Gunst et al. 1989; Montgomery and Runger 1994; Box, Hunter et al. 2005; National Institute of Standards and Technology (NIST) and International Sematech 2005]

In any experiment, one or more process variables (or factors) are intentionally changed by the experimenter in order to observe the effect the changes have on one or more response variables.

Any process can be modeled in the form of a `black box', with several discrete or continuous input factors that can be controlled and varied intentionally with one or more measured output responses (Figure 3-1). The output responses are assumed to be continuous. Then, the obtained experimental data are used to derive a practical approximation model linking the outputs and inputs.

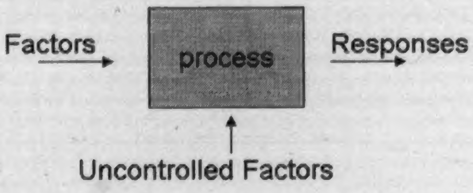

Figure 3-1: Black-Box Model.

3.1.1. Introduction to Experimental Design

In scientific research, experiments are performed to obtain an approximation model of a system. The object of using a statistical design of experiments (DOE) is to perform such experiments as efficiently as possible. These experiments are designed so that the data obtained can be analyzed to yield valid and objective conclusions.

In DOE the detailed experimental process is planned in advance of doing the experiment. If the design is well chosen, the amount of information and learning that can be obtained from the experimental effort are maximized.

DOE is a powerful tool that can be used in many situations and can be applied to a diverse range of applications. One common use of DOE is for decision making between two or more alternatives. It can also be used to select the key factors affecting a process. Such DOE designs are called screening experiments, in which a minimal number of experimental runs are used to determine the most important factors among a wide range of possible factors. The screening tests may be used as a first step when the ultimate goal is to model a response with a response surface, which itself may be obtained using DOE. Response surface method (RSM) experiments allow for estimation of interaction effects, while presenting an idea of the (local) shape of the response surface being investigated. The RSM is important for the following reasons:

- good graphical analysis is obtained through simple data patterns,
- the response function is obtained in the region of interest,
- the sensitivity of the response to the factors of interest becomes apparent,
- factor levels optimizing one or more response variables can be determined,
- when trying to optimize several response variables spontaneously, trade-offs are readily apparent, and
- factor levels can be determined if the response should hit a specific target, be maximized or minimized.

The RSM can also be used to reduce variation in the process, to make a process robust, or when seeking multiple goals.

Lastly, DOE can be used for regression modeling to estimate a precise model or quantifying the dependence of response variables on process inputs.

3.1.2. Design Selection

The experimental design can be chosen by considering the design objectives, the number of control factors and their levels.

The key objectives of the design should be considered and prioritization of the objectives helps in the selection of the factors, responses, and the particular design. Types of design objectives were discussed in the previous section and are summarized into four categories: comparative designs, screening designs, response surface modeling, and regression modeling.

After identifying the objective of the design, the experimental variables are selected including both factors and responses (inputs and outputs). All responses (outputs) relevant to the objective are determined. The responses corresponding to the combination of two or more measurements are broken down into the individual responses of the process and treated separately. For example, if one is interested in the ratio of two outputs, both are measured and not just the ratio. Engineering judgment and experiments are the basis for choosing all important factors (inputs) in the process. Then, the levels of each factor are determined based on the knowledge of the system or previous experiments. Choosing random extreme values may give runs that are not feasible or move one out of a smooth continuous range of the response surface.

Two-level designs are the most popular experimental designs, since they are the most simple and economical. As the standard layout, +1 and -1 notation are used in a matrix format to denote the "high" and the "low" levels respectively for each factor. The use of

±1 for the factor settings is called coding the data, which helps in the interpretation of the coefficients fit to any experimental model. For some designs center points are required and are coded to have the value “0”.

Once the design objectives, the number of control factors, and their levels are determined, a design can be chosen using the following design selection guideline. Choice of a design from these various types also depends on the amount of resources available. It is recommended to add center point runs to check for curvature and reproducibility.

Table 3-1: Design selection guidelines [National Institute of Standards and Technology (NIST) and International Sematech 2005].

Number of Factors	**Objective**		
	Comparative	**Screening**	**Response Surface**
1	1-factor completely randomized design		
2-4	Randomized block design	Full or fractional factorial	Central composite or Box-Behnken
5 or more	Randomized block design	Fractional factorial or Plackett-Burman	Screen first to reduce number of factors

The Box-Behnken design is explained in detail in the next section, since it is the design used in this thesis work.

3.1.2.1. Box- Behnken Design

The Box-Behnken design is used for fitting quadratic models. It is an independent quadratic design and does not contain an embedded factorial or fractional factorial design. It is used when it is necessary or preferred that factors should be run at only three levels.

In the Box-Behnken design the experimental points are specifically chosen to allow the efficient estimation of the coefficients of a second order model. These experimental points are at the midpoints of edges of the process space and at the center. These designs are rotatable[1] (or near rotatable) and have limited capability for orthogonal blocking compared to the central composite designs. Figure 3-2 illustrates different representations of the Box-Behnken design for three factors.

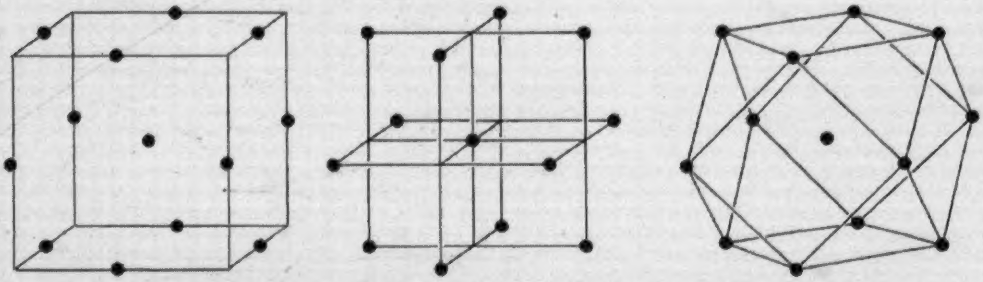

Figure 3-2: Box-Behnken design illustrations for 3 factors [Box, Hunter et al. 2005; National Institute of Standards and Technology (NIST) and International Sematech 2005].

The geometry of the Box-Behnken design implies a sphere within the process space. The surface of the sphere extends beyond each face of the cube while the surface of the sphere is tangential to the midpoint of each edge of the space box.

The matrix representation of the Box-Behnken design for three factors is

$$\begin{bmatrix} \pm 1 & \pm 1 & 0 \\ \pm 1 & 0 & \pm 1 \\ 0 & \pm 1 & \pm 1 \\ 0 & 0 & 0 \end{bmatrix}.$$

---

[1] Rotatable: If the variance of the predicted response at any point x depends only on the distance of x from the design center point, then the design is rotatable. A design with this property can be rotated around its center point without changing the prediction variance at a point x.

This matrix notation indicates the factor settings shown in Table 3-2. The center point (0,0,0) is repeated to provide a measure of process stability, inherent variability and to check for curvature.

Table 3-2: Factor settings for Box-Behnken design [National Institute of Standards and Technology (NIST) and International Sematech 2005].

Box-Behnken			
Repeats	**Factor 1**	**Factor 2**	**Factor 3**
1	-1	-1	0
1	+1	-1	0
1	-1	+1	0
1	+1	+1	0
1	-1	0	-1
1	+1	0	-1
1	-1	0	+1
1	+1	0	+1
1	0	-1	-1
1	0	+1	-1
1	0	-1	+1
1	0	+1	+1
3	0	0	0
Total Runs = 15			

The Box-Behnken designs require fewer experimental runs than a central composite design in cases involving 3 or 4 factors. However, it should be kept in mind that these designs contain regions of poor prediction quality due to the "missing corners" of the design space. In other words there is poor prediction at points that combine the extreme levels of factors.

3.1.3. Data Analysis

In a DOE analysis, first the data should be examined for outliers, typos, and obvious problems. Then, by using software or graphical tools several plots are constructed to analyze the data and find answers to the objective questions. It is important that the data is examined using a wide array of plots or visual displays which can reveal any irregularity, incongruity, or provide insights that most quantitative techniques are not capable of discovering. Examples of such plots are mean plots, interaction plots, normal or half-normal probability plots for effects, and Youden plots[1].

Sometimes the obtained graphs and data plots lead to obvious answers to the objective questions. However, in most cases the analysis is followed by fitting and validating a model that can be used to answer the objective questions. Examples of the plots used for testing and validating models are contour plots, response vs. prediction plots, residuals vs. prediction plots, residuals vs. independent variables plots, residual histograms, and normal probability plots of residuals.

An iterative approach can be taken in DOE, in which each stage provides insight for the next stage. Learning is done through each DOE stage. Also, once the data is analysed and an optimum combination of factors is obtained, the real response from the optimum combination can be tested and put back in the design to improve the model.

3.1.3.1. Response Surface Modeling

Response surface initial models include quadratic terms and may occasionally also include cubic terms. The full equation including all possible terms for a quadratic model is:

$$\begin{aligned}\hat{y} = b_0 + b_1x_1 + b_2x_2 + b_3x_3 + b_{12}x_1x_2 + b_{13}x_1x_3 + \\ b_{23}x_2x_3 + b_{11}x_1^2 + b_{22}x_2^2 + b_{33}x_3^2\end{aligned} \qquad \textbf{(Equation 3-1)}$$

---

[1] Youden plot: a graphical technique used for interlab comparison of results. It checks for reproducibility and repeatability.

The full equation including all possible terms for a cubic model is:

$$\begin{aligned}\hat{y} &= quadratic + b_{123}x_1x_2x_3 + b_{112}x_1^2x_2 + b_{113}x_1^2x_3 + \\ &b_{122}x_1x_2^2 + b_{133}x_1x_3^2 + b_{223}x_2^2x_3 + b_{233}x_2x_3^2 + b_{111}x_1^3 + \\ &b_{222}x_2^3 + b_{333}x_3^3\end{aligned} \qquad \textbf{(Equation 3-2)}$$

However, rarely are all the terms needed in an application.

3.1.3.2. Multiple Response Regression Tables

Once all the experimental data for all the responses are gathered, the multiple response regression table can be obtained. This table contains the coefficients of the RSM model obtained for each response. The closeness of fit of the models are shown using R^2 values. Furthermore, this table also contains a prediction region, in which a combination of factor values can be entered to obtain predicted responses.

3.1.3.3. Surface and Contour Plots

Regression tables of each experimental design are used to graph surface and contour plots. Surface plots graphically present the predicted model in three dimensions, where the x, y and z axes present the two independent variables and the response respectively. Contour plots are another way of representing a 3-dimensional surface. In a contour plot iso-response lines are graphed while two independent variables are displayed on the x and y axes. Contour plots used to graph the general quadratic model can be divided into four main types as shown in Figure 3-3.

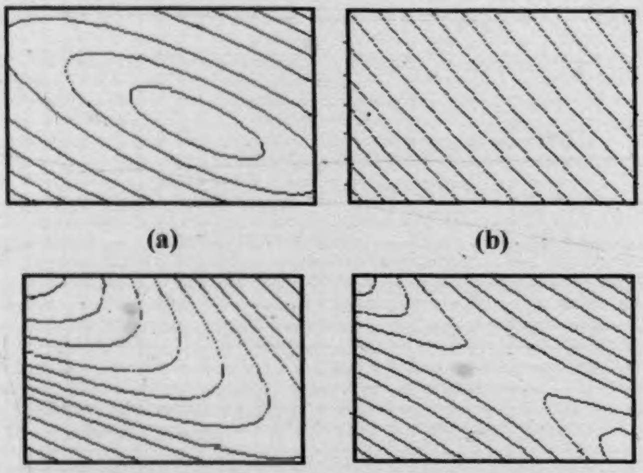

(a) (b)

(c) (d)

Figure 3-3: Contour plots: (a) peak, (b) hillside, (c) rising ridge, (d) saddle [National Institute of Standards and Technology (NIST) and International Sematech 2005].

3.1.3.4. Interaction Plots

Interaction plots, as the name implies, are used to determine the existence of interaction between factors. Interaction exists when the effect of each factor depends on the levels of the other factors. If interactions occur, the factors involved cannot be evaluated individually.

Consider the designs with two factors and one response. Design 1 has factor 1 and factor 2, and design 2 has factor 2 and factor 3. An interaction plot displays the response value and the levels of one of the factors on the y and x axis respectively. Separate lines are graphed for each level of the other factor. Examples of interaction plots are shown in Figure 3-4.

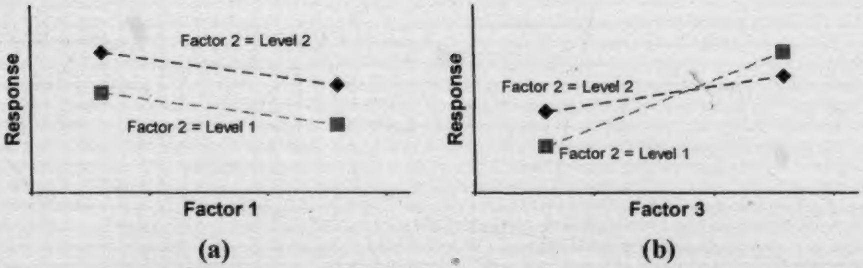

Figure 3-4: Interaction plots: (a) no interaction, (b) two-factor interaction.

The effect of factor 1 on the response is the same for all levels of factor 2 if the lines, corresponding to different levels of factor 2 are parallel. Therefore, the factors do not interact if the lines in the corresponding interaction plot are parallel. The interaction plot in Figure 3-4 (a) suggests that there is no two-factor interaction between factor 1 and factor 2. However, the interaction plot in Figure 3-4 (b) suggests that two-factor interaction exists between factor 2 and 3. In this example, to obtain a higher response value both factor 2 and factor 3 levels should be considered. For the higher response value, if the system is operated at the lower (or higher) level of factor 3, then factor 2 should be operated in level 2 (or level 1) respectively. In general, interactions are indicated by any nonparallel changes in the response. Moreover, experimental variations should be considered, and the lack of parallelism in the changes of the response must be sufficiently large to represent a real factor interaction effect.

Mathematically, if the model equation for a two level design can be expressed as

$$f(x_1, x_2) = f_1(x_1) + f_2(x_2), \qquad \textbf{(Equation 3-3)}$$

then there is no interaction between X_1 and X_2. This implies that a change in the response due to a change in X_1 (or X_2) does not depend on the level of X_2 (or X_1). Whenever Equation 3-3 does not hold, interaction between the two factors exists. In that case a change in the response due to a change in x_1 (or X_2) does depend on the level of X_2 (or X_1).

The interaction plots for designs of more than two factors display the average of the response values on the y-axis. In these designs, the interaction plots are done for all the pair combinations of the factors separately. Considering an example with three factors and one response, if the plots for both factor 1-factor 2 and factor 2-factor 3 indicate interaction, then there is a three-factor interaction among the three design factors as shown in Figure 3-5.

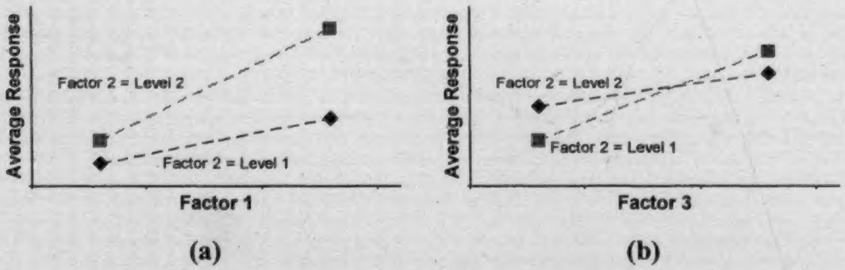

Figure 3-5: Three-factor interaction: (a) factor 1 & factor 2 interaction, (b) factor 1 & factor 3 interaction.

The presence of interactions requires that factors be evaluated jointly rather than individually.

3.1.3.5. Process Optimization

At times when the primary DOE goal is to find the optimum operating conditions, it is desired to maximize or minimize the system responses. A sequence of experiments is conducted, and the obtained empirical models are used to find the optimal region to run the process. In these experiments, the objective is to find the factor levels $X_1, X_2, ..., X_k$ that maximize or minimize the system response variables $Y_1, Y_2, ..., Y_r$.

Different optimization techniques can be applied to the fitted response equations. The obtained optimal operating conditions are good approximations of the real system, if the fitted equations are an adequate approximation of true system responses. One technique for optimization is to find approximate models and iteratively search for optimal operating conditions. If the experimental design is done in blocks (sets), the results from one block of experiments indicate where to search for improved operating conditions in the next set of experiments. Thus, the coefficients in the fitted equations may change during the optimization process.

Simultaneously optimizing for multiple responses is very difficult and often impossible. Therefore, the process engineer must make some trade-offs in order to find process operating conditions that are satisfactory for most of the responses.

3.2. Summary

In this chapter, the fundamental concepts of statistical design of experiments (DOE) were covered.

DOE was introduced, followed by the design selection method. Further, data analysis techniques including response surface modeling, multiple response regression tables, process optimization, and different plotting techniques were discussed.

The next chapter will cover the long term stability study of the standard electroplating bath developed by Ivey's group. This study gives a better understanding of the solution aging behaviour before proceeding with improvements.

Chapter 4: Long Term Stability Study

4.1. Overview of the Study

The long term stability of the standard electroplating bath developed by Ivey's group is studied in this chapter. This study was performed to obtain a better understanding of the solution aging behaviour before proceeding with improvements.

The composition of the plated deposits from the bath should be monitored over time to study the long term stability behaviour of the standard electroplating bath developed by Ivey's group (referred to as the standard solution from here on). Also, the gold precipitation behaviour and change in concentration of constituents in the bath should be studied over time. For these purposes, films were electroplated from fresh and aged standard solution, and the compositions of the deposited films were monitored using energy dispersive X-ray spectroscopy (EDS) within a scanning electron microscope (SEM). Further, a turbidity curve was obtained, which gives information about the relative amount of precipitates in the solution overtime. Atomic absorption spectroscopy was performed to monitor the concentration of gold and tin within the bath over time. These techniques are described in the following sections.

4.1.1. Scanning Electron Microscopy

This section provides a very brief introduction to SEM as the amount of information to cover is beyond the scope of this thesis. Complete information on scanning electron microscopy techniques and concepts can be found in [Goldstein, Newbury et al. 2003] and [Goodhew, Humphreys et al. 2001].

SEM is primarily used to study the surface topography and composition of specimens. SEM employs a finely focused beam of electrons (e.g., 20 keV) swept in a raster across the surface of the specimen. An electron gun, condenser and objective lenses, a vacuum system, scan generators, and detectors are some of the features of this microscope (Figure 4-1).

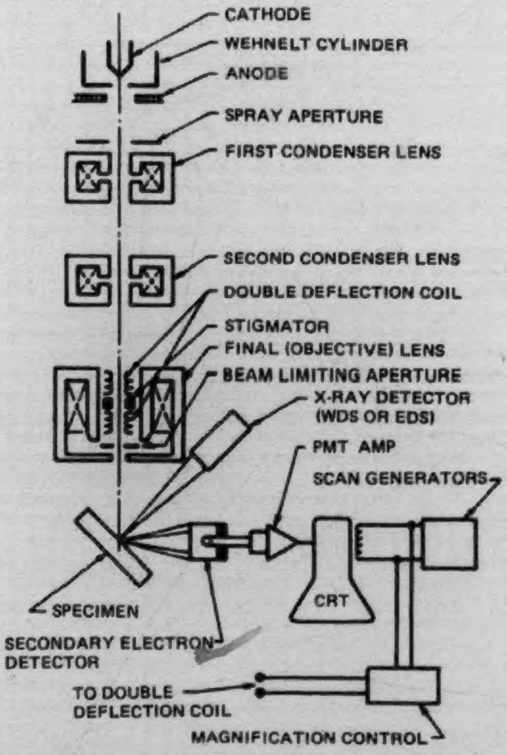
CATHODE
WEHNELT CYLINDER
ANODE
SPRAY APERTURE
FIRST CONDENSER LENS
SECOND CONDENSER LENS
DOUBLE DEFLECTION COIL
STIGMATOR
FINAL (OBJECTIVE) LENS
BEAM LIMITING APERTURE
X-RAY DETECTOR (WDS OR EDS)
PMT AMP
SCAN GENERATORS
CRT
SPECIMEN
SECONDARY ELECTRON DETECTOR
TO DOUBLE DEFLECTION COIL
MAGNIFICATION CONTROL

Figure 4-1: Schematic drawing of the electron and X-ray optics of a combined SEM-EPMA[1] [Goldstein, Newbury et al. 2003].

---

[1] EPMA: electron probe microanalyzer used to obtain localized chemical analysis of solid samples [Goldstein J. et al. 2003].

A thick specimen dissipates the energy of the incident electrons and results in various secondary emissions from the specimen. The signals of greatest interest in SEM are the secondary electrons, backscattered electrons, and the emitted X-rays. These signals are explained very briefly below.

Secondary electrons (SE) are ejected from orbitals in atoms and have low energy causing them to move only few atomic spacings before escaping the specimen. A small attractive voltage of +200 volts (positive bias) is used on the detector to attract the SE. The signal from the detector is then amplified to make signals for the gun in cathode ray tube (CRT). Since SE come from a small region of the sample, images with good resolution can be obtained from the sample.

Backscattered electrons (BSE) have much higher energy, since they occur when the incident beam interacts with the nucleus of the atoms on the sample. Therefore, the probability of their occurrence is lower than secondary electrons. Having higher energies than SE, a small bias voltage does not affect the BSE. To collect them, the detector is placed close to sample and it only detects the BSE that happen to hit the detector (line of sight). A repulsive voltage (-50 V) can be used to repel the SE electrons from the detector, if it is only desired to collect the BSE.

During the inelastic scattering of the electron beam, Bremsstrahlung and characteristic X-rays can be formed. A characteristic X-ray can occur when an outer-shell electron jumps in to fill an inner-shell vacancy. Energy dispersive spectroscopy (EDS) is the method used in this project to analyze the X-rays. The diameters of the effective signal producing area are 0.4 and 1.5 μm for gold and tin respectively. The calculation of these values was done assuming a beam spot size of 50 nm in diameter, incident beam energy of 20 keV, and bulk densities.

In the EDS technique, the detector consists of a semiconductor that is held in such a position that as many as possible of the X-rays emitted fall upon it. The number of electron hole pairs excited in the semiconductor by the X-rays is proportional to the energy of the X-ray photon being detected. The signal from the semiconductor is then amplified using a field emitting transistor (FET). A multi-channel analyzer is used to count the amount of X-rays detected in each energy range.

BSE imaging provides better contrast from different phases of different atomic numbers since they have different mass nuclei. Heavier elements produce many more BSE. Furthermore, SE imaging has better imaging resolution than BSE imaging since they come from a smaller region of the sample. For more accurate analysis of images, both SE and BSE images can be obtained and compared. Furthermore, X-ray analysis of the regions of different contrast can be done to gain a better understanding of whether the contrast is a result of composition or topography when needed. It should be noted that mostly SE imaging and EDS was used in this study.

4.1.2. Turbidity

Turbidity (τ) is the optical measurement of scattering of visible light dealing with the electromagnetic radiation with wavelengths between 380 and 780 nm. Ideally, a focused beam of light is undisturbed in intensity and direction when transmitted through a clear liquid containing no particles. If the beam of light encounters particulate matter, some of the light is absorbed or redirected (scattered) resulting in a decreased intensity of the transmitted beam of light [Elimelech, Gregory et al. 1998; McMillan and Considine 1999].

In a turbidity measurement, the scattered beams return to a detector causing a response correlating to the level of turbidity. Higher turbidity values correspond to higher levels of scattered light reaching the detector. The properties of the particles suspended in the liquid and the properties of the liquid itself determine the intensity and direction of scattered light. Refractive index, size, shape, color, and concentration of particles are some of the properties that affect the scattered light [Elimelech, Gregory et al. 1998; McMillan and Considine 1999]. Further, interferences have impact on turbidity measurements, and the type and magnitude of the interference often depend on the turbidity level being measured. Primary interferences are stray light, bubbles, ambient light, and contamination for low-level turbidity measurements (<5 NTU). Color, particle absorption, and particle density are interferences with greater impact for high turbidity testing (≥ 5 NTU) [Sadar 2002]. Typical interferences associated with turbidity measurement and their effects on measurement are summarized in Table 4-1.

Table 4-1: Interferences associated with turbidity measurement [Sadar 2002].

Interference	Effect on the Measurement
Absorbing particles (colored)	Negative bias[1]
Color in the matrix	Negative if the incident light wavelengths overlap the absorptive sprectra within the sample matrix
Particle size	Either positive or negative (wavelength dependent) a) Large particles scatter long wavelengths of light more readily than small particles. b) Small particles scatter short wavelengths of light more efficiently than long wavelengths.
Stray light	Positive bias[1]
Particle density	Negative bias
Contamination	Positive bias

The simple instrument to measure turbidity is the turbidity meter, which consists of three components, a light source, detectors, and a sample cell. Figure 4-2 illustrates a basic turbidity meter, where I_o, I_s, and I_t represent the initial, scattered, and transmitted light respectively.

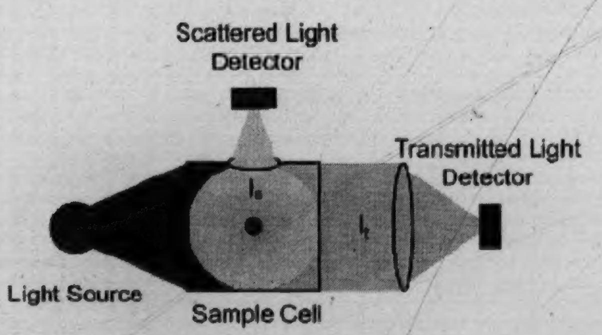

Figure 4-2: Basic turbidity meter [McMillan and Considine 1999].

---

[1] Negative bias: reported measurement is lower than actual turbidity.

There are many types of turbidity meters on the market due to variations in the arrangement of the three components in the instrument. Three main methods of scattered light measurement are forward scatter, 90° scatter, and backscatter. Figure 4-3 shows the difference between these methods.

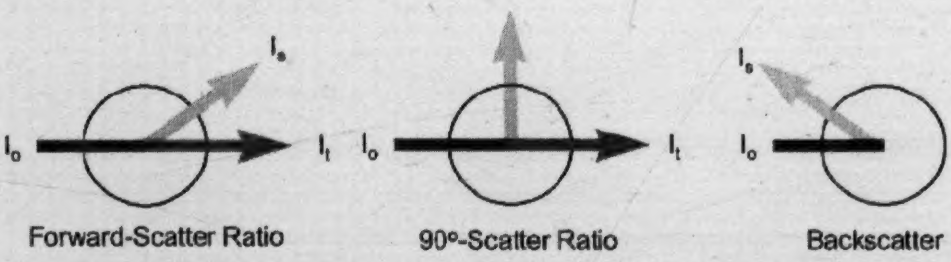

Figure 4-3: Methods of light scatter measurement [McMillan and Considine 1999].

There are many units of measure associated with the measurement of turbidity. These units depend on the calibration standard or the type of turbidity meter used, or are defined differently by various organizations. Some of the most common standard units are shown in Table 4-2 along with the description of the compliant technology. The units for reporting turbidity measurements are important, because the instrument design can have a dramatic effect on the reported result [Sadar 2002].

Table 4-2: Common standard turbidity units [McMillan and Considine 1999; Sadar 2002].

Unit	Name	Description of Compliant Technology
NTU	Nephelometric Turbidity Unit	White light, 90 degree detection only (American regulations)
FNU	Formazin Nephelometric Unit	860-nm light (near IR) with 90-degree detection (ISO7027 compliance)
TE/F or FE	Formazin Turbidity Units	860-nm light (near IR) with 90-degree detection (German Standard)
JTU or JCU	Jackson Turbidity Units	Forward-scattering, suspending specified diatomaceous earth in distilled water

---

[1] Positive bias: reported measurement is higher than actual turbidity.

Turbidity instrumentation is used in many industries. Some examples of turbidity applications are summarized in Table 4-3 for water and waste water, chemical and petrochemical, food, and beverage industries.

Table 4-3: Turbidity applications [McMillan and Considine 1999].

Water & Waste Water Industry	Chemical & Petrochemical	Food & Beverage
Municipal water quality Suspended solids in aeration basin Return activated sludge suspended solids concentration Filtered lake water clarity Drinking water turbidity Dishwasher wastewater	Sodium silicate after tank filter Viscous polymer solutions Brine clarity and filtration Water in liquid hydrocarbon stream Check for precipitates Monitor the filtrate from the processing of clay slurries use to manufacture high voltage ceramic	Concentration of tomato juice Concentration of tea after centrifuge Crude sugar syrup turbidity Phosphorus content of corn and soybean oil Fruit juice clarity for product uniformity Fermentor cell count

In this study, turbidity measurements were obtained from the standard solution to obtain information about the relative amount of precipitates in the solution over time.

4.1.3. Atomic Absorption Spectroscopy

For the determination of metallic elements in solution, atomic absorption (AA) spectroscopy is one of the most sensitive analytical methods available. The element of interest in the sample is merely dissociated from its chemical bonds, and placed in an unexcited "ground" state [Rosato et al. 2000]. The term atomic in this context relates to the fact that atomic spectra are being monitored.

Normally the sample is burned in a flame of the appropriate gas or gases for dissociation. A flame temperature in excess of 2000 K is required for this method. Commonly, an acetylene/air flame is used, which gives a temperature of around 2400 K. A hydrogen/air flame is another choice that provides a similar temperature. However, nitrous oxide addition to the fuel provides a much higher temperature for dealing with potentially refractory metals such as aluminium or titanium [Willoughby 2003].

In the "ground" state, the element is capable of absorbing the characteristic radiation of the proper wavelength. A radiant source of correct wavelength in the instrumentation is usually achieved by emission from the same element as that to be determined. A hollow cathode lamp, where the cathode is made of the specific metal of interest, or a discharge tube, containing a small amount of the required element, can be used for this purpose. Either way, a different lamp is required for each different analysed metal [Willoughby 2003].

The sample for AA must be in solution form, and normally this is an aqueous solution. However, some organic solvents can be tolerated if there is no disturbance to the flame. The detection limits vary with each element, and the sample to be analysed should fall within the appropriate range. Thus, some adjustment of sample concentration may be required prior to actual measurements [Willoughby 2003].

The basic AA instrument is shown in Figure 4-4, which contains a hollow cathode lamp, a flame of the appropriate gas(es) for dissociation, the monochromator[1], the detector and the signal processing units [Ramachandran 1995].

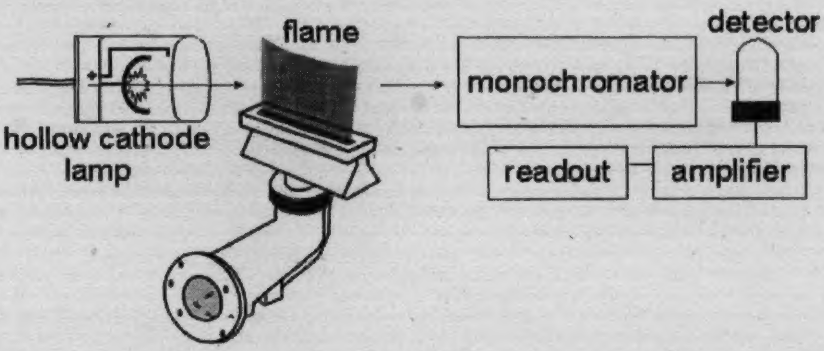

Figure 4-4: Schematic of an atomic absorption instrument [Ramachandran 1995].

---

[1] Monochromator: Apparatus that filters a particular wavelength or energy.

In this study, atomic absorption spectroscopy was performed to monitor the concentration of gold and tin in the standard solution over time. Characteristic data for flame atomic absorption spectroscopy for gold and tin are given in Table 4-4.

Table 4-4: Characteristic data for flame atomic absorptions [Perkin-Elmer].

Element	Wavelength (nm)	Flame Type	Linear Range (mg/l)
Tin	286.3	Nitrous oxide-acetylene, reducing (rich, red)	400
Gold	242.8	Air-acetylene, oxidizing (lean, blue)	50

4.2. Experimental Procedure

4.2.1. Solution Preparation

150 ml of standard solution was mixed as described in the following.

A 250 ml Erlenmeyer flask and Mettler Toledo PB303-S analytical balance were used to weigh 30.000 g of tri-ammonium citrate. About 120 ml of de-ionized water was added, and the flask was swirled. As the ammonium citrate was dissolved, the solution became clear and colorless.

The weighing procedure was repeated, and 0.750 g of potassium tetrachloroaurate was added to the ammonium citrate buffer solution. After swirling and dissolving the gold salt completely, the solution became clear with a golden yellow color.

9.000 g of sodium sulfite was then added to the solution, and the flask was swirled. As the sodium sulfite dissolved in the solution, the color of the solution brightened slightly. Once all the powder seemed to be dissolved, the solution was left to stand for an hour to turn colorless.

Further, 2.250 g of L-ascorbic acid was added to the solution followed by 0.750 g of tin (II) chloride. Once again, the flask was swirled after each addition to ensure that the powders dissolved. It should be noted that, once L-ascorbic acid was added to the colorless solution, the solution turned a light yellow in color.

The solution was transferred into a glass graduated cylinder, and de-ionized water was added to give a total solution volume of 150 ml. This final solution, which was clear with a yellow tinge, was poured back into the flask and swirled to ensure uniformity.

The prepared solution was divided into five portions. These portions were labelled and used as shown in Table 4-5.

Table 4-5: Solutions used for long term stability study.

Label	Container	Solution Volume	Purpose
LTP1	30 ml amber glass bottle with screw lid	30 ml	Long term plating
LTP2	30 ml amber glass bottle with screw lid	30 ml	Long term plating
LTP3	30 ml amber glass bottle with screw lid	30 ml	Long term plating
AA	30 ml amber glass bottle with screw lid	30 ml	AA spectroscopy
T	15 ml glass turbidity vial	15 ml	Turbidity

4.2.2. Long Term Plating

Films were electrodeposited daily to monitor the composition of the deposited film as the solution aged. To minimize environmental variations throughout this study, this set of electroplating experiments was performed in an Aldrich AtmosBag glove bag containing nitrogen.

This flexible, inflatable polyethylene chamber with built-in gloves allowed for an isolated and controlled environment. Inlet ports on each side of the AtmosBag were used for electrical lines and nitrogen gas ports. The AtmosBag with zipper-lock closure was used to allow for repeated access to the experimental setup after each plating experiment.

For each plating test, a water spray bottle, a beaker, an elastic band, tissue, and Parafilm were placed in the glove bag in advance. The solution from the proper container was poured into the plating tank, and the cathode and anode were placed in the cathode and anode holders. The solution used for each plated sample is shown in Table 4-6 along with the solution age. Each portion of the solution was not used for more than four plating experiments to ensure any change in deposit composition is due to aging and not Au or Sn depletion of the solution.

The tank, cathode holder, and anode holder used for electroplating tests were made of polypropylene. The tank was cylindrical with a diameter of about 6.5 cm and height of 5 cm. The spacing between the cathode and anode holders was about 37 mm; the anode and cathode were secured with two polypropylene clips.

The cathodes and anodes were cleaved pieces of Si wafers coated with Ti/Au and Ti/Pt metallization, respectively. The plating area of the cathode was defined using stop-off lacquer. The plating areas of the used cathodes are shown in Table 4-6. The samples were cleaned in de-ionized water and dried in air before and after each plating experiment.

The electroplating setup was moved into the glove bag after preparation. Then the glove bag was sealed and filled with nitrogen. To ensure nitrogen flow in the glove bag, a tube was connected to the bag. The other side of the tube was placed in a beaker filled with water. When the nitrogen flow was adjusted properly, bubbles formed in the beaker. An image of the experimental set up is shown in Figure 4-5.

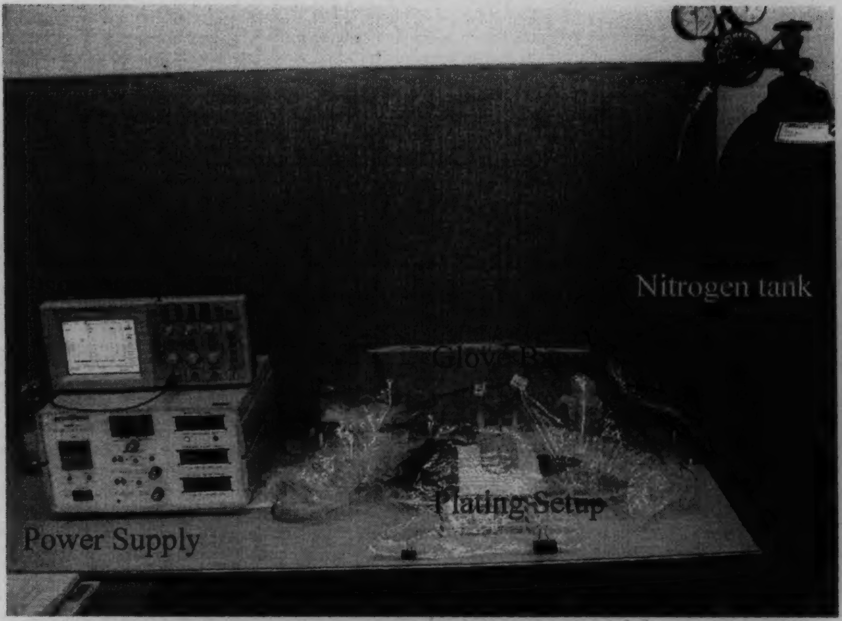

Figure 4-5: Experimental setup.

A Dynatronix PR 0.1-10 pulsed current power supply, with ON and OFF time ranges of 0-9.9 ms, was used for the experiments. A pulse current, with an ON time of 2 ms, an OFF time of 8 ms, and average current density of 2.4 mA/cm^2, was used for all the plating experiments. Each sample was electrodeposited for a period of 90 minutes. A 50 ohm resistor was connected in series with the plating circuit and the peak current density of the waveform was measured using a Tektronix TDS 1002 digital oscilloscope connected in parallel with the resistor. The peak currents and corresponding measured peak voltages for each experiment are shown in Table 4-6. A schematic diagram of the electroplating circuit is shown in Figure 4-6.

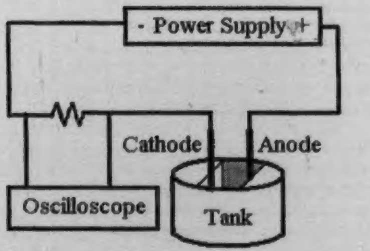

Figure 4-6: Schematic diagram of the electroplating circuit.

Table 4-6: Long term plating conditions and comments.

Sample	Solution	Age (hr:mm)	Area (cm^2)	I_{PK} (mA)	V_{PK} (mV)	Comments
LTP1	LTP1	0:45	1.00	12	600	Solution was left in the tank after plating.
LTP2	LTP1	22:23	0.95	11.4	570	Solution was left in the tank after plating.
LTP3	LTP1	46:13	1.00	12	600	Solution was left in the tank after plating.
LTP6b	LTP1	121:23	1.00	12	600	Precipitates were observed.
LTP6c	LTP2	125:28	1.00	12	600	Solution appeared clear when poured into a clean tank.
LTP8	LTP2	171:28	1.00	12	600	Precipitates were observed.

After each plating experiment, the sample was removed from the solution, the tank was covered with Parafilm, an elastic band was used to keep the Parafilm in place, and then the sample was removed from the glove bag. If the solution was not being reused the following day, the tank was also removed from the glove bag and cleaned thoroughly. The glove bag was resealed and filled with nitrogen. After electroplating the samples were placed in a sample box ready for further examination in the scanning electron microscope.

4.2.3. Scanning Electron Microscope Analysis

The Hitachi S2700 SEM was used to examine the electroplated samples. Images of the surface were taken followed by EDS. The following sections provide the specific procedure regarding sample preparation, obtaining secondary electron images, and EDS.

4.2.3.1. Sample Preparation

The samples were mounted on a pin mount for plan view examination. Then, they were cleaved and mounted on a modified pin mount for cross sectional examination.

In each case double-sided sticky tape made of carbon, was used to attach the sample to the holding mount, which made the sample stable and flat against the mount.

Conductive tape made of copper was used to ground the sample and prevent charging effects. The copper tape used contained nickel embedded in the adhesive side of the tape. Carbon or gold coatings were not required since the gold-tin deposit is electrically conductive.

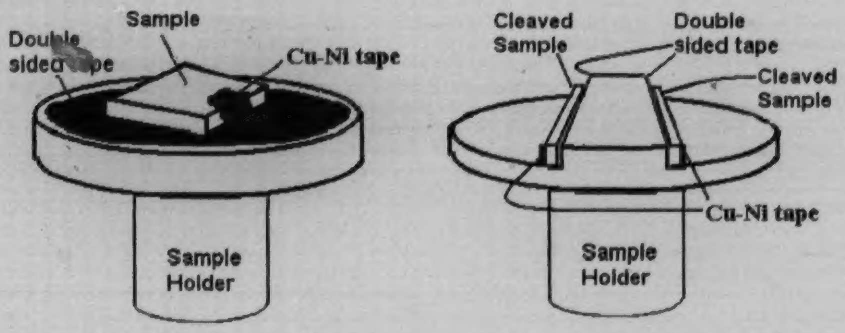
Sample
Double sided tape
Cu-Ni tape
Sample Holder
Cleaved Sample
Double sided tape
Cleaved Sample
Cu-Ni tape
Sample Holder

(a) (b)

Figure 4-7: SEM sample preparation: (a) plan view, (b) cross section.

4.2.3.2. Obtaining Secondary Electron (SE) Images

The secondary electron detector used in the Hitachi SEM was an Everhart-Thornley detector (E-T) positioned on the left side of the stage in the main chamber. The positively biased E-T detector was used to obtain SE images.

An accelerating voltage of 20 kV was used. The working distance (WD) was set to 17 mm, and the 50 μm aperture was used (position 3 of the Molybdenum (Mo) strip aperture).

For each sample, the focus and stigmatism were adjusted to obtain a clear image. Various areas of each sample, for both plan view and cross section samples, were examined at different magnifications to ensure uniformity. Areas of interest were selected, and SE images were captured and saved.

4.2.3.3. Energy Dispersive X-Ray Spectroscopy (EDS)

The X-ray detector in the Hitachi SEM, which is a Prism Intrinsic Germanium (IG) semiconductor detector, was used to detect X-rays. An accelerating voltage of 20 kV was used. The probe current was increased to obtain count rates of 2000-3500 counts/second. For all samples, a working distance of 17 mm and an aperture size of 50 μm were used. The real time collection time was set to 80 seconds.

The take off angle of the detector was calculated by the software to be 30.5° using the spectrometer location (35 mm) and rotation angle (2°). Pure gold and tin standards were chosen for quantitative analysis of the composition of the electroplated coatings. For each sample, three areas were selected for EDS analysis, and the average composition of these areas was used in the results.

4.2.4. Turbidity

The turbidity of the solution was measured frequently to obtain a turbidity curve with the turbidity value and solution age on the y and x axis respectively.

A VWR model 66120-200 turbidity meter was used (Figure 4-8). This meter reads the amount of reflected light at 90° to the incident angle of a light source. The specifications of this turbidity meter are shown in Table 4-7. Two permanently sealed standards of 0 NTU and 10 NTU were used to calibrate the meter before each use.

Figure 4-8: VWR 66120-200 turbidity meter.

Table 4-7: Specifications of VWR 66120-200 turbidity meter.

Resolution	**Accuracy**	**Display**
0.01(0-20) 0.1 (0-200)	+ 2%	1.25 cm LCD

4.2.5. Atomic Absorption Spectroscopy

A Perkin-Elmer 4000 atomic absorption spectrometer was used to monitor the concentration of gold and tin in the standard solution over time for this study. An image of the experimental set up is shown in Figure 4-9.

Figure 4-9: Perkin-Elmer 4000 atomic absorption spectrometer.

Stock standard solutions for gold and tin were available for use. The stock standard solution for gold (1000 mg/L) was previously prepared by dissolving 0.1000 g of gold in a minimum volume of aqua regia, and drying it. Then, the residue was dissolved in 5 ml HCl, cooled and diluted with de-ionized water. The stock standard gold solution was stored in an amber bottle. The stock standard gold solution was diluted and mixed with 10% (v/v) HCl to obtain a 30 mg/L standard solution for this study.

The stock standard solution for tin (1000 mg/L) was previously prepared by dissolving 1.000 g tin in 100 ml of concentrated HCl and diluting it to 1 litre with de-ionized water. The stock standard tin solution was diluted and mixed with 10% (v/v) HCl to obtain a 250 mg/L standard solution for this study.

For gold analysis, a gold hollow cathode lamp and air-acetylene flame type were used. A 10-cm burner head was used and a lean blue flame was formed. This burner provides the best sensitivity for air-acetylene due to its long burner path length.

For tin analysis, a tin hollow cathode lamp and nitrous oxide-acetylene flame type were used. A 5-cm burner head or nitrous oxide burner head was used, and a rich red flame was formed.

Prior to each AA spectroscopic measurement, the gold-tin standard solution was diluted to assure operation in the linear range. Since the linear range for gold and tin are different, separate samples were prepared for analysis for each metal. The samples prepared for gold analysis were diluted 200 times, while the samples prepared for tin analysis were diluted 20 times.

For each AA spectroscopic measurement, the proper hollow cathode lamp and burner were installed. The instrument was set up to the correct wavelength and the proper flame was turned on. Once the prepared standard solution was burned and the instrument was calibrated, the properly diluted sample was burned. Then the reading was recorded. This procedure was repeated once for gold and then for tin analysis.

4.3. Results and Discussions

Plan view and cross section SEM images for an electroplated deposit at 2.4 mA/cm^2 from a fresh solution are shown in Figure 4-10. The deposit is smooth and dense, and EDS analysis showed a composition of 51.2 at % Sn. The thickness of the deposited film was measured to be 2.9 μm from the cross section image. This thickness corresponds to a plating rate of about 1.9 μm/hr.

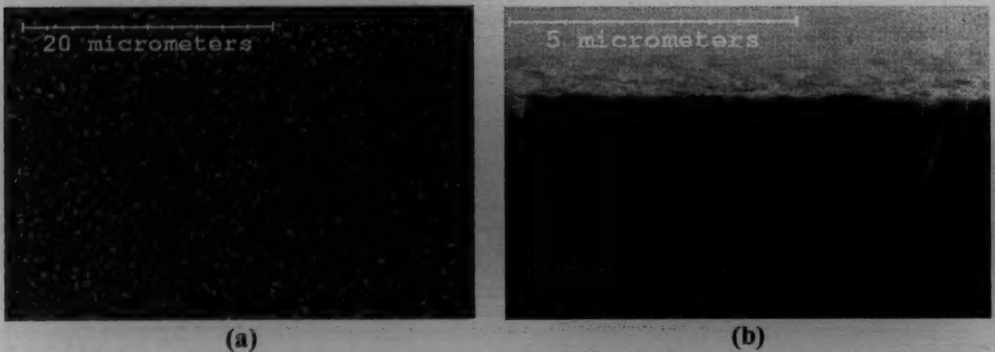

(a) (b)

Figure 4-10: SE images of deposit from a fresh standard solution: (a) plan view (b) cross section.

Plan view images, along with corresponding cross section SEM images, for electroplated deposits from the aged solution are shown in Figure 4-11. The deposit morphology deteriorates as the solution ages. The deposits from the aged standard solution are rougher and less dense compared to the deposit from the fresh solution.

Samples LTP6b and LTP6c were both plated from the solution with an age of 5 days. LTP6b was plated from the portion of the solution which was stored in the plating tank (LTP1), and 3 other samples were plated from this portion. This solution contained precipitates at the time of plating LTP6b. However, LTP6c was plated from the portion of the solution which was stored in an amber glass bottle and not used. Once the stored solution was poured into a clean tank, most of the precipitates were left behind in the bottle. Thus, this portion of the solution did not contain as many precipitates at the time of plating LTP6c. The difference in the morphology of these two samples shows that the differently stored solutions perform differently, and the amount of precipitates in the solution at the time of plating affects the deposit morphology.

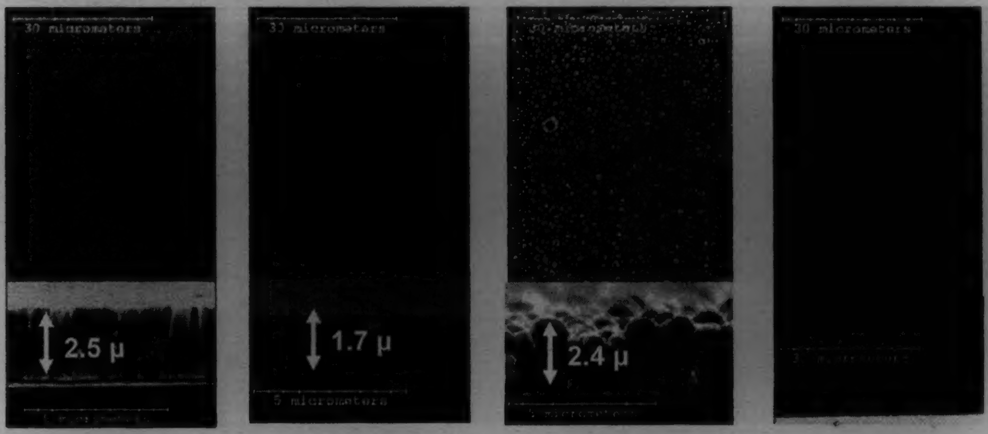

(a) (b) (c) (d)

Figure 4-11: SE plan view and cross section images of deposits from an aged solution: (a) LTP2-1 day (b) LTP3-2 days old (c) LTP6b-5 days old (d) LTP6c-5 days old.

The composition of the plated deposits from the standard solution over time was measured using EDS within the SEM. Figure 4-12 show the change in tin content of the deposited films over time. For all graphs presented in this thesis the measurement error is contained within the point size represented on the graph.

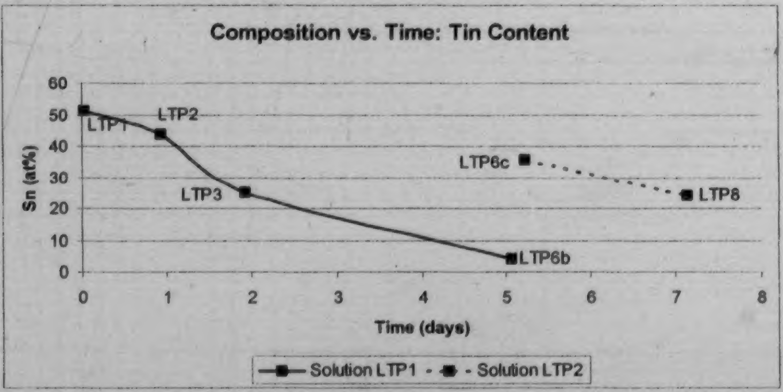

Figure 4-12: Tin content of the deposited film as a function of aging time.

The difference in the composition of samples LTP6b and LTP6c shows that the depletion in the solution due to electrodeposition affects the amount of change in the composition of the deposits over time. The difference in the composition is also due to the amount of precipitates in the solution at the time of electrodeposition. Sample LTP6b has a higher gold content (or lower tin content), since more of the fine gold precipitates in the solution may have been incorporated in the deposit at the time of electroplating.

The tin content of the electroplated deposits decreases, while the gold content of the electroplated deposits increases as the solution ages. Figure 4-12 suggests that the useful shelf life of the standard solution is about one day.

A turbidity curve was obtained and is shown in Figure 4-13. Solution turbidity was initially low for the fresh solution (solution remained transparent with a faint yellow color). This value increased with time and peaked out at 28 hours. The turbidity dropped gradually to near zero the next day and stayed at very low values. This obtained curve follows the same trend of a typical turbidity plot of the electroplating solution as a function of aging time reported previously by [He, Liu et al. 2005]. The only difference was in the time periods it took to complete each stage. In some previously reported instances the maximum turbidity occurred after two or three days. It should be noted that soon after the peak turbidity was reached, small, suspended particles were visible in the solution. These particles agglomerated over time and gradually deposited on the bottom and sidewalls of the bottles. The time corresponding to the peak of the turbidity curve correlates with the useful shelf life of the solution.

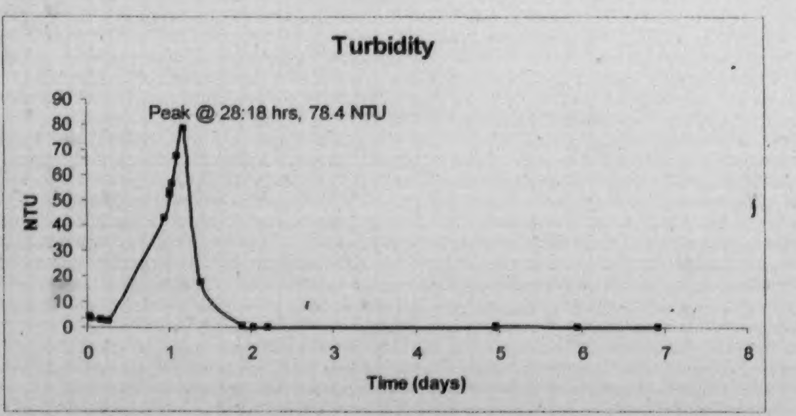

Figure 4-13: Sample turbidity curve for the standard solution.

The initial increase in turbidity has been attributed to reduction and precipitation of small gold particles that are not visible to the naked eye. The decrease in the turbidity value, after reaching the peak, has been attributed to agglomeration and settling of the precipitated gold [He, Liu et al. 2005].

Atomic absorption spectroscopy results are plotted and are shown in Figure 4-14 and Figure 4-15. The concentration values in both graphs are normalized with respect to the initial measured values. The initial concentration of tin and gold in the solution were measured to be 2.24 and 3.62 g/L respectively. The initial concentration that was measured using atomic absorption spectroscopy corresponded with the amount of gold and tin that was added to the solution.

The concentration of tin in the standard solution remained constant as the solution aged. However, the concentration of gold in the standard solution remained constant for about 24 hours. During this time period, a decrease in concentration of gold in the solution was expected due to reduction and precipitation of small gold particles, which was suggested by the turbidity behaviour. The reason for this unexpected result could be due to the size of the precipitated gold particles. These initial particles were small enough to be detected by the AA spectrometer although they were not in solution form. The gold concentration decreased after about 24 hours and dropped to zero somewhere between 2 and 5 days. This behavior roughly correlated to the turbidity bahavior; better agreement may have been obtained if additional AA measurements were done between 2 and 5 days. The results combined suggest a useful shelf life of one day.

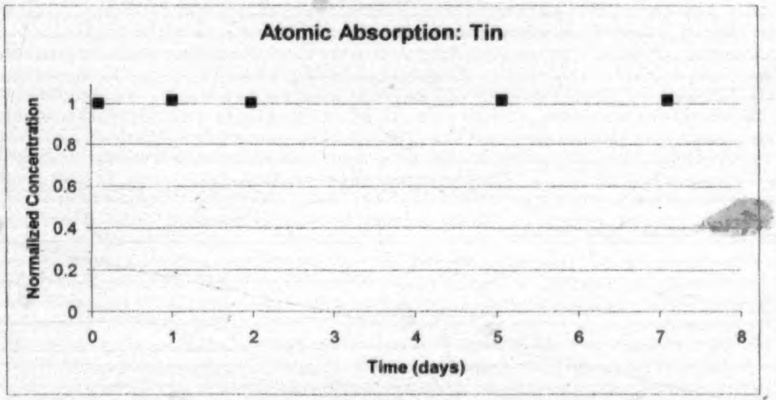

Figure 4-14: Atomic absorption spectroscopy results for tin.

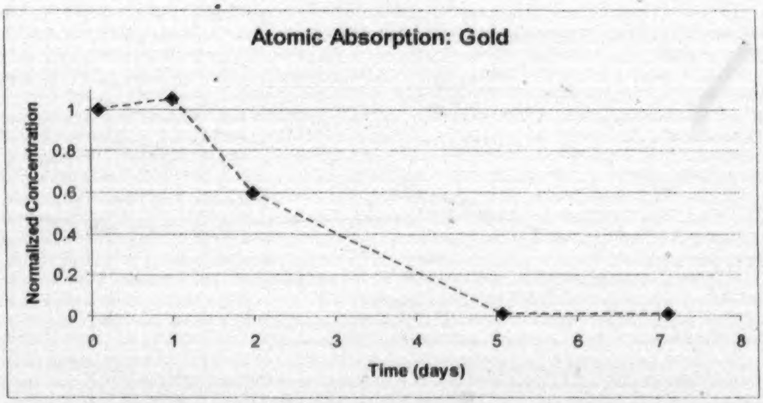

Figure 4-15: Atomic absorption spectroscopy results for gold.

4.4. Conclusions

The long term stability of the standard electroplating bath developed by Ivey's group was studied to obtain a better understanding of the solution aging behaviour.

The study of composition of the plated deposits over time suggested a useful shelf life of one day for the standard solution. The tin content of the electroplated deposits decreased, while the gold content of the electroplated deposits increased as the solution aged. The difference in the composition of differently stored samples showed that the depletion in the solution due to electrodeposition affects the amount of change in the composition of the deposits over time. The difference in storage also demonstrated that the amount of precipitates in the solution at the time of electrodeposition affects the composition of the deposit.

Plan view and cross section SEM images of electroplated deposits plated at different times showed that morphology deteriorates as the solution ages. Deposits from the aged standard solution were rougher and less dense compared to the deposit from the fresh solution. The morphology of differently stored solutions was different and demonstrated that the amount of precipitates in the solution at the time of plating affects the deposit morphology.

The turbidity of the standard solution was initially low, increased with time, and peaked out at 28 hours. The turbidity value dropped gradually to near zero the next day and stayed at very low values. The peak of the turbidity curve correlated with the useful shelf life of the solution.

The concentration of tin in the standard solution remained constant as the solution aged. However, the concentration of gold in the standard solution decreased after about 24 hours. This behaviour also correlated with the turbidity and composition curves and suggests a useful shelf life of one day. The next chapter covers the screening tests performed to determine the key factors affecting the stability and the plating rate.

Chapter 5: Screening Tests

5.1. Overview

This Chapter addresses the screening tests performed to determine the key factors affecting the stability and the plating rate. The term screening used in this chapter refers to a filtering process, in which a list of factors affecting the performance of a process are initially considered and a few of the most vital ones are chosen and studied thoroughly.

The lifetime of the bath solution is limited due to gold precipitation, and previous studies had shown that nano-size gold particles were present in freshly mixed solutions [He, Liu et al. 2005]. Transmission electron microscopy (TEM) analysis was done to monitor gold precipitation during the solution mixing procedure to find the origin of formation of the gold particles. Also, experiments were performed in which the concentration of solution constituents was changed and a few additives were added. The effects of these changes to the standard solution were studied, and the most vital factors were chosen for the statistical design of experiments.

The composition of the plated deposits from the modified baths was monitored as a function of aging time to study their stability behavior. Similar to the long term stability study, films were electroplated from fresh and aged standard solutions, and the compositions of the deposited films were monitored using EDS within the SEM. Turbidity curves were also obtained to monitor the gold precipitation behavior as a function of aging time. These techniques, except TEM, are described in Chapter 4, and the next section provides an introduction to TEM.

5.1.1. Transmission Electron Microscopy

This section provides a very brief introduction to TEM as the amount of information to cover is beyond the scope of this thesis. Complete information on transmission electron microscopy techniques and concepts can be found in [Williams and Carter 1996].

In TEM an image is formed using electron-optical techniques. A beam of highly energetic electrons is produced by an electron gun, and it is guided in vacuum using electromagnetic lenses (pressures lower than 10^{-10} Pa). The produced beam passes through the specimen and creates an image on the fluorescent screen. TEM can have resolution of up to 0.2 nm.

Bright field (BF) images were taken using the JEOL-2010 TEM with the help of PhD student Heather Kaminsky. Figure 5-1 shows how BF images were obtained. BF images are used to observe any nano-scale gold precipitates within the prepared samples.

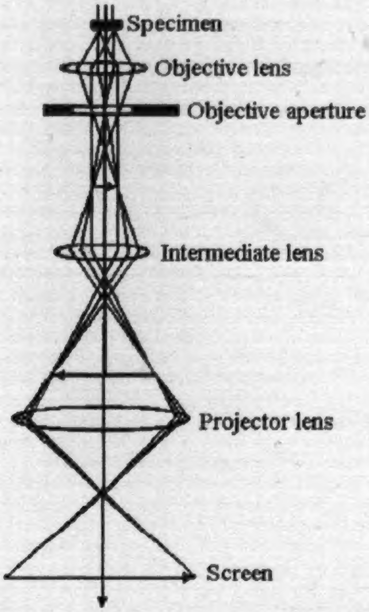

Figure 5-1: BF imaging within the TEM [Goodhew, Humphreys et al. 2001].

5.2. Experimental Procedure

5.2.1. TEM Sample Preparation

Transmission electron microscopy (TEM) analysis was done to monitor gold precipitation during the solution mixing procedure to find the origin of formation of the gold particles that exist in a freshly made solution. The same procedure as explained in Section 4.2.1 was followed to prepare a standard solution. However, the quantity of each constituent was calculated to make 10 ml of the solution. After mixing each constituent thoroughly, one drop from the solution was taken and placed on a lacy carbon coated copper grid. Then, the grids were left to dry in air. Thus, samples were collected after each step of the mixing process. Table 5-1 includes the sample names and the content of each sample.

Table 5-1: TEM Samples.

Name	Content
TEM1	Ammonium citrate + $KAuCl_4$
TEM2	Ammonium citrate + $KAuCl_4$ + sodium sulfite (as mixed)
TEM3	Ammonium citrate + $KAuCl_4$ + sodium sulfite (after 30 minutes)
TEM4	Ammonium citrate + $KAuCl_4$ + sodium sulfite + ascorbic acid
TEM5	Ammonium citrate + $KAuCl_4$ + sodium sulfite + ascorbic acid + $SnCl_2.2H_2O$

5.2.2. Concentration of Solution Constituents

The concentration of solution constituents was modified to observe the effect of each component. The composition of the plated deposits from the modified baths was monitored as a function of aging time to study their stability behavior. Films were electroplated from fresh and aged standard solutions, and the compositions of the deposited films were monitored using EDS within SEM. Turbidity curves were also obtained to monitor the gold precipitation behavior as a function of time.

Initially, there were attempts to eliminate ammonium citrate from the solution. In the first attempt, a solution was mixed following the standard procedure without any ammonium citrate (i.e., $KAuCl_4$ was mixed with water and sodium sulfite was added to the solution). In the second attempt, $KAuCl_4$ and sodium sulfite were dissolved in DI-water separately. Then, these solutions were mixed, and the rest of the components were added following the standard procedure. In the last attempt, a solution similar to the second attempt was mixed, but $SnCl_2.2H_2O$ was also added as a solution through the last step of the mixing procedure.

More solutions were mixed with modified concentration of components following the standard procedure. 30 mL of each solution was mixed. Table 5-2 shows the modified concentrations of the constituents within each solution. All values listed in Table 5-2 are in g/L (unless specified). Whenever a component was added as a solution, the amount of DI-water used, has been stated. Further, whenever the same concentration as the standard solution was added, no value has been stated in the table.

Table 5-2: Solutions with modified concentrations.

	Ammonium citrate	$KAuCl_4$	Sodium sulfite	L-ascorbic acid	$SnCl_2.2H_2O$
Ci-free1	0				
Ci-free2	0	+ 10 ml DI-water	+ 10 ml DI-water		
Ci-free3	0	+ 10 ml DI-water	+ 10 ml DI-water		+ 10 ml DI-water
50Ci	50				
50Ci10Au	50	10			
50Ci15Au	50	15			
30Ci10Au10Sn	30	10			10
7AA				7	
5AA				5	
25Au		25			
100SS			100		

These solutions were examined using turbidity techniques and EDS analysis of the deposited films.

5.2.3. Modified Mixing Procedure and Additives

The mixing procedure was modified to observe the effects of the change. Also, a new additive and the effect of tin sponge were summarily examined. The experimental procedures for these investigations are discussed below.

5.2.3.1. A3 + L-Ascorbic Acid Solution + B3

An alternative to a single gold-tin electroplating solution was developed by [He, Liu et al. 2006], in which separate stable gold and tin solutions are prepared and then mixed as needed. Ascorbic acid is claimed to be an important bridge component between the two solutions. The separate gold and tin solutions were claimed to be stable for at least 12 months. However, once the two solutions and ascorbic acid were mixed, the plating solution had limited stability.

The gold and tin solutions were called A3 and B3 respectively in the previous work, and the same notation will be used here. The mixing procedure was modified by bridging the two solutions using ascorbic acid in solution form as an attempt to improve the stability of the final solution. The concentrations of components in A3 and B3 were adjusted to obtain the standard concentrations in the final solution.

5.000 g of tri-ammonium citrate was weighed. About 19 ml of DI-water were added, and the ammonium citrate was completely dissolved. 0.250 g of potassium tetrachloroaurate was added to the ammonium citrate buffer solution. After swirling and dissolving the gold salt completely, 3.007 g of sodium sulfite were then added to the solution. Once all the powder appeared to be dissolved, the solution was left to stand for an hour until it became colorless. The solution was transferred into a glass graduated cylinder, and DI-water was added to give a total solution volume of 20 ml. This final solution was called A3.

Meanwhile, 5.000 g of tri-ammonium citrate was weighed. About 19 ml of DI-water were added, and the ammonium citrate was completely dissolved. 0.250 g of tin (II) chloride were added and dissolved thoroughly. The solution was transferred into a glass graduated cylinder, and DI-water was added to give a total solution volume of 20 ml. This solution was called B3.

Finally, 0.752 g of l-ascorbic acid were dissolved in 10 ml of DI-water, and added to the A3 solution. Then, the B3 solution was added to the A3 plus ascorbic acid solution. A clear solution with a yellow tinge was obtained.

The shelf life of this solutions was examined using the turbidity technique and EDS analysis of the deposited films as a function of aging time.

5.2.3.2. Cupferron

In some unpublished work done in Ivey's group in 2004, cupferron ($C_6H_5N(NO)ONH_4$) was introduced as a possible additive to improve stability of the standard solution. The turbidity value of a standard solution containing 0.010 g/L of cupferron stayed low for at least one week. Thus, this additive was studied further in this work.

A solution was mixed using the standard procedure and concentrations. However, just before adding DI-water for final volume adjustment, 0.010 g/L of cupferron was added to the solution. Since the amount of cupferron to be added was fairly small, it was added in solution form as follows. 0.050 g of cupferron was added to 100 mL of DI-water, and 1 ml of this solution was added to the standard solution. The final volume of the solution was then adjusted to be 50 ml.

The compositions of the films deposited from the solution containing cupferron at various current densities and as a function of ageing time were examined.

5.2.3.3. Tin Sponge

Oxidation of tin can cause a loss in the deposition rate and productivity. As suggested by [Schlesinger and Paunovic 2000], one way to minimize tin (IV) formation is to add a piece of tin sponge in the plating tank according to the equation:

$$\text{Sn(IV)} + \text{Sn} \rightarrow 2\text{Sn(II)}. \qquad \textbf{(Equation 5-1)}$$

A piece of tin sponge was made using the following procedure found in [Flinn Scientific 2003]. 16 mL of DI-water was added to 5.625 g of tin (II) chloride in a 200-mL beaker followed by addition of 34 mL of 3 M hydrochloric acid solution. The solution was mixed thoroughly to enhance dissolution, and the solution turned cloudy and milky-white. This observation refers to formation of tin oxide within the solution. 3.700 g of zinc was added to the solution. Finely divided tin crystals on the zinc surface were formed, and hydrogen gas bubbles were generated by reaction of zinc with hydrochloric acid. The cloudy solution eventually turned clear as the reaction proceeded, and the tin began to resemble a sponge. The tin sponge rose slowly to the surface, floated by the hydrogen gas bubbles and the presence of pockets of air. After the reaction was completed, the tin sponge was removed from the solution using tweezers and rinsed under running DI-water. The tin sponge was allowed to air dry in a fume hood. The tin sponge was soft and spongy.

In this experiment, two oxidation–reduction reactions take place simultaneously. These reactions as suggested by [Flinn Scientific 2003] are shown below.

$$\text{Zn}_{(s)} + \text{SnCl}_{2(aq)} \rightarrow \text{Sn}_{(s)} + \text{ZnCl}_{2(aq)} \qquad \textbf{(Equation 5-2)}$$

$$\text{Zn}_{(s)} + 2\ \text{HCl}_{(aq)} \rightarrow \text{H}_{2(g)} + \text{ZnCl}_{2(aq)} \qquad \textbf{(Equation 5-3)}$$

However, due to observation of tin oxide in the solution one other possible reaction would be:

$$\text{SnO}_2 + 4\ \text{H}^+ + 2\ \text{Zn} \rightarrow \text{Sn} + 2\ \text{Zn}^{2+} + 2\ \text{H}_2\text{O} \qquad \textbf{(Equation 5-4)}$$

A small piece of tin sponge (about 1 cm^3 in size) was placed in the tank containing 30 mL of standard solution, and two samples were plated at current densities of 0.8 and 2.4 mA/cm^2. The used standard solution was then divided into two 15 mL portions. One half was stored containing the used tin sponge, and the other half was stored without any tin sponge.

5.3. Results and Discussions

5.3.1. TEM Results

The BF TEM images from all prepared samples are shown in Figure 5-2 to Figure 5-6. Gold was detected from EDS analysis of all observed precipitates. Precipitates were observed as early as the very first step in the mixing procedure. The image from the TEM sample containing the mixture of ammonium citrate and $KAuCl_4$ shows precipitates ranging in size from 10 nm to 1000 nm (Figure 5-2).

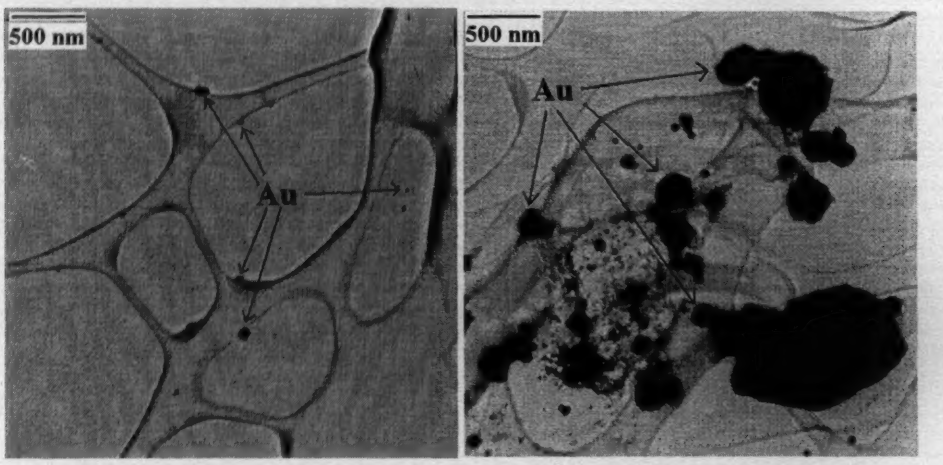

Figure 5-2: BF TEM images of sample TEM1 (ammonium citrate + $KAuCl_4$).

The image from the TEM sample after addition of sodium sulfite shows precipitates of about 10 nm in size. These fine precipitates were observed in the dark regions (circled) of the left hand image in Figure 5-3. These regions are shown at higher magnifications in the right hand image in Figure 5-3. However, the image of the sample from the same solution after standing for 30 minutes shows a particle size of 10nm to 100nm (Figure 5-6).

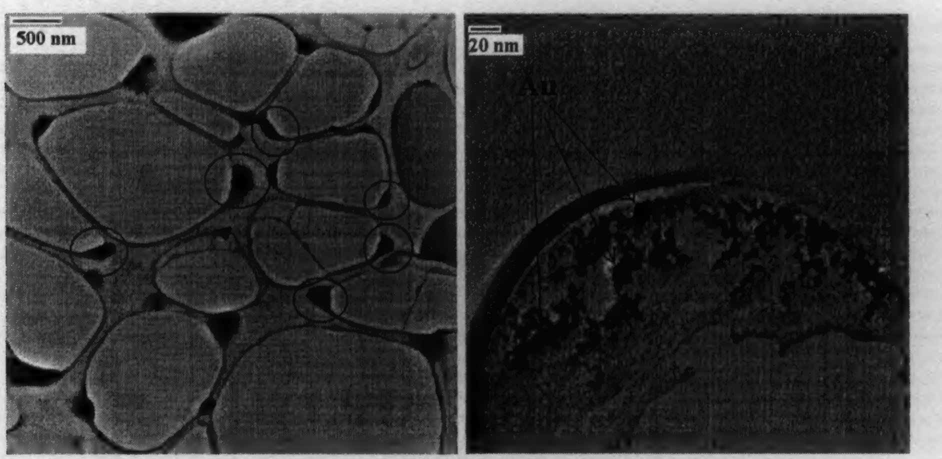

Figure 5-3: BF TEM image of sample TEM2 (ammonium citrate + KAuCl$_4$ + sodium sulfite (as mixed)).

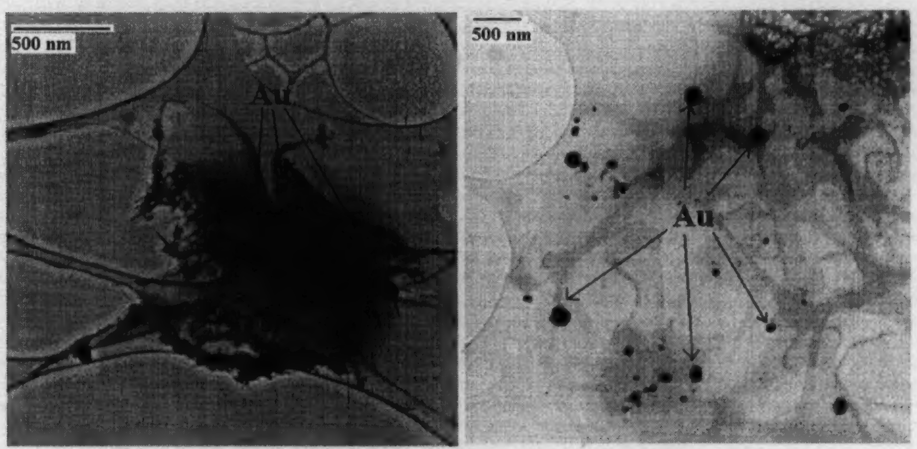

Figure 5-4: BF TEM images of sample TEM3 (ammonium citrate + KAuCl$_4$ + sodium sulfite (after 30 minutes)).

The TEM images of the sample after addition of ascorbic acid show precipitates in the size range of 10 nm to 70 nm (Figure 5-5). Finally, the images from the sample from the final solution (TEM5) contain precipitates in the range of 6 nm to 20 nm (Figure 5-4).

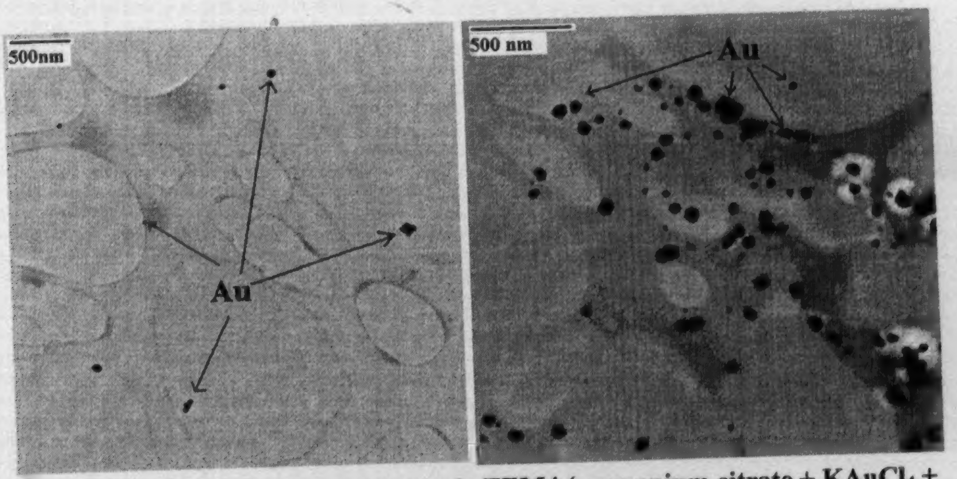

Figure 5-5: BF TEM images of sample TEM4 (ammonium citrate + $KAuCl_4$ + sodium sulfite + ascorbic acid).

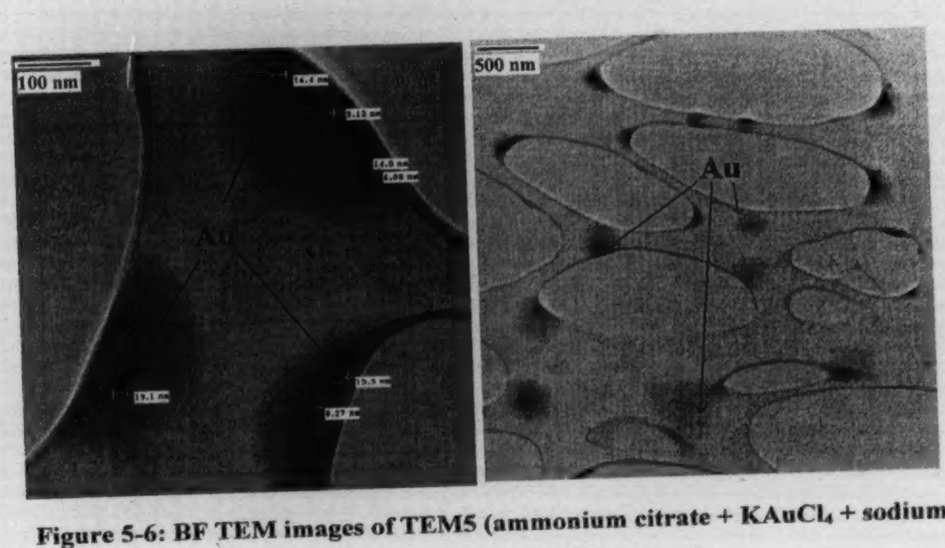

Figure 5-6: BF TEM images of TEM5 (ammonium citrate + $KAuCl_4$ + sodium sulfite + ascorbic acid + $SnCl_2.2H_2O$).

It is important to note that the particle sizes measured through the TEM analysis do not have statistical significance. In this study the particle size is not of interest, and the measured particle sizes are not reliable for any comparison between samples. However, it can be concluded from this study that gold precipitation occurs as soon as ammonium citrate and $KAuCl_4$ are mixed. These nano-size particles remain within the solution throughout the mixing procedure. Thus, the final fresh solution contains nano-size gold particles.

5.3.2. Concentration of Solution Constituents

Since the TEM analysis showed that ammonium citrate contributes to gold precipitation and solution instability, initial attempts were made to eliminate ammonium citrate from the solution.

In the first attempt, a solution (Ci-free1) was mixed following the standard procedure except without any ammonium citrate. The clear yellow solution of $KAuCl_4$ and DI-water turned brown and precipitation occurred as soon as sodium sulfite powder was added. Therefore, the experiment was stopped at this point.

In the second attempt, $KAuCl_4$ and sodium sulfite were mixed as solutions, and the rest of the components were added following the standard procedure (Ci-free2). Although brown precipitation did not occur after the mixture of sodium sulfite and $KAuCl_4$ in this attempt, the solution turned milky and white particles were observed when tin (II) chloride was added to the solution at the last step.

In the last attempt, a solution (Ci-free3) similar to the second attempt was mixed, but tin (II) chloride was also added as a solution through the last step of the mixing procedure. This solution turned milky with a very bright yellow color, and precipitation occurred.

It was concluded that the ammonium citrate cannot be eliminated from the solution. Thus, solutions with reduced concentrations of 50 and 30 g/L of ammonium citrate were mixed and examined. The following section contains the results and discussion for the solutions with reduced ammonium citrate concentrations. Due to the results obtained from reducing the concentration of ammonium citrate, as well as the aim of increasing the plating rate, the concentration of metal salts in the solution was increased. The results and discussion for these solutions are also presented in the following section. The section is then followed by results and discussion obtained from solutions with modified concentrations of ascorbic acid and sodium sulfite.

5.3.2.1. Concentration of Ammonium Citrate and Metal Salts

A solution containing 50 g/L ammonium citrate (one fourth of the standard amount) was used to electroplate films at various current densities. The composition of the plated deposits was measured using EDS within the SEM. Figure 5-7 shows the tin content of the deposited films over the current density range of 0.8 to 2.4 mA/cm^2. Current densities lower than 0.8 mA/cm^2 were not of interest due to their low inconvenient plating rates. The film deposited at a current density of 2.4 mA/cm^2 was stressed (Figure 5-8), and therefore higher current densities were not used. Figure 5-7 shows that the decrease in the ammonium citrate concentration shifts the plateaus shown in Figure 2-11 towards lower current densities, and only the phase containing 50 at % Sn (AuSn) is obtainable.

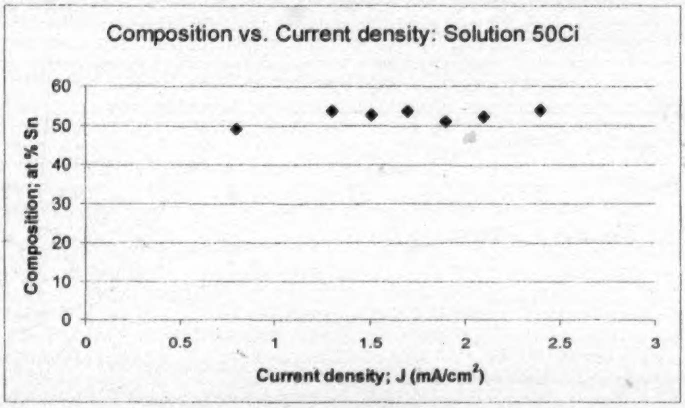

Figure 5-7: Tin content of the deposited films at various current densities using the 50Ci solution.

20 micrometers

Figure 5-8: SE image of deposit from 50Ci solution at $j = 2.4$ mA/cm^2.

The turbidity behavior of this solution was studied, and the obtained curve is shown in Figure 5-9. Solution turbidity was initially low for the fresh solution, and this value stayed low for at least 43 days. Also, the solution stayed clear for this period although the color of the solution turned to a slightly darker shade of yellow over time.

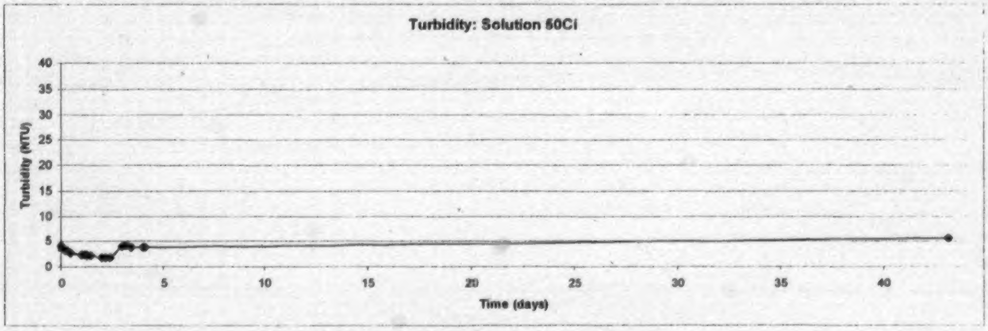

Figure 5-9: Turbidity curve for 50Ci solution.

To determine the useful shelf life of the solution, films were electroplated daily. The change in tin content of the deposited films as a function of time is shown in Figure 5-10. These films were electroplated at a current density of 1.5 mA/cm^2. Figure 5-10 shows that the tin content of the plated deposits stayed unchanged for about seven days, after which the tin content started to decrease.

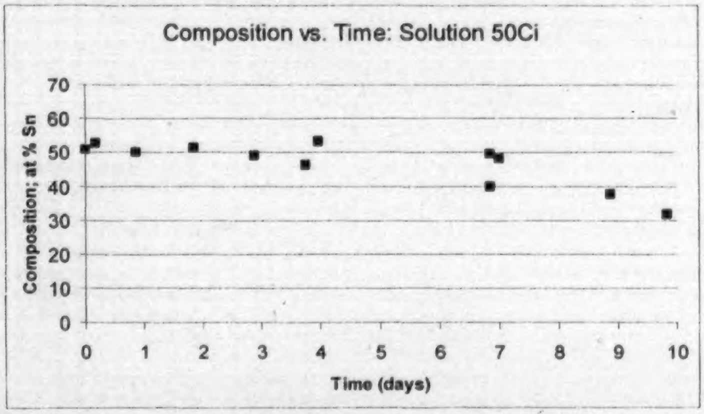

Figure 5-10: Tin content of the deposited films at 1.5 mA/cm^2 from 50Ci solution as a function of aging time.

Since the shelf life of the solution improved, this experiment was repeated. Solutions 50ci1 to 50ci4 were mixed in a manner similar to the solution 50Ci, and films were electroplated from these solutions as a function of ageing time. However, this time 5 g/l of tin (II) chloride was added to the solution whenever the tin content of the solution decreased and films were electroplated after the addition of tin (II) chloride. The change in tin content of the deposited films is shown in Figure 5-11. These films were also electroplated at a current density of 1.5 mA/cm^2. In Figure 5-11 any increase in tin content of the solution corresponds to the addition of tin (II) chloride to the solution.

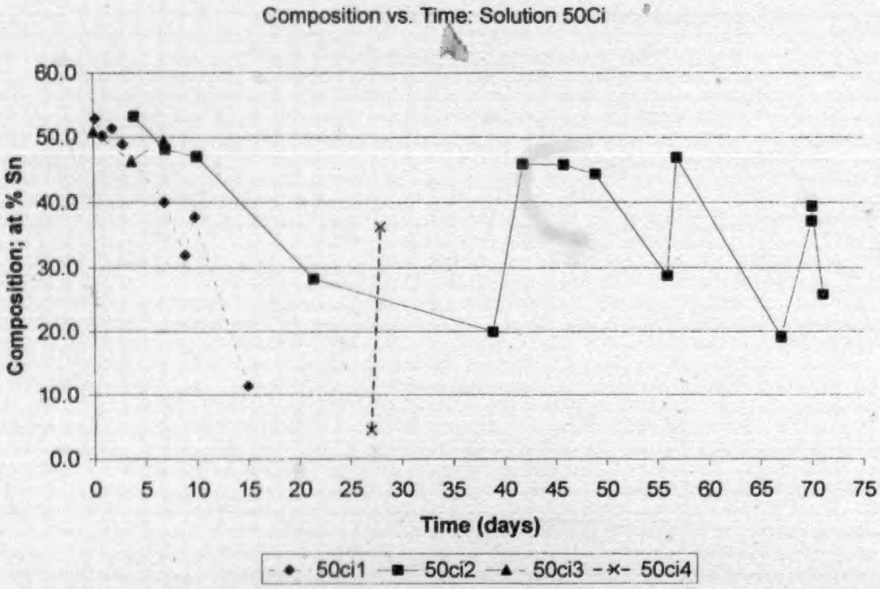

Figure 5-11: Change in tin content of films deposited at 1.5 mA/cm^2 from the 50Ci solution as a function of ageing time. The addition of tin (II) chloride corresponds to abrupt increases in deposit tin composition.

The 50Ci solution looked promising, except that the electrodeposition of both phases AuSn and Au_5Sn was not possible. In attempts to obtain the Au_5Sn phase, the concentration of $KAuCl_4$ in the solution was increased to 10 g/L (solution 50Ci10Au) and 15 g/L (solution 50Ci15Au). The tin content of the deposited films at various current densities using 50Ci10Au and 50Ci15Au solutions is shown in Figure 5-12 and Figure 5-13 respectively. The concentration increase to 10 g/L slightly shifted the plateaus shown in Figure 5-7 towards higher current densities. However, a plateau of the phase containing ~16 at % Sn (Au_5Sn) was still not obtainable. The concentration increase to 15 g/L significantly shifted the plateaus shown in Figure 5-7 towards higher current densities. However, the AuSn plateau was not obtainable.

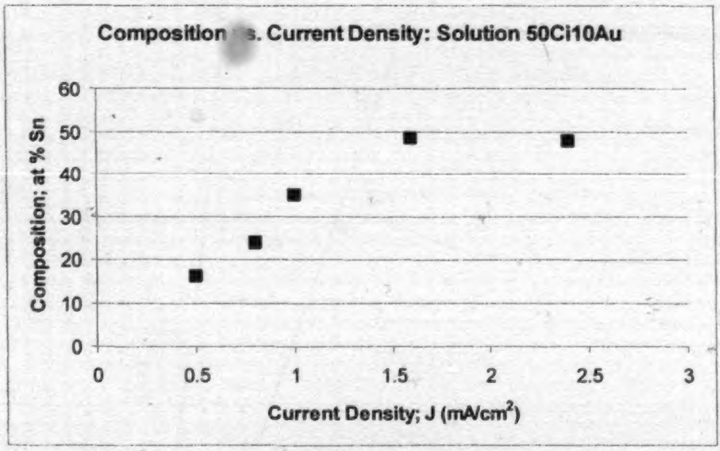

Figure 5-12: Tin content of the deposited films at various current densities using the 50Ci10Au solution.

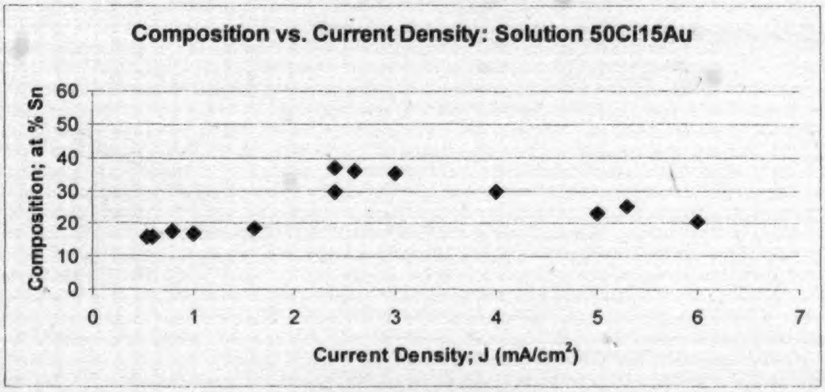

Figure 5-13: Tin content of the deposited films at various current densities using the 50Ci15Au solution.

To get an idea of how the increase in concentration of gold in the solution affects the shelf life, films were electroplated from the 50Ci15Au solution as a function of aging time (Figure 5-14). The shelf life of this solution appeared to be one day, since the concentration of tin in the deposited films dropped after 24 hours. Thus, increasing the gold concentration in the 50Ci solution resulted in a decrease of the useful shelf life of the solution.

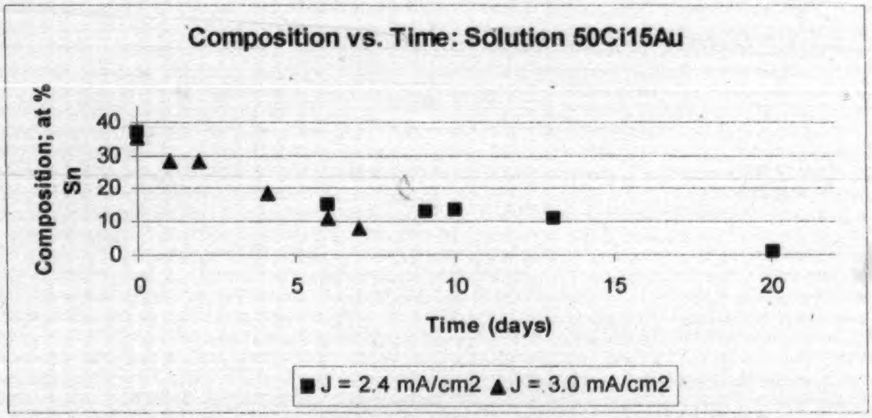

Figure 5-14: Tin content of the deposited films from 50Ci15Au solution as a function of aging time.

To get an idea of how the increase in gold concentration in the solution affects the plating rate, the thickness of deposits from fresh solutions were measured. Figure 5-15 shows SE plan view and cross section images of deposits at different current densities from solutions 50Ci10Au and 50Ci15Au. The deposition rates from solution 50Ci10Au at 0.8 and 2.4 mA/cm^2 were 0.7 and 3.0 µm/hr respectively. Moreover, the deposition rate from the 50Ci15Au solution at 0.8 mA/cm^2 was 0.9 µm/hr. The measurements showed that the deposition rate increased with an increase in the concentration of gold in the solution.

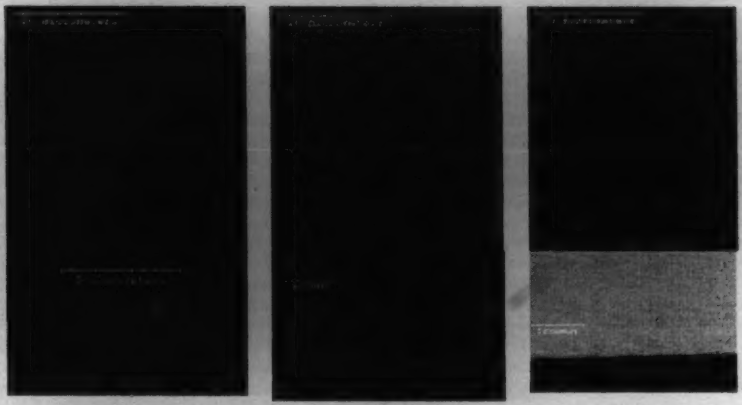

(a) (b) (c)

Figure 5-15: SE plan view and cross section images of deposits: (a) from 50Ci10Au solution at 0.8 mA/cm^2 (b) from 50Ci10Au solution at 2.4 mA/cm^2 (c) from 50Ci15Au solution at 0.8 mA/cm^2.

Solution 30Ci10Au10Sn was mixed with an even lower ammonium citrate concentration. Also, the gold and tin concentrations were increased in the solution. Since the increase in concentration of gold increased the plating rate, the main reason for increasing the concentration of metals in the solution was to try to increase the plating rate.

The composition of the deposits plated at three different current densities (0.5, 0.8, 2.4 mA/cm^2) was measured using EDS within the SEM. Figure 5-16, showing the tin content of these deposited films, illustrates that AuSn and Au_5Sn are obtainable at high and low current densities respectively.

To determine the useful shelf life, two solutions, 30Ci10Au10Sn-1 and 30Ci10Au10Sn-2, were mixed using the same procedure to perform the experiment in duplicate. Films were electroplated at 2.4 mA/cm^2 after different ageing times. The change in tin content of the deposited films as a function of ageing time is shown in Figure 5-17. The tin content of the plated deposits from 30Ci10Au10Sn-1 stayed unchanged for about seven days. Tin content values obtained from the plated deposits from 30Ci10Au10Sn-2 seemed to drop after only three days. The difference is shelf life of these two solutions is either due to scatter in data or lack of repeatability.

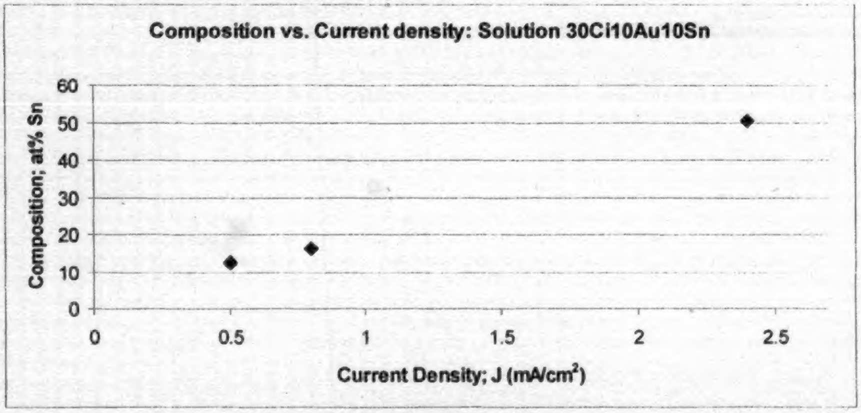

Figure 5-16: Tin content of deposited films at various current densities using the 30Ci10Au10Sn solution.

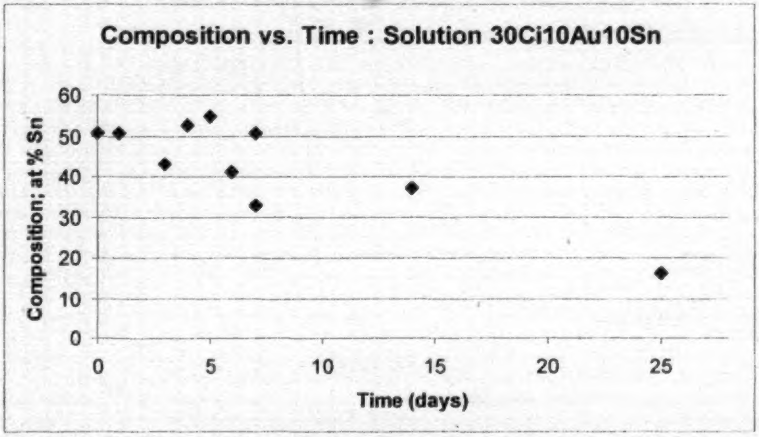

Figure 5-17: Tin content of films deposited at 2.4 mA/cm^2 from the 30Ci10Au10Sn solution as a function of ageing time.

The thickness of the film deposited at 2.4 mA/cm^2 from the 30Ci10Au10Sn fresh solution was measured to obtain the plating rate. Figure 5-18 shows the SE plan view and cross section images from this deposit. At a current density of 2.4 mA/cm^2 and composition of

50 at % tin, the deposition rate from solution 30Ci10Au10Sn (2.7 µm/hr) is higher than the deposition rate obtained from the standard solution (1.9 µm/hr). Further, the plan view image shown in Figure 5-18 shows that the electrodeposited film is stressed.

20 micrometers
10 micrometers

Figure 5-18: SE plan view and cross section images of deposit from 30Ci10Au10Sn solution at 2.4 mA/cm^2.

Solution 25Au was mixed using a higher concentration of $KAuCl_4$ (25 g/L), while the concentration of ammonium citrate was kept at the standard level (200g/L). This solution was mixed to observe the effect of an increase in the concentration of gold in the solution.

The composition of deposits plated at various current densities was measured using EDS within the SEM. Figure 5-19, showing the tin content of these deposited films, illustrates that a composition higher than 20 at% Sn was not obtainable.

To obtain the useful shelf life of the solution, films were electroplated at current densities of 2.4 and 4.0 mA/cm^2 at various ageing times. The tin content of the deposited films at 4.0 mA/cm^2 decreased faster as the solution aged compared to the deposited films at 2.4

mA/cm^2 (Figure 5-20). Films were not deposited after one day of ageing, because gold precipitation was visible at this time and the solution was visibly unstable after one day.

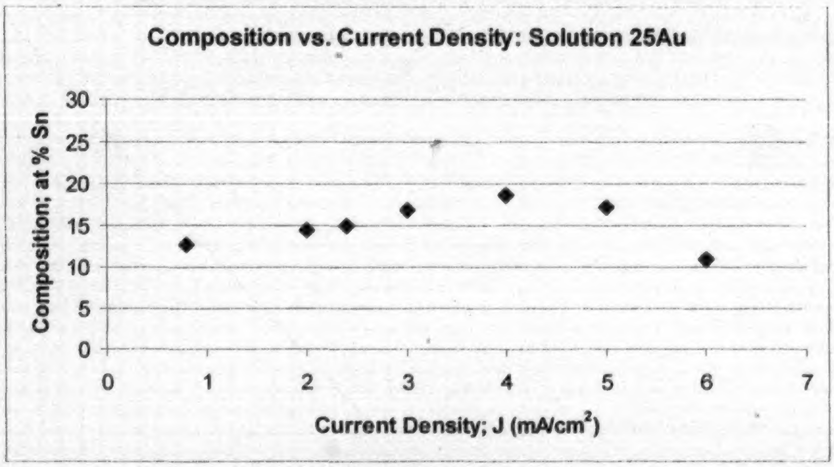

Figure 5-19: Tin content of the deposited films at various current densities using the 25Au solution.

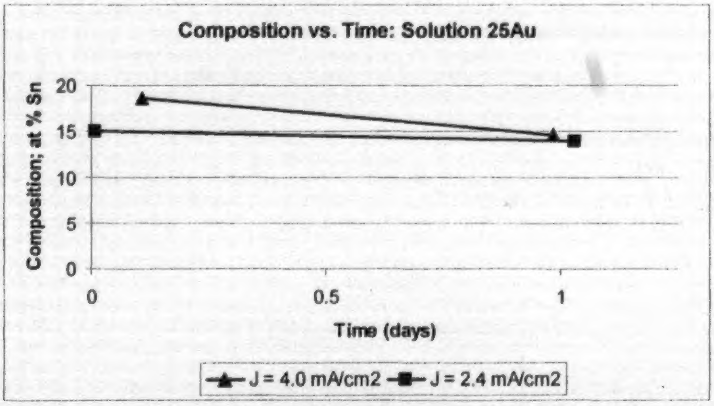

Figure 5-20: Tin content of deposited films from the 25Au solution as a function of ageing time.

The thickness of the films deposited at 2.4 mA/cm^2 and 5.0 mA/cm^2 from the 25Au fresh solution was measured to obtain the plating rate. Figure 5-21 shows SE cross section images of these deposits. At current densities of 2.4 and 5.0 mA/cm^2, the deposition rates were 4.9 and 7.0 μm/hr respectively. Considering the composition of these deposits (about 15-20 at % Sn), the deposition rates are 7 to 10 times faster than the deposition rate at 0.8 mA/cm^2 from the standard solution (0.7 μm/hr). The increase in concentration of gold increased the limiting current density and allowed for the deposition of Au_5Sn phase at higher current densities leading to higher deposition rates.

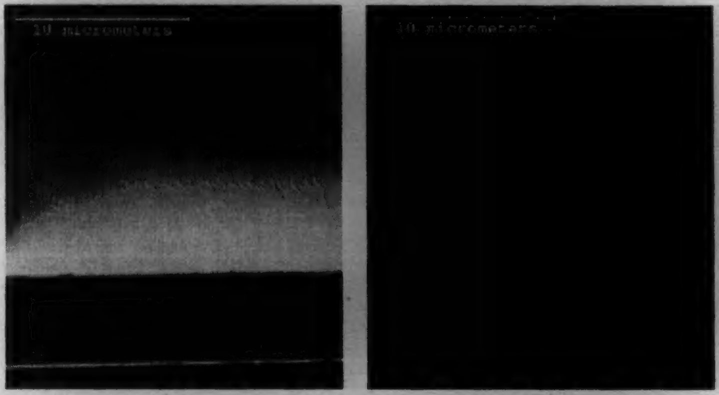

(a) (b)

Figure 5-21: SE cross section images of deposits from the 25Au solution: (a) j = 2.4 mA/cm^2 (plating rate = 4.9 μm/hr) (b) j = 5.0 mA/cm^2 (plating rate = 7.0 μm/hr).

5.3.2.2. Concentration of Ascorbic Acid

UV/Vis spectroscopic analysis presented in [He, Liu et al. 2005] showed that ascorbic acid acted as a reducing agent for the ionic complexes of gold. In an attempt to increase stability and decrease reduction of gold, the concentration of ascorbic acid was decreased to 7 g/L (approximately half the standard amount) and 5 g/L (one third of the standard amount) to observe the effect of ascorbic acid on solution behavior.

The composition of deposits plated at various current densities, from the solution containing 7 g/L of ascorbic acid, was measured using EDS within the SEM . Figure 5-22, showing the tin content of these deposited films, illustrates that decreasing the ascorbic acid concentration shifts the plateaus, shown in Figure 2-11, towards lower current densities, and under most current densities only the phase containing 50 at% Sn

(AuSn) is obtainable. The Au_5Sn phase is obtainable at very low current densities. However, using the one point at current density 0.25 mA/cm^2 is not enough evidence for existence of a plateau for the Au_5Sn phase. Also, very low current densities (lower than 0.5 mA/cm^2) are not desirable due to very low deposition rates.

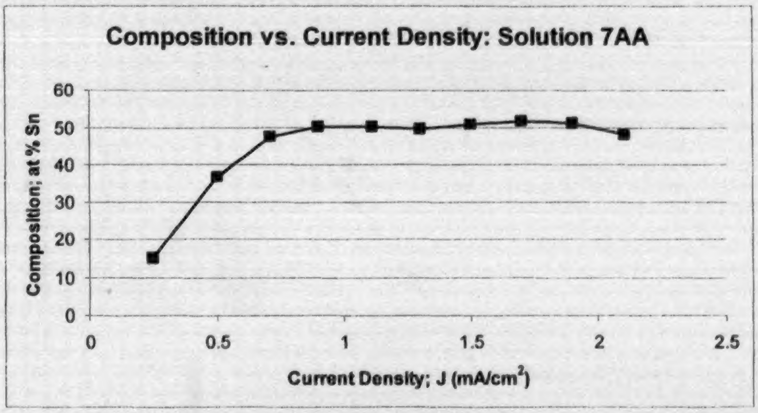

Figure 5-22: Tin content of films deposited at various current densities using the 7AA solution.

The turbidity behavior of the solution containing 5 g/L ascorbic acid was studied, and the resultant curve is shown in Figure 5-23. Similar to the turbidity behavior of the standard solution, the turbidity was initially low for the fresh solution. This value increased with time and peaked out after about 36 hours. Then, the turbidity dropped gradually to near zero and stayed at very low values. The turbidity peak for the 5AA solution appeared about 12 hours later than that for the standard solution. Since the turbidity curve did not show a significant change in the behavior of the solution containing 5 g/L ascorbic acid (one third of the standard amount), it was decided that the turbidity behavior of the solution containing 7 g/L ascorbic acid (about half the standard amount) would not be significantly different either. Thus, the turbidity test for the 7AA solution was not performed.

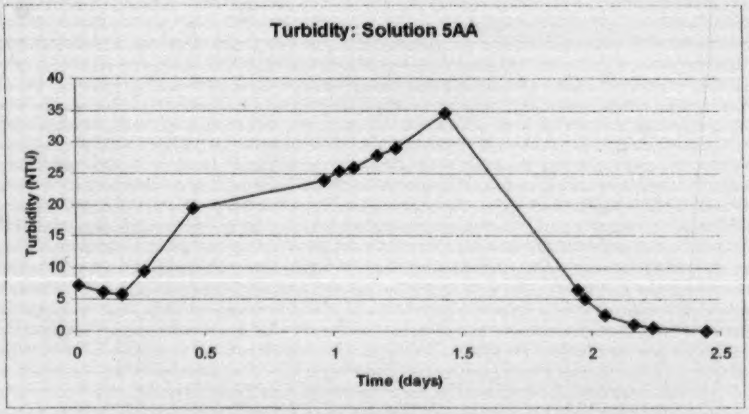

Figure 5-23: Turbidity curve for 5AA solution.

To obtain the useful shelf life of both solutions, films were electroplated at a current density of 1.6 mA/cm^2 after various ageing times. The change in the tin content of films deposited from solutions 7AA and 5AA is shown in Figure 5-24 and Figure 5-25 respectively. The tin content of the plated deposits was constant for at least 48 and 24 hours for 7AA and 5AA solutions respectively, after which the tin content started to decrease.

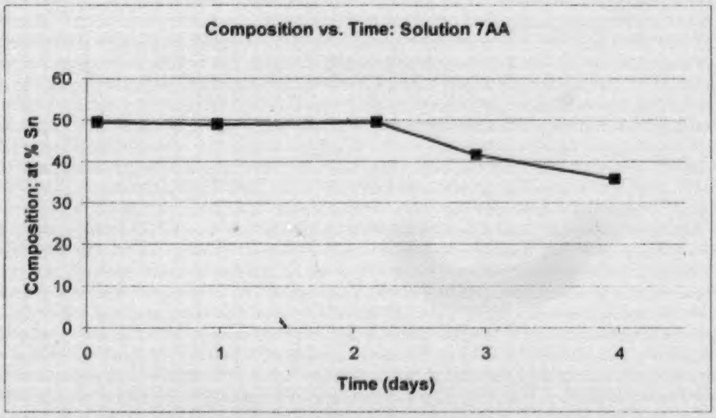

Figure 5-24: Tin content of films deposited at 1.6 mA/cm^2 from the 7AA solution as a function of ageing time.

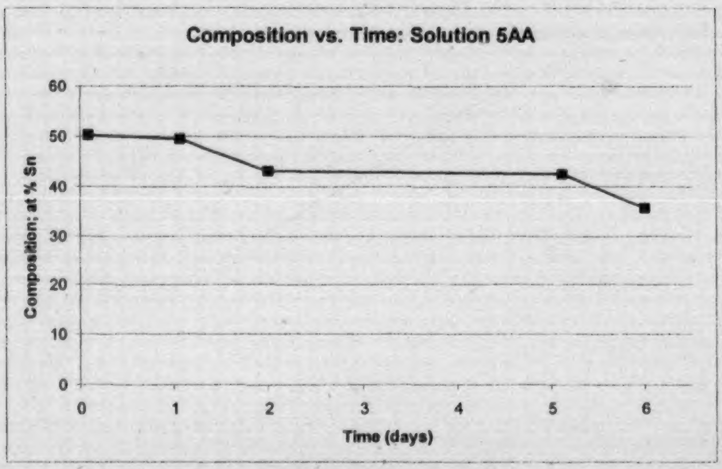

Figure 5-25: Tin content of the films deposited at 1.6 mA/cm^2 from the 5AA solution as a function of ageing time.

The turbidity peak in Figure 5-23 roughly correlates with the electrodeposition results from solution 5AA (Figure 5-25). The peak occurs after 36 hours of ageing, but electrodeposition was performed only after 24 hours and 48 hours of ageing.

Figure 5-26 shows SE plan view images of deposits from solution 7AA. Comparing Figure 5-26 (a) to (c) shows that deposits are smoother at lower current densities. Comparing Figure 5-24 (b) and (d) shows that at a current density of 1.6 mA/cm^2 the deposit morphology deteriorates as the solution ages.

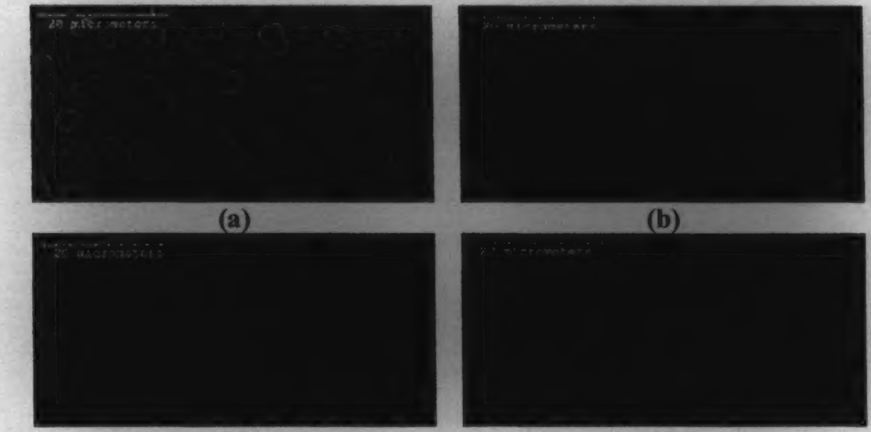

(a) (b) (c) (d)

Figure 5-26: SE plan view images of deposits from 7AA solution: (a) Fresh at 2.0 mA/cm^2 (b) Fresh at 1.6 mA/cm^2 (c) Fresh at 0.8 mA/cm^2 (d) 1 day old at 1.6 mA/cm^2.

5.3.2.3. Concentration of Sodium Sulfite

The concentration of sodium sulfite was increased to 100 g/L (solution 100SS) to observe its effect on the solution.

The turbidity behavior of solution 100SS was studied, and the results are shown in Figure 5-27. Similar to the turbidity behavior of the standard solution, the turbidity was initially low for the fresh solution. This value increased with time and peaked at 12 to 24 hours. Then, the turbidity dropped to near zero and stayed at very low values. The turbidity peak of this solution appeared about 12 hours earlier than that of standard solution. In other words, solutions containing a higher concentration of sodium sulfite showed a shorter shelf life.

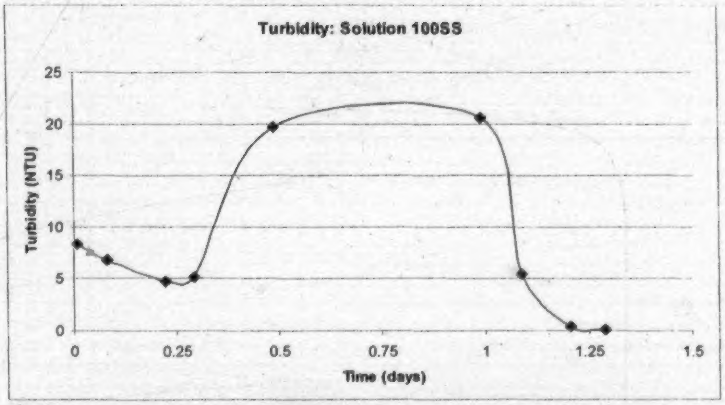

Figure 5-27: Turbidity curve for 100SS solution.

5.3.3. Modified Mixing Procedure and Additives

The results obtained from changes made to the mixing procedure and the addition of other additives to the solution are discussed in the following sections.

5.3.3.1. A3 + L-Ascorbic Acid Solution + B3

The turbidity behavior of the solution obtained following the procedure explained in Section 5.2.3.1 was studied (Figure 5-28). Similar to the turbidity behavior of the standard solution, the turbidity was initially low for the fresh solution. This value increased with time and peaked out after about 36 hours. Then the turbidity dropped gradually to near zero and stayed at very low values. The turbidity peak of this solution appeared about 12 hours later than that of standard solution. In other words, the shelf life of the solution was improved by about 12 hours.

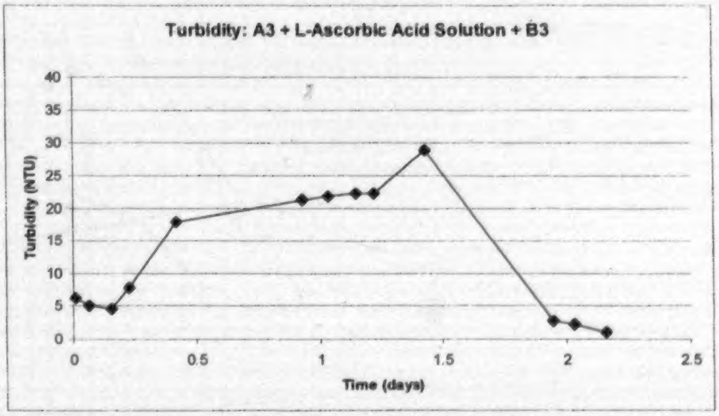

Figure 5-28: Turbidity curve for A3 + L-ascorbic acid Solution + B3 solution.

To obtain the useful shelf life of the solution, films were electroplated at a current density of 2.4 mA/cm^2 after various ageing times. Since the tin content of the deposited films decreased after one day, the rest of the samples were electrodeposited at a lower current density of 1.6 mA/cm^2. Figure 5-29 shows the change in tin content for these deposited films.

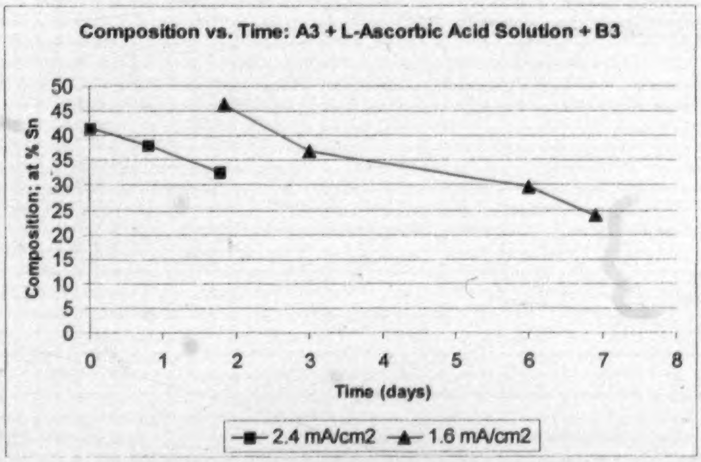

Figure 5-29: Tin content of the deposited films from the A3 + L-ascorbic acid solution + B3 solution as a function of solution age.

Figure 5-30 shows SE plan view images of deposits from the aged A3 + L-ascorbic acid solution + B3 solution. Comparing Figure 5-30 (a) and (b) shows that the deposits are rougher at higher current densities. Comparing Figure 5-30 (b) and (c) shows that at a current density of 1.6 mA/cm^2 the deposit morphology deteriorates as the solution ages. These deposits are rougher than deposits obtained from an aged standard solution.

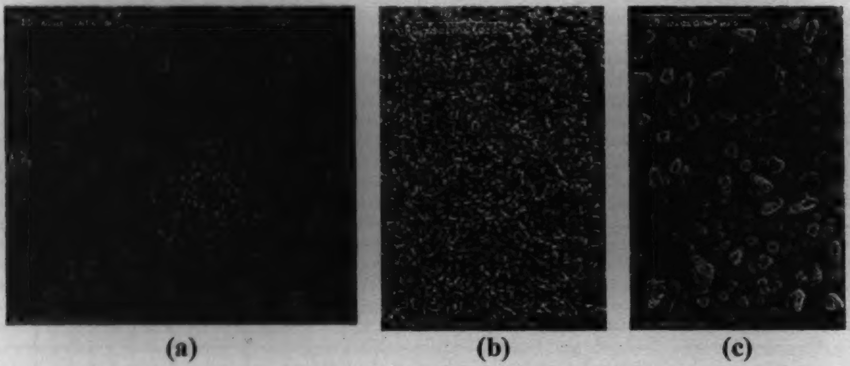

Figure 5-30: SE plan view images of deposits from the A3 + L-ascorbic acid solution + B3 solution: (a) 2 days old at 2.3 mA/cm^2 (b) 2 days old at 1.6 mA/cm^2 (c) 3 days old at 1.6 mA/cm^2.

5.3.3.2. Cupferron

The composition of the plated deposits was measured using EDS within the SEM at various current densities from a solution containing 0.010 g/L of cupferron. Figure 5-31, showing the tin content of these deposited films, illustrates that the addition of cupferron to the solution shifts the plateaus shown in Figure 2-11, towards lower current densities, so that the phase containing 50 at % Sn (AuSn) is obtained at most current densities. The Au_5Sn phase deposits at very low current densities. However, low current densities (lower than 0.5 mA/cm^2) are not desirable for plating due to the very low deposition rates.

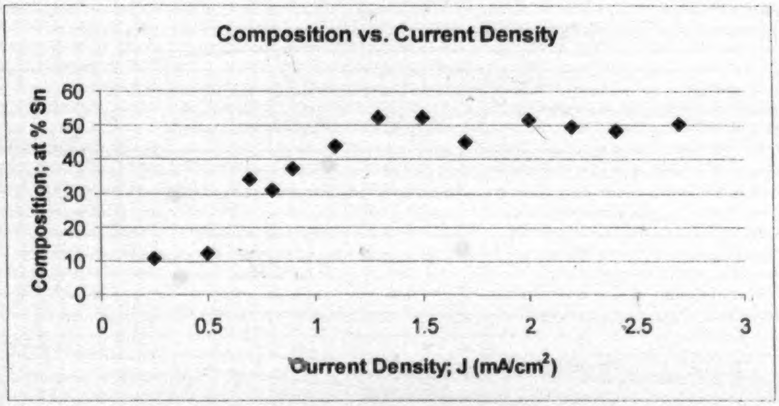

Figure 5-31: Tin content of the films deposited at various current densities from a solution containing cupferron.

To obtain the useful shelf life of the solution, films were electroplated at current densities of 0.8 and 2.4 mA/cm^2 after various ageing times. Figure 5-32 shows the change in tin content of the deposited films. The tin content of the deposits begins to decrease after ageing times of 24 hours or less (for 0.8 mA/cm^2). Thus, the shelf life of the solution was not improved by addition of 0.010 g/L of cupferron.

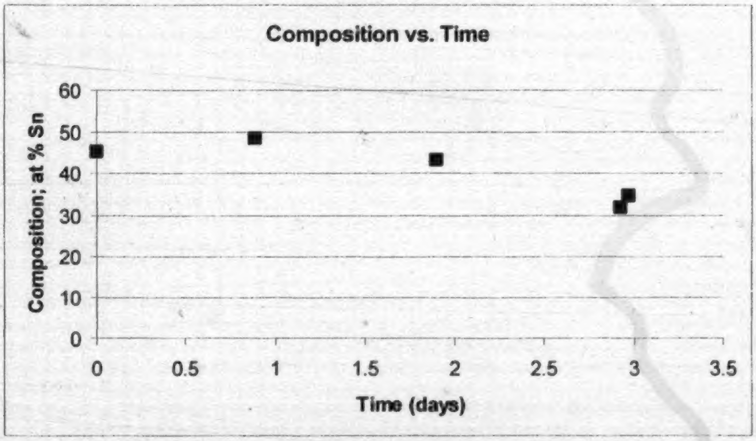

Figure 5-32: Tin content of the films deposited at 2.4 mA/cm^2 from a solution containing cupferron after ageing for various times.

5.3.3.3. Tin Sponge

The composition of deposited films plated from a standard solution containing a small piece of tin sponge was measured using EDS within the SEM. Figure 5-33 shows that a deposit obtained at current density of 0.8 mA/cm^2 from the solution with tin sponge contained a higher amount of tin (about 40 at % Sn) compared with a deposit at the same current density from the standard solution (about 20 at % Sn). This point could belong to the AuSn plateau or a transition region, while for the standard solution this point belongs to the Au_5Sn plateau. This fact shows that the addition of tin sponge to the solution shifts the plateaus, shown in Figure 2-11, towards lower current densities, and mostly the phase containing 50 at % Sn (AuSn) is obtainable. This result is expected, since previous studies showed that higher tin content in the solution results in a higher tin content in the deposits [Sun 1998].

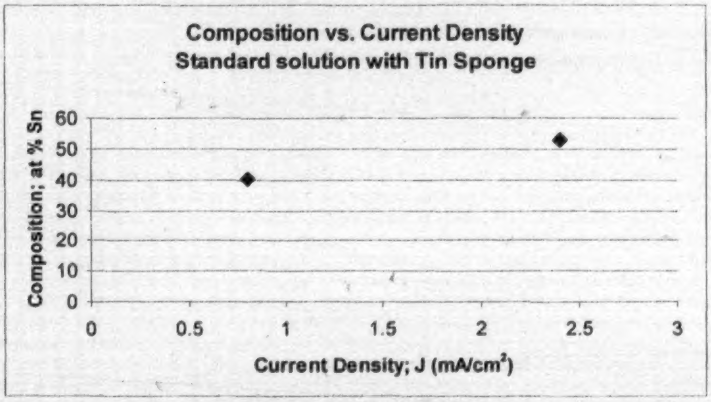

Figure 5-33: Tin content of the deposited films at various current densities from a solution containing tin sponge.

To get an idea of how the increase in concentration of tin in the solution affects the plating rate, the thickness of deposits from fresh solutions were measured. Figure 5-34 shows the SE plan view and cross section images of the deposited films. Using the solution with tin sponge, deposition rates at current densities of 0.8 and 2.4 mA/cm^2 were 0.8 and 2.9 μm/hr respectively. Comparing these measurements with that of a standard solution showed that the deposition rate increased with an increase in the concentration of tin in the solution (i.e., the deposition rate at 2.4 mA/cm^2 from standard solution is 1.9 μm/hr). SE plan view images in Figure 5-34 shows that the deposited films from the solution containing tin sponge are rougher than those from a standard solution.

20 micrometers
20 micrometers

(a) **(b)**

Figure 5-34: SE plan view and cross section images of deposits from a solution containing tin sponge: (a) at 0.8 mA/cm^2 (1.3 μm/hr) (b) at 2.4 mA/cm^2 (2.9 μm/hr).

If the solutions containing tin sponge were stored for more than 12 hours, films formed on the walls of the beaker. Initially the films were believed to be gold due to their golden color, and gold etch (potassium iodide) was used to clean the beaker. However, after cleaning the beaker with gold etch, a film of metallic color was left behind. This film was considered to be tin, and tin etch (hydrochloric acid) was used to clean the beaker further. It was concluded that gold-tin films were electrolessly plated on the walls of the beaker, and the solution was visibly unstable. However, any solution stored with the tin sponge removed remained clear. Thus, storing the solution containing tin sponge did not improve the stability.

5.4. Conclusions

The screening tests explained in this chapter were used to determine the key factors affecting the stability and the plating rate from the Au-Sn solution. Transmission electron microscopy (TEM) analysis was done to monitor gold precipitation during the solution mixing procedure. This TEM study showed that gold precipitates form as soon as ammonium citrate and $KAuCl_4$ are mixed. These nano-size particles remain within the solution throughout the mixing procedure. Thus, the final fresh solution contains nano-size gold particles.

Attempts to eliminate ammonium citrate from the solution were inconclusive, and it was decided to minimize the concentration of ammonium citrate in the solution.

The concentration of solution constituents was modified, which affected deposition behavior. The composition plateaus corresponding to Au_5Sn and AuSn for a standard solution (Figure 2-11) were shifted as solution composition was modified. In some instances both plateaus were not attainable. Plating rates and deposit properties (morphology, stress) were affected changing in the solution concentration. Changing the concentration of ammonium citrate had the most effect on the solution stability, while changing in gold and tin concentrations had the most effect on plating rates.

Attempts to modify the mixing procedure and additives did not improve the stability or plating rate of the solution significantly.

The next chapter covers the statistical design of the experiments approach used to try and optimize the solution concentration. The concentration of ammonium citrate, potassium tetrachloroaurate, and tin (II) chloride are chosen as the three main factors affecting the stability and plating rate for use in the statistical design. This chapter defines the experiment design and covers the experimental procedure. Then, the data are presented, discussed, and analyzed.

Chapter 6: Statistical Design of Experiments for Gold Tin Electrodeposition Process

6.1. Overview

This chapter defines the DOE for the gold tin electrodeposition process. It covers the experimental procedures to obtain data followed by data analysis.

All the obtained data are presented and discussed followed by the data analysis. The data analysis section covers the regression table and examples of the response surface models including the surface, contour and interaction plots. In addition, obtained improved and optimal process settings are presented.

Finally, the data analysis and optimization results are summarized and concluded at the end of this chapter.

6.2. Experimental Design Procedure

6.2.1. Black Box Model

The Au-Sn 'black box' process can be modeled if the factors (inputs) and responses (outputs) are known.

The most effective factors influencing the lifetime and the plating rate were determined using screening tests in Chapter 5. TEM analysis was done to monitor gold precipitation during the mixing procedure. When ammonium citrate and $KAuCl_4$ were mixed, gold precipitation occurred early in the mixing process. Since gold precipitation is observed as a result of aging of the solution, the concentration of ammonium citrate in the solution was believed to be an important factor for the bath lifetime. Furthermore, the experiments in Chapter 5 showed that lifetime increased as the concentration of ammonium citrate decreased. Further experiments revealed that the plating rate was increased (by up to a factor of 3) as the concentration of gold and tin salts in the solution was increased (by up to a factor of 4). Although changes in the concentration of all bath constituents affected the process, only the most vital ones were chosen as key factors for these experiments due to time constraints.

Since the objective of the work involved in this thesis is to find optimal process settings to improve stability and the plating rate, the two main categories of responses include stability (shelf life) and plating rate. The total plating rate of a multilayer film can be improved if the plating rate of each phase (AuSn and Au_5Sn) is improved. To be able to monitor the changes in the plating rate of each phase, the composition of each film should be taken into account.

Deposit composition, plating rate, and quality (roughness, stress) depend on the current density at which the film is electroplated. Thus, deposits are plated from each solution at three different current densities. Current densities of 0.8 and 2.4 mA/cm^2 were chosen, because they are used to electroplate phases Au_5Sn and AuSn from the standard solution respectively. By knowing the composition at these current densities, one could estimate the shifts in the plateaus in Figure 2-11. Further, a current density of 3.5 mA/cm^2 was also chosen. This current density was selected to check for possibility of electrodeposition at higher current densities, which is desirable due to higher electrodeposition rates.

The final Au-Sn 'black box' process model is shown in Figure 6-1.

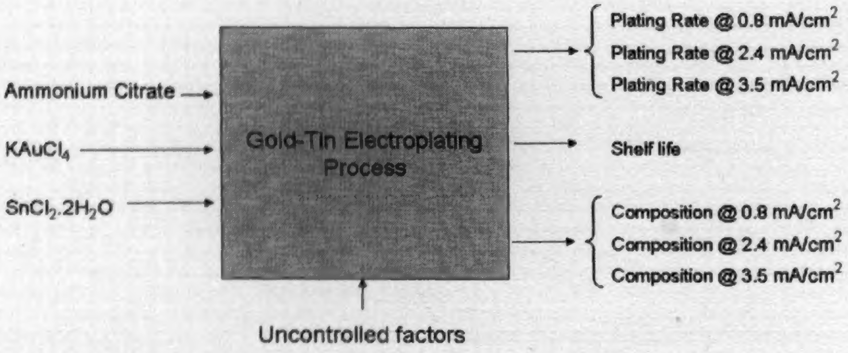
Ammonium Citrate
KAuCl$_4$
SnCl$_2$.2H$_2$O
Gold-Tin Electroplating Process
Uncontrolled factors
Plating Rate @ 0.8 mA/cm^2
Plating Rate @ 2.4 mA/cm^2
Plating Rate @ 3.5 mA/cm^2
Shelf life
Composition @ 0.8 mA/cm^2
Composition @ 2.4 mA/cm^2
Composition @ 3.5 mA/cm^2

Figure 6-1: Black box model of the gold tin electroplating process.

6.2.2. Design Selection

The experimental design can be chosen by considering the design objectives and the number of control factors. As mentioned previously, the objective of these experiments is to find improved and optimal process settings. Therefore, the experiment should be designed to allow for estimation of interaction and quadratic effects, while presenting an idea of the (local) shape of the response surface being investigated. These types of experiments are called response surface method (RSM) designs. The number of control factors for this experimental design is three as chosen from screening tests. Using the design selection guideline table in Chapter 3 (Table 3-1), either of the central composite or the Box-Behnken designs can be used.

The Box-Behnken design was chosen, since it requires fewer runs for the case of three factors compared with a central composite design.

6.2.3. Box-Behnken Design

Since three levels are required for the Box-Behnken design, low, medium, and high levels were chosen for each factor. These values are shown in Table 6-1, and the logic used for selection of these levels for each factor is explained as follows.

Table 6-1: Factor levels for Box-Behnken design.

	Levels		
	Low	**Medium**	**High**
Ammonium Citrate	30 g/L	50 g/L	70 g/L
$KAuCl_4$	5 g/L	10 g/L	15 g/L
$SnCl_2.2H_2O$	5 g/L	10 g/L	15 g/L

Through screening tests, electrodeposition (at a current density of 2.4 mA/cm^2) from solutions containing 30 and 50 g/L ammonium citrate introduced stress in the deposits. Thus, decreasing the concentration of ammonium citrate in the solution was believed to lead to stress in the deposits, and it was decided to set the low level to 30 g/L (the lowest concentration tested). The lower concentration of ammonium citrate was believed to introduce stress even when plating at lower current densities. The first choice for the high level for ammonium citrate factor would be 200 g/L, which is the concentration used for the standard solution. However, the concentration range for the ammonium citrate factor was kept relatively small to get a better idea of the local shape of the responses within the region. Thus, a medium level was chosen first and the high level was calculated based on the chosen low and medium levels. A concentration of 50 g/L was chosen to be the medium level. The combination of all factors is desired to be optimized while the design is centered on this ammonium citrate concentration. This would ideally result in a solution which has the improved shelf life of the solutions containing 50 g/L ammonium citrate, while gold and tin concentrations are adjusted for both phases to be obtained in plating. Since a medium level should be located half way between the high and low levels, the high level was chosen to be 70 g/L.

The low level for both factors $KAuCl_4$ and $SnCl_2.2H_2O$ was chosen to be 5 g/L, which is the concentration used in the standard solution. Screening tests revealed that the plating rate was increased as the concentration of gold and tin salts in the solution increased. Therefore, it was not desirable to decrease the concentration of these factors lower than that of the standard solution, which would result in even lower plating rates. The high level for $KAuCl_4$ was chosen to be 15 g/L, which is three times the standard amount. Higher gold concentrations were not chosen due to its high cost. Higher concentrations could be selected for future work, if this approach proves to be promising. The high level for $SnCl_2.2H_2O$ was also chosen to be 15 g/L to keep the same range of concentration for both metal salts. From the low and high level values, the medium level was chosen to be 10 g/L.

The computer aided design selection feature of DOE PRO XL software was used to create the 3 factors with 3 levels of quantitative design using the Box-Behnken design type. Then the name, low values, and high values of each factor were entered in the software using the values shown in Table 6-1. Further, the number and the names of responses were entered into the software from the black box model of the gold tin electroplating process (Figure 6-1). Seven design sheets were created (one for each response).

Table 6-2 shows the experimental runs required for the Box-Behnken design of the gold tin electroplating process. The center point (sequence number 8) is repeated to provide a measure of process stability, inherent variability and to check for curvature. This repeated run is called sequence 16. Further, sequence numbers 7 and 9 are added to the Box-Behnken design, since these combinations of concentrations were studied briefly in the screening tests. The sequence numbers 7 and 9 correspond to solutions 30Ci10Au10Sn and 50Ci10Au respectively (see Chapter 5). Note that sequence number is the order in which the experiments were performed, and they are also referred to as experimental run or run numbers in the following text.

Table 6-2: Box-Behnken design for gold-tin electroplating process.

Sequence Number	Ammonium Citrate	$KAuCl_4$	$SnCl_2.2H_2O$
1	Low (30)	High (15)	Mid (10)
2	Mid (50)	High (15)	Low (5)
3	Mid (50)	High (15)	High (15)
4	High (70)	High (15)	Mid (10)
5	Low (30)	Mid (10)	Low (5)
6	Low (30)	Mid (10)	High (15)
7	Low (30)	Mid (10)	Mid (10)
8	Mid (50)	Mid (10)	Mid (10)
9	Mid (50)	Mid (10)	Low (5)
10	High (70)	Mid (10)	High (15)
11	High (70)	Mid (10)	Low (5)
12	Low (30)	Low (5)	Mid (10)
13	Mid (50)	Low (5)	Low (5)
14	Mid (50)	Low (5)	High (15)
15	High (70)	Low (5)	Mid (10)

6.3. Experimental Procedure

Solutions were mixed for each experimental run of the Box-Behnken design following a similar procedure to the standard procedure.

120 ml clear glass bottles with a screw lid were used to mix and store the solutions. A Corning PC-420 stirrer/hot plate and a Mettler H32 balance were used for stirring and weighing throughout the procedure.

For each solution of the experimental runs, an appropriate amount of tri-ammonium citrate was weighed, and de-ionized water was added as about 60 percent of the total volume of the solution. The ammonium citrate was dissolved, and the solution became clear and colorless.

The weighing procedure was repeated, and an appropriate amount of potassium tetrachloroaurate was added to the ammonium citrate buffer solution. After dissolving the gold salt completely, the solution became clear with a golden, yellow color. For the experimental runs containing 15 g/L of potassium tetrachloroaurate, the clear solution had an orange color at this point.

60 g/L of sodium sulfite was then added to the solution. As the sodium sulfite dissolved in the solution, the color of the solution brightened slightly. Once all the powder seemed to be dissolved, the solution was left to stand to turn colorless. This time varied for each experimental run. The solutions with higher potassium tetrachloroaurate concentration took longer to turn clear. The solutions were left over night to assure complete dissolution. No solution degradation is expected during this time, since previous research had shown that a solution of $KAuCl_4$, ammonium citrate, and sodium sulfite (with the same order of mixing used in this work) could be stored for twelve months without any further color change or visual precipitation and with very little change in turbidity [He, Liu et al. 2006].

15 g/L of L-ascorbic acid was then added to the solution followed by the appropriate amount of tin (II) chloride. It should be noted that once L-ascorbic acid was added to the colorless solution, the solution turned light yellow in color.

The solution was transferred into a glass graduated cylinder, and de-ionized water was added to give the desired total volume. This final solution, which was clear with a yellow tinge, was poured back into the bottle and stirred to ensure uniformity.

As mentioned before, deposit composition, deposition rate, and shelf life were monitored as process responses. Films were electroplated at each of the three chosen current densities for 60 minutes from a fresh solution. A Dynatronix PR 0.1-10 pulsed current power supply with ON and OFF time ranges of 0-9.9 ms was used for the experiments. A pulse current, with an ON time of 2 ms and an OFF time of 8 ms, was used for all the plating experiments. A 50 ohm resistor was connected in series with the plating circuit and the peak current density of the waveform was measured using a Fluke 123 Scopemeter connected in parallel with the resistor. A schematic diagram of the electroplating circuit is identical to that shown in Figure 4-7.

The cathodes and anodes were cleaved pieces of Si wafers coated with Ti/Au and Ti/Pt metallization respectively. The plating area of the cathode was defined using blue tape. The plating areas of the used cathodes were in the range of 0.5 to 0.9 cm^2.
The compositions of the deposited films were measured using EDS in a LEO 435VP SEM. For each sample, three areas were selected for EDS analysis, and these composition values were used in the analysis. The plating rate of each deposit was measured through thickness measurements of the deposited films using profilometry. This technique is described at the end of this section. Before deposition a small "v" shape mark was drawn on the cathode using a Sharpie ultra fine marker. After deposition, the mark was rinsed off using acetone, and a Tencor AlphaStep 200 profiler was used to measure the thickness of the deposited film. Thickness was measured at two or three points relative to the "v" shape mark, and these values were used in the analysis. Note, that all measured values for composition and plating rates were used in the analysis as opposed to using an average value.

The stability of each solution was monitored through turbidity measurements using a VWR model 66120-200 turbidity meter. The time corresponding to the peak of the turbidity versus time curve was chosen as the shelf life. However, if precipitation was observed before occurrence of a turbidity peak, the time corresponding to precipitate observation was chosen as the shelf life. The turbidity measurements were performed at least two times, and all obtained values were considered in the data analysis (as opposed to an average value). It should be noted that there are limitations to the shelf life measurements using turbidity, since the shelf life is not monitored directly. To monitor the shelf life directly requires electrodeposition from a solution for each experimental run as a function of aging, which due to time constraints was not feasible.

All obtained values for turbidity, composition and plating rate at three current densities were entered in the design sheets created in DOE PRO XL.

6.3.1. Profilometry

Profilometry is a non-destructive and easy technique for thickness measurement. It consists of electromagnetically sensing the mechanical movement of a stylus while it scans across the topography of a substrate. In this study, a step was made by the thickness difference between the untouched area under the "v" shape mark and the deposited solder. The measurement resolution depends on the radius of the stylus and the geometries of the features. The factors that limit the accuracy of the measurement are stylus penetration and scratching of films (i.e., soft films), substrate roughness (introduces noise), and vibration of the equipment [Ohring 2002].

Tencor AlphaStep 200 profiler, used in this study, was equipped with a diamond-tipped stylus of 12.5 μm radius. This profiler was capable of probing maximum sample thickness and diameter of 16.5 mm and 162 mm respectively. The resolution for the kilo Angstrom and micron modes were 5 Angstrom and 5 nanometers respectively.

6.4. Results and Discussions

6.4.1. Composition and Plating Rate

The average composition values for the deposited films obtained using EDS are summarized in Table 6-3. The compositions between 10 and 20 at% tin are considered to be the Au_5Sn phase and are underlined and in italics. The compositions between 45 and 55 at% tin are considered to be the AuSn phase and the values appear in bold. Any compositions between 20 and 45 at% tin are considered to be a mixture of the two phases. The average values of plating rates measured through thickness measurements are also summarized in Table 6-3. The deposited film from experimental run 3 at current density of 3.5 mA/cm^2 was stressed, and the film peeled off. Therefore, the deposition rate of this experiment is unknown and a value of zero was entered for analysis purposes. All the measured values for composition and plating rates are presented in complete design sheets in Appendix B.

Table 6-3: Compositions and plating rate results for the Box-Behnken design.

Run #	J_1= 0.8 mA/cm^2 Comp. (Sn at%)	Rate (µm/hr)	J_2= 2.4 mA/cm^2 Comp. (Sn at%)	Rate (µm/hr)	J_3= 3.5 mA/cm^2 Comp. (Sn at%)	Rate (µm/hr)
1	*15.5*	0.8	**49.0**	3.2	**49.2**	4.8
2	*15.7*	1.0	40.1	3.2	30.7	5.1
3	*15.9*	0.8	44.9	4.5	**49.7**	0
4	*12.0*	1.0	39.5	4.1	43.3	6.5
5	34.9	1.4	**45.3**	4.1	39.3	4.9
6	**47.1**	0.8	**47.0**	3.0	**52.0**	4.1
7	21.4	0.5	**46.5**	3.7	**50.4**	6.3
8	*14.8*	0.6	42.6	3.1	**46.9**	6.9
9	*16.4*	1.0	44.9	3.5	37.0	5.5
10	*15.9*	0.7	**45.7**	3.4	**45.8**	4.1
11	*14.9*	1.0	41.5	4.6	33.3	4.9
12	**47.0**	0.7	**52.4**	3.4	**54.0**	5.2
13	43.8	1.3	40.4	2.1	**48.2**	3.6
14	42.0	1.2	**53.4**	3.0	**47.7**	3.8
15	40.3	1.2	**51.0**	2.9	43.2	4.4
16	*12.2*	0.5	38.6	3.7	**50.9**	6.4

6.4.1.1. Deposit Quality

Secondary electron SEM images of the deposited films for all the experimental runs for the Box-Behnken DOE are shown in Table 6-4. The roughness of the deposited films increases as the current density increases. Also, in some runs an increase in the current density causes stress in the deposited films. Run 3 and 7 show examples of stressed films at high current densities. However, in some runs an increase in current density does not change the morphology of the deposits substantially (i.e., run 9).

Table 6-4: SE plan view images of deposits for the Box-Behnken design.

Run #	J_1= 0.8 mA/cm^2	J_2= 2.4 mA/cm^2	J_3= 3.5 mA/cm^2
1	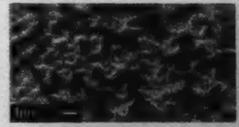	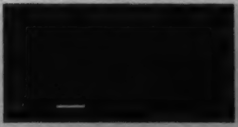	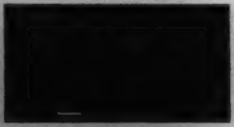
2	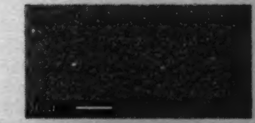		
3			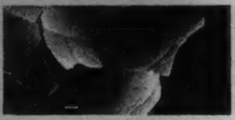
4	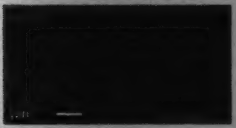	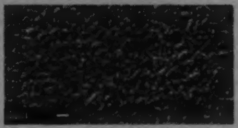	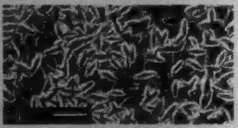
5			
6			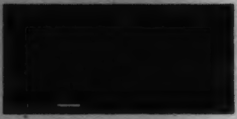
7	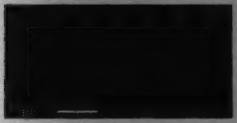		
8		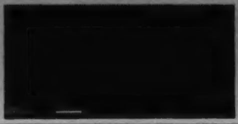	

Table 6-4: SE plan view images of deposits from DOE experimental runs (continued).

Run #	J_1= 0.8 mA/cm^2	J_2= 2.4 mA/cm^2	J_3= 3.5 mA/cm^2
9	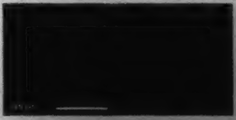		
10	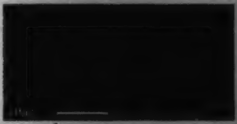	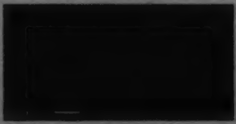	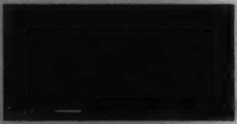
11			
12		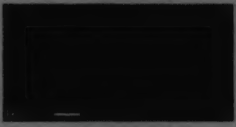	
13			
14			
15			
16			

6.4.2. Shelf Life

The shelf life values obtained from the turbidity curves are shown in Table 6-5. These values relate to the time corresponding either to the peak of the turbidity curve or the precipitation time, which ever was lower. The value from the turbidity curve was recorded, unless precipitation was observed before a turbidity peak, in which case the precipitation time was recorded. These shelf life values were rounded down to the closest half day. For example, the turbidity peaks of experimental run 6 were at 4.1 and 4.9 days which were rounded down to 4.0 and 4.5 days respectively. Turbidity curves obtained from all experimental runs are shown in Appendix A.

Table 6-5: Shelf life results for the Box-Behnken design.

Run #	Trial 1 (days)	Trial 2 (days)
1	5.5	6.0
2	6.0	11.0
3	3.0	2.5
4	2.5	4.0
5	10.5	11.0
6	4.5	4.0
7	7.5	9.0
8	6.0	5.0
9	9.0	11.0
10	3.0	2.5
11	8.0	8.0
12	3.0	11.0
13	13.0	15.0
14	3.5	4.0
15	4.5	5.0
16	3.5	1.0

Examination of the turbidity curves shows that the turbidity behavior of the solution for each experimental run may vary through replications. Examples of solutions with excellent and poor repeatability through replications are runs 11 and 12 respectively. For run number 10, the peaks of the two obtained turbidity curves were very close. One peak appeared just after three days, while the other peak appeared just before three days. To be consistent with the method of obtaining all the shelf life values, the value was rounded down to 2.5 days for the peak appearing just before 3 days.

The turbidity behavior of solutions for some experimental runs differs from that of the standard behavior. As an example, precipitation occurs before a peak is reached (i.e., run 3). Since the precipitate size is small initially, observing visible precipitates is not expected before agglomeration and settling of the precipitated gold, which occurs after reaching a peak. The reason for this behavior is unclear to the author. However, one possible explanation is that there may have been a sharp undetected peak between two consecutive turbidity measurements. Another difference from the standard behavior, for some solutions, was the high value of the initial turbidity for fresh solutions (i.e., runs 3 and 6). This is believed to be due to the higher concentration of tin (II) chloride in these solutions. Although the powder seems to be dissolved upon visual examination, the time required for tin to dissolve thoroughly may vary. At higher tin (II) chloride concentrations, the high turbidity value may correspond to the undissolved tin salt in the solution during early stages of aging. However, no tin particles were observed in the deposits (using the SEM) from these fresh solutions.

6.5. Data Analysis

The completed design sheets created in DOE PRO XL (presented in Appendix B) were used to analyze the design. The regression tables and the response surface models (RSM) including the surface, contour, and interaction plots are presented and discussed in the following sections. These sections are followed by presentation of improved and optimal process settings obtained from design analysis.

6.5.1. Regression Tables

Once the design sheets were completed, multiple response regression tables were created using the software. The software calculates the coefficients for the quadratic equation describing the surface model for each response. The Box-Behnken design in DOE PRO

XL software is coded automatically (i.e., the actual high and low values will be mapped to 1 and -1). Two regression tables based upon coded and actual inputs were created. However, the uncoded table p-values (explained below) are not guaranteed to be correct. Thus, the p-values from the coded table were used for analysis.

The coded and un-coded $\hat{Y}$ (Y-hat) model regression tables for shelf life, composition, and plating rate responses are shown in Tables 6-6 to 6-8. The coefficients for the RSM model obtained for each response are shown under the heading "Coeff". Titles Const, A, B, and C correspond to coefficients b_0, b_1, b_2, and b_3 used in Equation 3-1 (see Chapter 3). Further, x_1, x_2, and x_3 refer to the three factors ammonium citrate, $KAuCl_4$, and $SnCl_2.2H_2O$ respectively.

R^2 values, which are a measure of the fit of the regression model, for each response are presented. The R^2 value is the square of the correlation between the response values and the predicted response values. A value of 1 indicates a perfect fit of the model, and a value closer to 1 indicates a better fit. For example, an R^2 of 0.7809 (for the shelf life response) means that the fit explains 78.09% of the total variation in the data about the average. The best model was fitted to plating rate response at a current density of 3.5 mA/cm^2 with an R^2 value of 0.8777, meaning this response can be modeled well with a quadratic equation (compared to the other responses). However, the worst fit model was for plating rate response at current density of 2.4 mA/cm^2 with an R^2 value of 0.4423. In other words, only about 44 percent of the total variation in the data about the average could be fitted to a quadratic model for this response. Thus this response does not fit to a quadratic equation well.

Values under the heading P (2 Tail) are a measure of the significance of an effect and refer to the probability that a term does not belong in a regression model. As a rule of thumb, the factor is considered highly significant if this value is less than 0.05. If the P (2 Tail) value is less than 0.05, the number is shown in bold. If this value is slightly more than 0.05, the number is shown in italics.

As expected from the screening tests, all factors are significant for the shelf life response. Further, the $SnCl_2.2H_2O$ factor is the most significant among them. Comparing the P (2 Tail) values shows that, although all factors are significant, the concentration of tin (II) chloride in the solution has the most effect on the stability of the solution. However, the concentration of ammonium citrate was shown to be a key factor for stability through screening tests, and it was expected to be the most significant factor for shelf life response. One reason for ammonium citrate not having the most significant coefficient for shelf life response might be its low concentration value compared to the standard solution. The average concentration of ammonium citrate for these experiments was one fourth of the standard amount (50 g/L vs. 200 g/L). The small change in the concentration of ammonium citrate ($\pm$20 g/L) at such a low level might not be as significant for the shelf life response as it might have been at higher concentrations.

For the composition responses, ammonium citrate and $KAuCl_4$ factors are significant for plating at all three current densities. However, $SnCl_2.2H_2O$ is only significant for composition at 2.4 and 3.5 mA/cm^2. This is expected, since more tin is usually plated at higher current densities. The coefficients AA, BB, CC are all significant for the response at 0.8 mA/cm^2. Further, the P (2 Tail) value for coefficient AC is close to 0.05 at this low current density corresponding to a joint effect of ammonium citrate and tin concentrations in the solution. Based on this result, the ratio of concentrations of ammonium citrate and $SnCl_2.H_2O$ in the solution may affect the composition of the deposit at the low current density. The same applies for the coefficients AB and BC at a current density of 2.4 mA/cm^2. Finally, the coefficient BC is significant for electrodeposition at 3.5 mA/cm^2, and the relative amount of gold and tin in the solution plays a significant role in determining which gold-tin phase is obtainable.

For the plating rate responses, the ammonium citrate factor is not significant at the three current densities. This implies that ammonium citrate concentrations in the solution do not play a significant role in determining the plating rates. This was expected, since screening tests showed that the plating rate was affected by the amount of the metal salts in the solution. $KAuCl_4$ is only significant for plating rates at current densities of 0.8 and 2.4 mA/cm^2, while $SnCl_2.2H_2O$ is only significant for 0.8 and 3.5 mA/cm^2. Similar to composition, the coefficients AA, BB, CC are all significant for the plating rate response at 0.8 mA/cm^2. The value of coefficient AA (ammonium citrate) is very small, however, and a small change in its concentration will not lead to a large change in the plating rate. Further, the P (2 Tail) value for coefficients AB and BB are close to 0.05 at 2.4 mA/cm^2. This result corresponds to a possible significance of a joint effect of ammonium citrate and gold concentrations in the solution, meaning that although ammonium citrate itself is not significant at this current density, its relative amount to the gold concentration in the solution may affect the results. Finally, the coefficients AB, BC, BB and CC are significant for electrodeposition at 3.5 mA/cm^2. The relative amount of gold to both ammonium citrate and tin in the solution plays a significant role in determining the deposition rates.

Table 6-6: Y-hat model regression table for shelf life response.

		Shelf Life		
		Coded		**Un-coded**
Factor	**Name**	**Coeff**	**P(2 Tail)**	**Coeff**
Const		4.43E+00	**0.0001**	3.54E+01
A	Ammonium citrate	-1.39E+00	**0.0079**	-1.82E-01
B	$KAuCl_4$	-1.16E+00	**0.0292**	-1.17E+00
C	$SnCl_2.2H_2O$	-3.49E+00	**0.0000**	-2.85E+00
AB		-6.25E-02	0.9298	-6.25E-04
AC		3.13E-01	0.6601	3.13E-03
BC		1.13E+00	0.1228	4.50E-02
AA		3.52E-01	0.6424	8.80E-04
BB		6.45E-01	0.3821	2.58E-02
CC		1.93E+00	**0.0170**	7.73E-02
R^2		0.7809		
Std Error		1.9828		

Table 6-7: Y-hat model regression tables for composition responses.

Factor	**Name**	**Composition at 0.8 mA/cm^2**			**Composition at 2.4 mA/cm^2**			**Composition at 3.5 mA/cm^2**		
		Coded		**Un-coded Coeff**	**Coded**		**Un-coded Coeff**	**Coded**		**Un-coded Coeff**
		Coeff	**P(2 Tail)**		**Coeff**	**P(2 Tail)**		**Coeff**	**P(2 Tail)**	
Const		1.18E+01	**0.0000**	1.63E+02	4.17E+01	**0.0000**	6.50E+01	4.85E+01	**0.0000**	5.03E+01
A	Ammonium citrate	-7.10E+00	**0.0000**	-1.94E+00	-2.00E+00	**0.0070**	-6.81E-01	-3.57E+00	**0.0005**	3.18E-02
B	$KAuCl_4$	-1.42E+01	**0.0000**	-1.10E+01	-2.97E+00	**0.0002**	-9.57E-01	-2.52E+00	**0.0149**	-3.29E+00
C	$SnCl_2.2H_2O$	1.71E+00	0.1301	-5.20E+00	2.36E+00	**0.0017**	3.36E-01	5.60E+00	**0.0000**	3.05E+00
AB		7.75E-01	0.6385	7.75E-03	-2.03E+00	*0.0579*	-2.03E-02	1.23E+00	0.3831	1.23E-02
AC		-2.78E+00	*0.0971*	-2.78E-02	6.33E-01	0.5444	6.33E-03	-5.00E-02	0.9716	-5.00E-04
BC		5.00E-01	0.7616	2.00E-02	-2.08E+00	*0.0522*	-8.30E-02	4.86E+00	**0.0013**	1.94E-01
AA		7.13E+00	**0.0002**	1.78E-02	2.88E+00	**0.0129**	7.20E-03	-1.31E+00	0.3839	-3.28E-03
BB		9.45E+00	**0.0000**	3.78E-01	2.76E+00	**0.0138**	1.10E-01	2.81E-01	0.8465	1.12E-02
CC		8.42E+00	**0.0000**	3.37E-01	8.13E-01	0.4664	3.25E-02	-4.81E+00	**0.0026**	-1.92E-01
	R^2	0.8658			0.6078			0.6914		
	Std Error	5.6682			3.5867			4.8413		

Table 6-8: Y-hat model regression tables for plating rate responses.

Factor	Name	Rate at 0.8 mA/cm^2			Rate at 2.4 mA/cm^2			Rate at 3.5 mA/cm^2		
		Coded		Un-coded Coeff	Coded		Un-coded Coeff	Coded		Un-coded Coeff
		Coeff	P(2 Tail)		Coeff	P(2 Tail)		Coeff	P(2 Tail)	
Const		5.0E-01	**0.0000**	4.41E+00	3.48E+00	**0.0000**	5.6E+00	6.67E+00	**0.0000**	-9.0E+00
A	Ammonium citrate	3.9E-02	0.3213	-4.4E-02	1.5E-01	0.2409	-9.8E-02	1.6E-01	0.2994	-5.1E-02
B	$KAuCl_4$	-8.8E-02	**0.0400**	-2.1E-01	4.4E-01	**0.0020**	1.3E-01	-1.0E-01	0.5359	1.4E+00
C	$SnCl_2.2H_2O$	-1.6E-01	**0.0005**	-3.1E-01	-7.7E-03	0.9512	-1.8E-01	-8.2E-01	**0.0000**	2.2E+00
AB		-3.8E-02	0.5113	-3.8E-04	3.6E-01	*0.0554*	3.6E-03	6.6E-01	**0.0090**	6.6E-03
AC		7.9E-02	0.1755	7.9E-04	1.1E-01	0.5528	1.1E-03	-1.1E-01	0.6395	-1.1E-03
BC		2.1E-02	0.7158	8.4E-04	1.9E-01	0.2977	7.7E-03	-1.4E+00	**0.0000**	-5.6E-02
AA		1.7E-01	**0.0129**	4.2E-04	2.4E-01	0.2538	5.9E-04	1.8E-02	0.9433	4.4E-05
BB		2.6E-01	**0.0002**	1.0E-02	-3.7E-01	*0.0647*	-1.5E-02	-1.4E+00	**0.0000**	-5.8E-02
CC		2.9E-01	**0.0001**	1.2E-02	6.5E-02	0.7454	2.6E-03	-2.1E+00	**0.0000**	-8.6E-02
	R^2	0.6629			0.4423			0.8777		
	Std Error	0.1783			0.5657			0.6922		

In the above tables, numbers listed under Std Error for each response can be used as an estimate of the standard deviation of that response. This value is about 2 days for the shelf life response. The reason for the relatively large Std Error value is the variation of shelf life values obtained through turbidity test replications. However, the worst case for the shelf life can be calculated by subtracting two days from the predicted age. Thus, the solutions with a predicted shelf life of three days (or less), are considered to have the worst case shelf life of one day (or less). When several solution options are available or through optimization, the solutions with a predicted shelf life of three days (or less) can be eliminated for further studies, because, they do not provide an effective improvement in the shelf life.

The standard error for the composition and plating rate responses are also shown in the Tables 6-6 to 6-8. These errors contain the possibility of composition and thickness variation across a substrate. This is because all the measured composition and rates for all the experimental runs, along with their standard deviation, were considered in the analysis.

The excel sheet containing the regression table, also contains a prediction region in which a combination of factor values can be entered to obtain predicted responses. This table uses the coefficients from the regression table and Equation 3-1 to calculate the predicted responses. An example of a prediction region is shown in Table 6-9.

Table 6-9: An example of the prediction region.

Factor	Name	Low	High	Factor Value
A	Ammonium Citrate	30	70	**45**
B	$KAuCl_4$	5	15	**7**
C	$SnCl_2.2H_2O$	5	15	**12**
Multiple Response Prediction				
		99% Confidence Interval		
Response	**Y-hat**	**Lower Bound**		**Upper Bound**
Sn at % @ 0.8 mA/cm^2	28.3	20.2		36.3
Sn at % @ 2.4 mA/cm^2	46.4	39.8		52.9
Sn at % @ 3.5 mA/cm^2	51.4	30.7		72.2
Rate @ 0.8 mA/cm^2	0.6	0.6		0.7
Rate @ 2.4 mA/cm^2	3.1	2.3		3.9
Rate @ 3.5 mA/cm^2	5.9	3.7		8.2
Shelf Life	6	4		7

6.5.2. Surface, Contour, and Interaction Plots

Surface plots graphically present the predicted model in three dimensions, where the x, y, and z axes present the two independent variables and the response respectively. Since there were three factors used for the Box-Behnken design, one factor had to be kept at a constant level to create each response surface plot. The DOE PRO XL software was utilized to create plots from the obtained coefficients in the coded regression table and the value of the constant factors. An example of one such plot is shown in Figure 6-2.

Contour plots are another way of representing a 3-dimensional surface. In a contour plot iso-response lines were graphed while two independent variables were displayed on the x and y axes. Table 6-10 to Table 6-12 summarize the contour plot types obtained from creating the contour and surface plots for all combinations of the factors while keeping one factor at the low, medium, and high levels. All plots created are available on a CD at Ivey's group Lab. The contour plot type "trough" refers to a pattern similar to the peak type with the inner iso-response circle referring to a minimum region. An example of a surface plot corresponding to the "trough" contour type is shown in Figure 6-2. The contour plot type "hill side/rising ridge" refers to a pattern similar to the hillside type with a small curvature to the iso-response lines (all other plot types are defined in

Chapter 3). An example of a contour plot with the “hill side/rising ridge” type is shown in Figure 6-3.

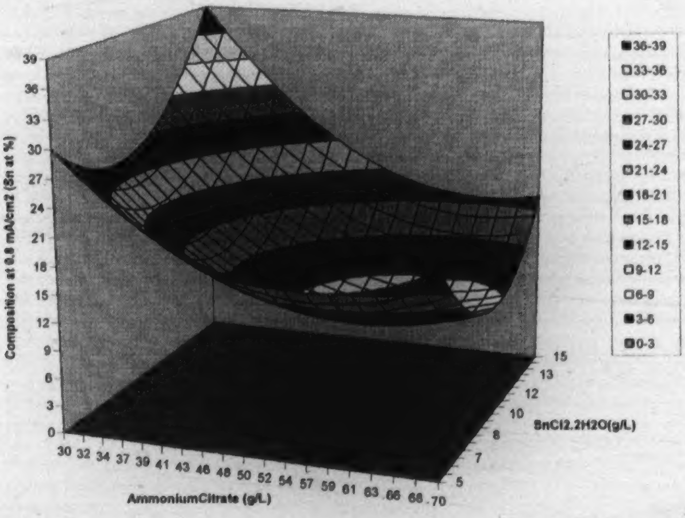

Figure 6-2: Y-hat model surface plot of composition at 0.8 mA/cm^2 for ammonium citrate vs. $SnCl_2.2H_2O$ while keeping $KAuCl_4$ constant at 15 g/L (trough type).

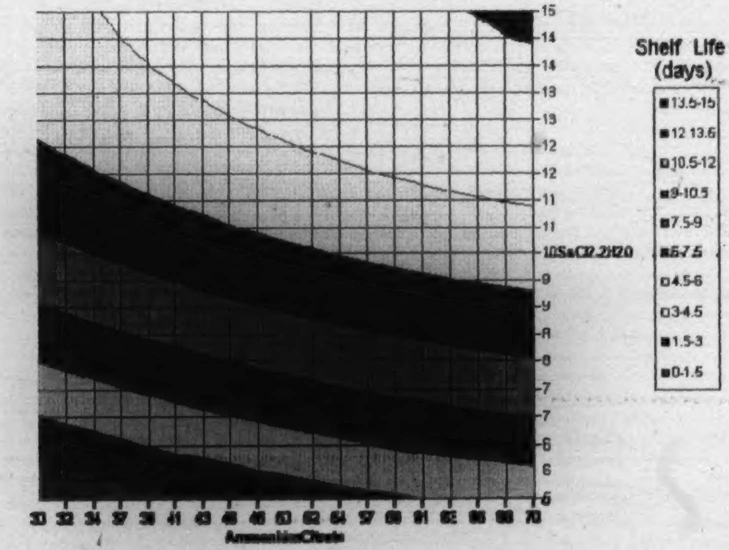

Figure 6-3: Y-hat model contour plot of shelf life for ammonium citrate vs. $SnCl_2.2H_2O$ while keeping KAuCl4 constant at 5 g/L.

Interaction plots, as the name implies, were used to determine the existence of interaction between factors. The created interaction plots display the response value and the levels of one of the factors on the y and x axis respectively, and separate lines are plotted for each level of the other factor. Interaction exists when the effect of each factor depends on the levels of the other factors, and the factors do not interact if the lines in the corresponding interaction plot are parallel.

Table 6-10 to Table 6-12 summarize the interactions obtained from plots for all combinations of the factors while keeping one factor at the low, medium and high levels. In these tables, yes and no refer to existence of or lack of interaction respectively. In some interaction plots, the lack of parallelism in the changes of the response is not readily obvious if the lines do not intersect. To decide if these factors were interacting, trend lines were fitted to the lines and their equations were compared. If the trend lines had similar equations with different intercepts, parallelism was confirmed. This confirmation represents a lack of a factor interaction effect. Figure 6-4 is an example of an interaction plot showing that for the rate response at 2.4 mA/cm^2, factors ammonium citrate and $KAuCl_4$ interact while the $SnCl_2.2H_2O$ concentration is kept constant at 5 g/L. Figure 6-5 is an example of an interaction plot showing that for the shelf life response, factors ammonium citrate and $KAuCl_4$ do not interact while $SnCl_2.2H_2O$ concentration is kept constant at 5 g/L. All the created interaction plots are available on a CD within Ivey's group.

Table 6-10: Interactions and contour plot types for ammonium citrate and KAuCl$_4$ at constant SnCl$_2$.2H$_2$O concentrations.

Ammonium Citrate vs. KAuCl$_4$						
	Interaction			Contour Plot Type		
Constant SnCl$_2$.2H$_2$O	5 g/L	10 g/L	15 g/L	5 g/L	10 g/L	15 g/L
Shelf Life	no	no	yes	hill side/rising ridge	rising ridge	rising ridge
Rate @ 3.5	yes	yes	yes	saddle	saddle	saddle
Rate @ 2.4	yes	yes	yes	saddle	saddle	saddle
Rate @ 0.8	yes	yes	yes	trough	trough	trough
Sn at % @ 3.5	yes	yes	yes	rising ridge	rising ridge	rising ridge
Sn at % @ 2.4	yes	yes	yes	trough	rising ridge	rising ridge
Sn at % @ 0.8	no	no	no	trough	trough	trough

Table 6-11: Interactions and contour plot types for ammonium citrate and SnCl$_2$.2H$_2$O at constant KAuCl$_4$ concentrations.

Ammonium Citrate vs. SnCl$_2$.2H$_2$O						
	Interaction			Contour Plot Type		
Constant KAuCl$_4$	5 g/L	10 g/L	15 g/L	5 g/L	10 g/L	15 g/L
Shelf Life	yes	yes	yes	hill side/rising ridge	rising ridge	rising ridge
Rate @ 3.5	yes	yes	yes	rising ridge	rising ridge	rising ridge
Rate @ 2.4	yes	yes	yes	rising ridge	trough	hill side/rising ridge
Rate @ 0.8	yes	yes	yes	trough	trough	trough
Sn at % @ 3.5	no	no	no	rising ridge	rising ridge	rising ridge
Sn at % @ 2.4	yes	yes	yes	rising ridge	rising ridge	trough
Sn at % @ 0.8	yes	yes	yes	trough	trough	trough

Table 6-12: Interactions and contour plot types for KAuCl$_4$ and SnCl$_2$.2H$_2$O at constant ammonium citrate concentrations.

KAuCl$_4$ vs. SnCl$_2$.2H$_2$O						
	Interaction			Contour Plot Type		
Constant Ammonium Citrate	30 g/L	50 g/L	70 g/L	30 g/L	50 g/L	70 g/L
Shelf Life	yes	yes	yes	rising ridge	rising ridge	rising ridge
Rate @ 3.5	yes	yes	yes	peak	peak	peak
Rate @ 2.4	yes	yes	yes	saddle	saddle	saddle
Rate @ 0.8	no	no	no	trough	trough	trough
Sn at % @ 3.5	yes	yes	yes	saddle	saddle	saddle
Sn at % @ 2.4	yes	yes	yes	rising ridge	rising ridge	rising ridge
Sn at % @ 0.8	no	no	no	trough	trough	trough

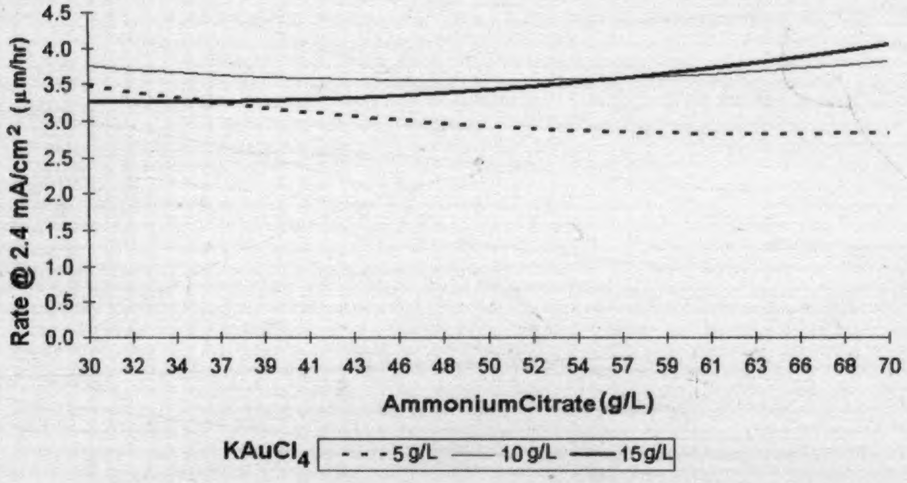

Figure 6-4: Y-hat model interaction plot of rate @ 2.4 mA/cm^2 as a function of ammonium citrate and KAuCl$_4$ concentration, keeping SnCl$_2$.2H$_2$O constant at 5 g/L (interaction effect).

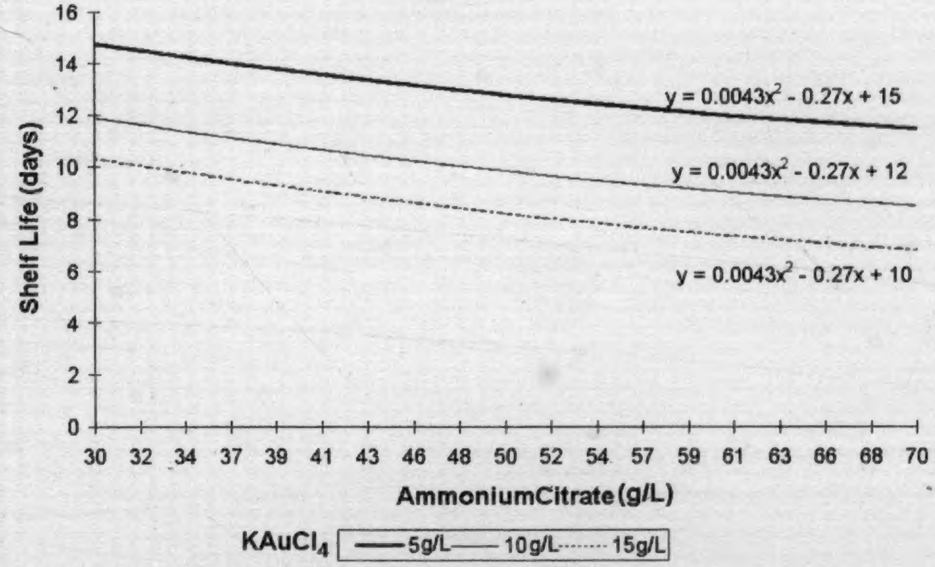

Figure 6-5: Y-hat model interaction plot of shelf life as a function of ammonium citrate & KAuCl$_4$ concentration, keeping SnCl$_2$.2H$_2$O constant at 5 g/L (no interaction).

6.5.3. Optimization

The multiple response optimizer function of the DOE PRO XL software was used to find optimal process settings. Using this function, the desired range of prediction for each factor was entered to be the same as the low and high levels used in the Box-Behnken design. Further, the factors were selected to be continuous.

Once the software computed the bounds for the responses automatically, the constraints for the problem could be defined. The Y-hat model was chosen for all the optimizations. For each constraint, the desired response was chosen, followed by the type of the optimization. In other words, the value of the response was set to be maximized or minimized. Also, the response could be chosen to be greater or equal to, smaller or equal to, or equal to an entered target value. Finally, the importance of meeting each constraint was determined by setting the weight of the constraint. A weight of 1 was given to the lowest priority while a weight of 100 was given to the highest. Table 6-13 shows examples of the constraints entered and the obtained optimal settings.

Table 6-13: Examples of optimization constraints and results.

Opt #		Sn at% @ .8	Weight	Sn at% @ 2.4	Weight	Sn at% @ 3.5	Weight	Rate @ 0.8	Weight	Rate @ 2.4	Weight	Rate @ 3.5	Weight	Shelf Life	Weight	Optimal Setting		
																Ammonium Citrate	$KAuCl_4$	$SnCl_2.2H_2O$
A	Const.	20	100	50	100	-	-	max	1	max	1	-	-	max	1	30.0	15.0	6.7
	Calc.	20.8		49.0		38.3		1.1		3.2		4.7		8.3				
B	Const.	20	100	-	-	-	-	max	100	-	-	-	-	-	-	34.6	15.0	5.0
	Calc.	20.1		47.3		32.0		1.3		3.3		4.5		9.8				
C	Const.	-	-	50	100	-	-	-	-	max	100	-	-	-	-	70.0	7.8	15.0
	Calc.	26.7		50.0		42.9		1.0		3.5		3.9		2.3				
D	Const.	15	100	50	100	-	-	max	1	max	1	-	-	max	1	30.0	15.0	6.3
	Calc.	21.4		49.1		36.9		1.1		3.3		4.7		8.7				
E	Const.	15	100	50	100	-	-	max	100	max	100	-	-	max	100	30.0	15.0	5.0
	Calc.	23.9		49.6		32.0		1.3		3.3		4.3		10.3				
F	Const.	10-20	100	45-55	100	-	-	max	50	max	50	-	-	max	50	34.6	13.4	5.0
	Calc.	20.0		45.6		34.5		1.1		3.5		5.0		10.1				
G	Const.	10-20	100	-	-	45-55	100	max	1	-	-	max	1	max	70	41.7	9.3	6.7
	Calc.	20.0		42.2		44.8		0.8		3.5		6.1		8.6				
H	Const.	-	-	-	-	30-33	100	-	-	-	-	-	-	-	-	56.5	13.1	5.1
	Calc.	12.2		39.7		32.9		1.0		3.7		5.9		8.0				
I	Const.	-	-	-	-	30-33	100	-	-	-	-	-	-	max	1	30	14.5	5.0
	Calc.	23.6		48.9		32.8		1.3		3.3		4.5		10.4				

Optimization A wass set to obtain 20 and 50 at % Sn at 0.8 and 2.4 mA/cm^2 respectively. Also, the deposition rates at these current densities and the shelf life were maximized. Weights of 100 were given to the composition constraints, while the weight for deposition rates and the shelf life were set to 1. This weight selection ensured that the optimizer does not allow the composition to differ in order to maximize the rates or shelf life weight. The small weights of rate and composition do not decrease the effectiveness of the optimizer to find the maximum, but it only ensures that rates and shelf life are not maximized at the cost of the compositions.

Optimizations B and C were set to obtain 20 at % Sn at 0.8 mA/cm^2 and 50 at % Sn and 2.4 mA/cm^2 respectively. For both optimizations, the deposition rates were also maximized.

Both optimizations D and E were set to obtain 15 and 50 at % Sn at 0.8 and 2.4 mA/cm^2 respectively. For both optimizations, the deposition rates and the shelf life were also maximized. The difference between these two optimizations was the weight set for the deposition rates and the shelf life.

Optimizations F and G were both set to obtain the phase Au_5Sn (composition range of 10 to 20 at % Sn) at 0.8 mA/cm^2. However, the phase AuSn (composition of 45 to 55 at % Sn) was set to be obtained at current densities of 2.4 and 3.5 mA/cm^2 for optimization F and G respectively. The deposition rates and shelf life were also maximized.

Finally, optimizations H and I were performed to obtain eutectic composition (30-33 at % Sn) at the higher current density of 3.5 mA/cm^2. The shelf life is also maximized for optimization I.

It should be noted that once the constraints are entered and optimization is performed once, only one suggested optimal setting is obtained. Using the same constraints, the optimization can be repeated to obtain more optimal settings. In other words, there may be several optimal combinations that would satisfy the same constraints. Also by changing the weight of each constraint, different optimal settings are obtained.

To find improved and optimal process settings for the gold tin electrodeposition process, several optimizations were chosen for further characterization. The following sections give details of the chosen optimal settings, and the constraints and the obtained optimal settings are summarized Table 6-14.

Table 6-14: Chosen optimal settings for characterization.

									Optimal Setting		
Opt #		Sn at% @ 0.8	Sn at% @ 2.4	Sn at% @ 3.5	Rate @ 0.8	Rate @ 2.4	Rate @ 3.5	Shelf Life	Ammonium Citrate	$KAuCl_4$	$SnCl_2.2H_2O$
1	Const.	10-20	45-55	-	max	max	-	max	30	15	5.7
	Weight	100	100	-	1	1	-	1			
	Calc.	22.4	49.3	34.7	1.2	3.3	4.6	9.4			
2	Const.	-	-	-	-	-	-	max	30	5	5
	Weight	-	-	-	-	-	-	100			
	Calc.	54.9	47.3	49.2	1.5	3.5	3.0	14.8			
3	Const.	-	-	30-33	-	-	max	Max	65	11	5
	Weight	-	-	100	-	-	100	100			
	Calc.	16.8	39.4	33.5	1.0	3.8	5.9	8.3			

6.5.3.1. Opt1

To improve the deposition process of multilayer of AuSn and Au_5Sn phases at the same current densities as of the standard procedure, Opt1 was obtained. For this optimization, while making sure that the correct range of composition was plated at each current density, the plating rates were maximized. Also, the shelf life was maximized. Weights of 100 were chosen for the composition responses to ensure the deposition of both AuSn and Au_5Sn phases. However, weights of 1 were chosen for the plating rates and the shelf life to ensure that rates and shelf life were not maximized at the cost of the compositions.

The calculated responses predict that compositions of 22.4 and 49.3 at % Sn are obtainable at current densities 0.8 and 2.4 mA/cm^2 respectively. The plating rates of 1.2 and 3.3 μm/hr are also predicted at current densities 0.8 and 2.4 mA/cm^2 respectively. These plating rates are higher than that of the standard solution (0.7 and 2 μm/hr at 0.8 and 2.4 mA/cm^2 respectively). Further, the shelf life of this solution is predicted to be 9.4 days, which is longer than 1 day shelf life for the standard solution.

6.5.3.2. Opt2

Optimization Opt2 was considered to merely maximize the shelf life of the solution. The obtainable compositions or plating rates were not considered. This optimization predicts that no combination of concentrations of the factors (within the low and high levels of factors) gives a shelf life longer than 14.8 days. Further, the calculated responses predict that compositions corresponding to Au_5Sn are not obtainable at any of the three current densities.

6.5.3.3. Opt3

To simplify the deposition process of the gold-tin eutectic composition, Opt3 was obtained. For this optimization, the higher current density of 3.5 mA/cm^2 was considered, because higher plating rates are obtained at higher current densities. The composition range of 30 to 33 at % Sn was chosen at this current density, which corresponds to the eutectic composition. Also, the plating rate at a current density of 3.5 mA/cm^2 and the shelf life were maximized for further improvements. A weighting of 100 were given to all constraints, because the composition could be compensated by a small amount (± 1 at % Sn) to obtain higher shelf life and plating rates.

This optimization, if repeatable, may suggest that eutectic composition is attainable at a single current density with little variation (similar to a plateau) by changing the concentrations of the factors in the standard solution. Note that such a plateau was not obtainable for the standard solution, and any eutectic composition belonged to the transition region between the AuSn and Au_5Sn plateaus and was not repeatable.

The calculated responses predict that a composition of 33.5 at % Sn is obtainable at current density of 3.5 mA/cm^2. A plating rate of 5.9 μm/hr is also predicted at this current density, which is higher than that of the standard solution (less than 2 μm/hr for the artificial eutectic composition). Further, the shelf life of this solution is predicted to be 8.3 days, which is longer than the 1 day shelf life for the standard solution.

To obtain an idea of the range of concentration for each factor that can be used to obtain constraints satisfying Opt 3, contour and surface plots were created for shelf life, rate, and composition at 3.5 mA/cm^2. Repeating the optimization within the multiple response optimizer function resulted in optimal settings that have a $SnCl_2.2H_2O$ concentration at 5 g/L. Thus, these surface and contour plots were created keeping the $SnCl_2.2H_2O$ concentration constant at 5 g/L. The created plots are shown in Figure 6-6 to Figure 6-8.

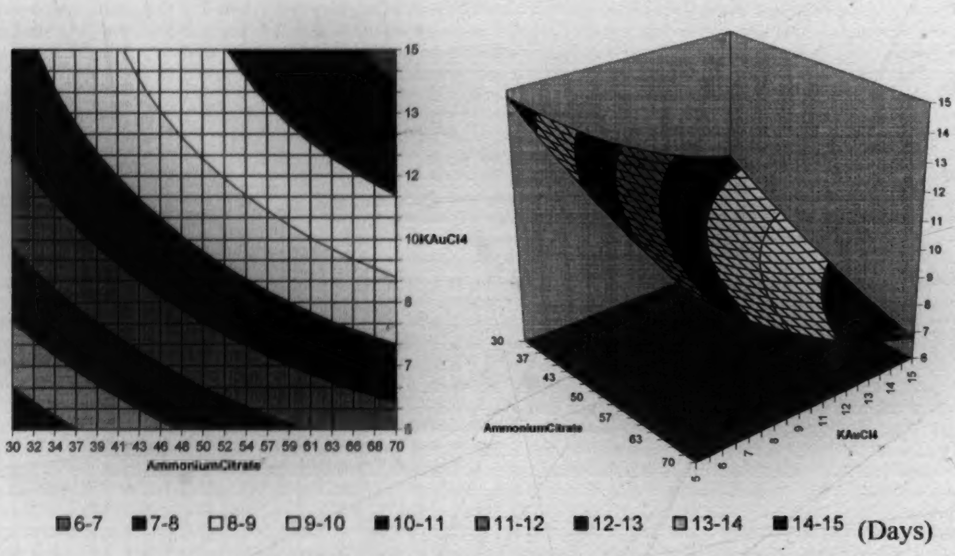

Figure 6-6: Y-hat model contour and surface plots of shelf life for ammonium citrate vs. $KAuCl_4$ while keeping $SnCl_2.2H_2O$ constant at 5 g/L.

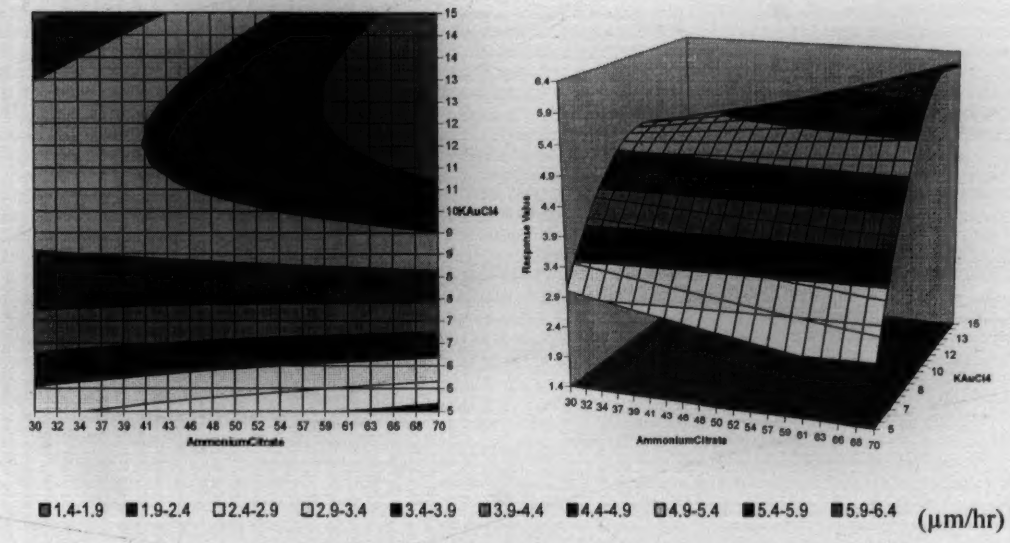

Figure 6-7: Y-hat model contour and surface plots of rate at 3.5mA/cm^2 for ammonium citrate vs. KAuCl$_4$ while keeping SnCl$_2$.2H$_2$O constant at 5 g/L.

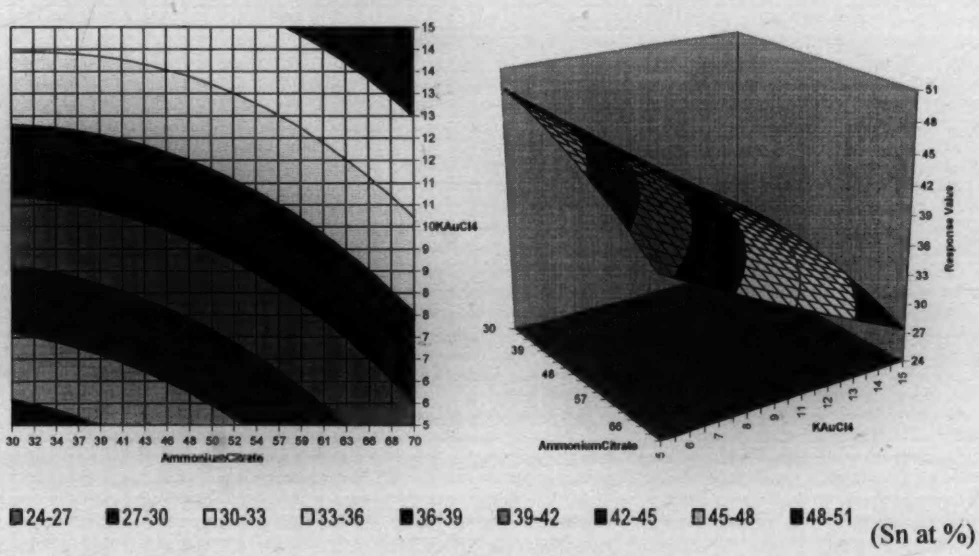

Figure 6-8: Y-hat model contour and surface plots of composition at 3.5mA/cm^2 for ammonium citrate vs. KAuCl$_4$ while keeping SnCl$_2$.2H$_2$O constant at 5 g/L.

Figure 6-6 shows that the maximum shelf life is obtainable at low concentration levels of ammonium citrate and $KAuCl_4$. However, Figure 6-7 shows that the maximum plating rate is obtainable at high concentration levels of ammonium citrate and $KAuCl_4$. Thus, by adjusting the concentration of ammonium citrate and $KAuCl_4$, shelf life and plating rate cannot be maximized simultaneously. As illustrated here, RSM is significant in determination of trade-offs. The inverse relationship of shelf life and plating rate are readily apparent from these contour and surface plots.

The eutectic composition of 30 to 33 at % Sn is obtainable in the region shown in Figure 6-8. Overlapping the contour plots of shelf life, composition, and plating rate would determine the region of optimal setting that would meet the constraints of eutectic composition with high plating rate and shelf life. The overlapped contour plots are shown in Figure 6-9. The green area corresponds to the region that meets the desired constraints. Within this region, the section with the darker shade of green predicts a higher shelf life.

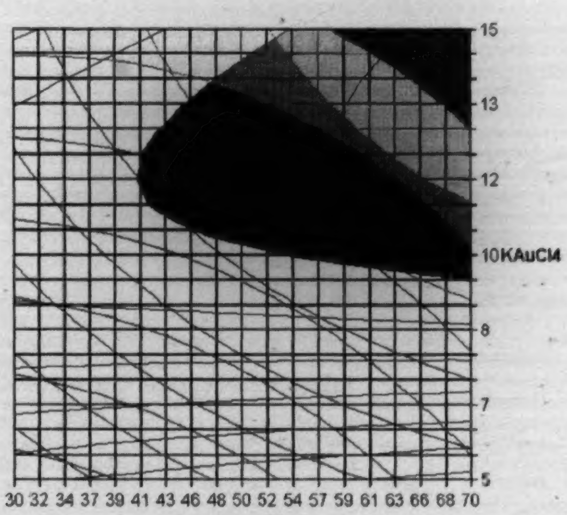

Figure 6-9: Overlapped contour plots from Figure 6-6 to Figure 6-8.

It should be noted that the optimal setting of Opt3 (65 g/L of ammonium citrate, 11 g/L $KAuCl_4$) is slightly below the green region. This means that composition is in the range of 33 to 36 (instead of the constraint range of 30-33). This compensation of composition was allowed to obtain higher shelf life and plating rates due to the chosen weighting of the constraints (a weighting of 100 were given to all constraints). However, the predicted composition differs only by 0.5 at % Sn from the higher limit of the desired constraint (predicted 33.5 at % Sn compared to 33 at % Sn), which is acceptable.

6.6. Conclusions

The statistical design of the experiments for the gold tin electrodeposition process was performed and Box-Behnken design type was used to study the process.

Composition, deposition rate, and shelf life data were obtained for each experimental run, and the regression tables obtained from these data were presented and analyzed. The response surface models including the surface, contour, and interaction plots were used to obtain a better understanding of the system behaviour.

Finally, the multiple response optimization function of the DOE PRO XL software was used to obtain improved and optimal process settings. Three optimal settings were chosen for further characterization. Optimization Opt1 was obtained to maximize the shelf life and the plating rates of AuSn and Au_5Sn phases at current densities of 0.8 and 2.4 mA/cm^2 respectively. Optimization Opt2 was obtained to merely maximize the shelf life of the solution, and the obtainable compositions or plating rates were not considered. Finally, optimization Opt3 was obtained to simplify the deposition process and to electroplate the gold-tin eutectic composition at one single step with a long shelf life and a higher plating rate.

The solutions with the optimized process settings (Opt1-3) are studied further in the next chapter. The predicted response values are compared with the experimental values, and the reproducibility and repeatability of these solutions are tested.

Chapter 7: Characterization of Optimized Solutions

7.1. Overview

In the previous chapter improved and optimal process settings were obtained. Three optimal settings were chosen for further characterization. These solutions, with the optimized process settings (Opt1-3), are studied further in this chapter (summarized in Table 7-1). The predicted response values are compared with the experimental values, and the reproducibility and repeatability of these solutions are briefly examined.

Table 7-1: Concentrations of the optimized solutions.

Optimized Solution	Ammonium Citrate	$KAuCl_4$	$SnCl_2.2H_2O$
Opt1	30	15	5.7
Opt2	30	5	5
Opt3	65	11	5

7.2. Experimental Procedure

Solutions were mixed for each optimized condition following the exactly the same procedure used for the runs of the Box-Behnken design. Further, the same methods used to obtain responses for the Box-Behnken design were employed to get the values of the compositions, plating rates, and shelf lives for the optimized solutions (see Chapter 6 for details of the experimental procedures).

Obtained responses of these optimized solutions were compared to the predicted values, and solutions were selected for further characterization. Films were electroplated at various current densities, and their composition and plating rates were measured using EDS within the SEM and profilometry respectively. Also, to determine the useful shelf life of the solution, the composition of the films electroplated as a function of aging time was measured with EDS within the SEM.

7.3. Results and Discussions

Secondary electron SEM images of the deposited films for all the optimized solutions are shown in Table 7-2. All deposits appear smooth, but the deposited film from Opt2 solution at 3.5 mA/cm^2 is stressed.

Table 7-2: SE plan view images of deposits for the optimized solutions.

Opt #	J_1= 0.8 mA/cm^2	J_2= 2.4 mA/cm^2	J_3= 3.5 mA/cm^2
1			
2			
3		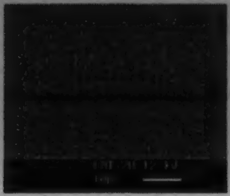	

The shelf life values obtained from the turbidity curves are shown in Table 7-3. As before, these values relate to the time corresponding either to the peak of the turbidity curve or the onset of precipitation, which ever was lower. The compositions of the deposited films obtained using EDS, and the plating rates measured through thickness measurements are also summarized in Table 7-3. Further, the calculated values along with the 99% confidence intervals are shown in this table for comparison purposes. The 99% confidence intervals are shown in the form of lower bound to upper bound separated by a dash.

Table 7-3: Measured and predicted response values for the optimized solutions.

Opt #		Sn at% @ 0.8	Sn at% @ 2.4	Sn at% @ 3.5	Rate @ 0.8	Rate @ 2.4	Rate @ 3.5	Shelf Life
1	Calculated	22.4	49.3	34.7	1.2	3.3	4.6	9.4
	99% Confidence	18.2-26.6	46.1-52.5	29.7-39.7	0.9-1.6	2.9-3.6	4.5-4.6	6.3-12.6
	Measured	21.2	42.4	23.8	0.8	4.3	6.5	9.2
2	Calculated	54.9	47.3	49.2	1.5	3.5	3.0	14.8
	99% Confidence	34.4-75.5	35.7-58.9	57.3-41.2	1.4-1.6	3.4-3.5	2.9-3.0	3.9-25.6
	Measured	43.6	45.1	51.0	1.3	3.1	3.8	7.5
3	Calculated	16.8	39.4	33.5	1.0	3.8	5.9	8.3
	99% Confidence	12.9-20.8	27.5-51.4	11.7-55.3	0.7-1.3	2.3-5.3	4.6-7.1	6.1-10.6
	Measured	10.3	34.9	31.1	1.0	4.1	4.8	7.5

Not all the measured values for the Opt1 and Opt2 optimizations match the predicted values. The reason for this poor prediction quality becomes apparent by noticing the location of these optimized combinations within the design space. All three optimized points are shown in Figure 7-1 within the Box-Behnken design space. These optimized points are labelled while all the other points correspond to the Box-Behnken experimental runs. The x, y, and z axes correspond to factors ammonium citrate, $KAuCl_4$, and $SnCl_2.2H_2O$ respectively.

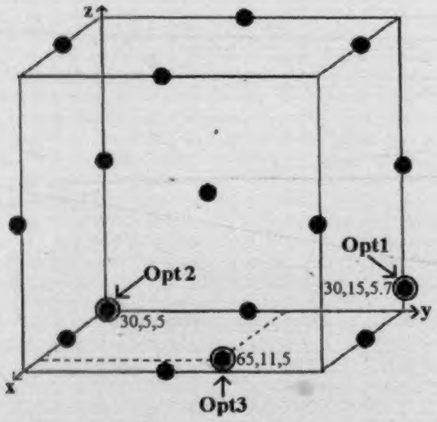

Figure 7-1: Illustration of optimized solutions on Box-Behnken design process space.

Figure 7-1 shows that Opt 1 and Opt2 are located at the corners of the Box-Behnken design space. Thus, these points are positioned at the region of poor predictability of the Box-Behnken design. For this design, the difference between the measured and predicted values is expected at the points that combine the extreme levels of factors.

Considering the limitation of the experimental design and the application of the responses, the obtained values for Opt1 solution are still acceptable. The compositions at current densities 0.8 and 2.4 mA/cm^2 are close to those of the Au_5Sn and AuSn phases respectively, and by adjusting the thickness of each layer the overall eutectic composition is still obtainable. The electrodeposition rates and the shelf life at both of these current densities are higher than the standard values. Further, since electrodeposition at a current density of 3.5 mA/cm^2 is not needed for this optimized process, the composition and the rate at this current density do not matter.

For solution Opt2, the compositions obtained at all three current densities correspond to the AuSn phase only. This formulation cannot substitute for the standard solution, because the eutectic composition is not obtainable.

The measured shelf life is about half of the predicted value for Opt2. Although, this shelf life (7.5 days) is longer than that of the standard solution, it is no more than that of Opt 1.

Considering this fact and comparing the obtainable compositions and plating rates, the Opt1 solution offers a better alternative to the standard process to improve plating rates and shelf life. However, further experiments were needed to confirm the process repeatability. Moreover, the shelf life of the new optimized solution had to be monitored directly to verify the turbidity measurement results. The shelf life can be monitored directly by measuring the composition of the plated films from the solution as a function of aging time.

The measured values of all responses for Opt3 are within the calculated 99% confidence interval except for the composition at 0.8 mA/cm^2. Although there is a difference of about 7 at % Sn between the predicted and the measured values at 0.8 mA/cm^2, the composition of 10 at % Sn is still considered to correspond to the Au_5Sn phase for the purpose of this study. These measurements show that the factor setting for Opt3 can be used to improve the plating rate and the solution shelf life of the standard process. By electroplating the eutectic composition directly using only one current density simplifies the standard process. However, similar to the Opt1 solution, further experiments were needed to confirm the process repeatability and the solution shelf life.

The results obtained from the characterization of the Opt1 and Opt3 solutions are presented in the following sections.

7.3.1. OP1

The change in tin content and the plating rate of the deposited films at various current densities are shown in Figure 7-2 and Figure 7-3 respectively. The diamond shape points correspond to the values obtained from measuring three regions of the deposited films, and the dashed lines correspond to the average values of the measurements. This presentation of the data provides a better understanding of the composition variation throughout the deposited films.

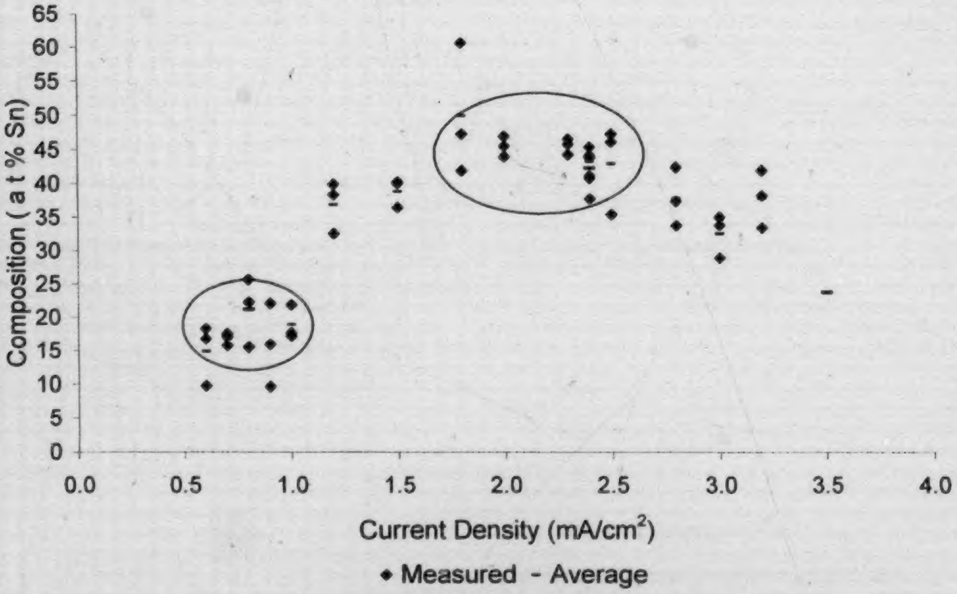

Figure 7-2: Tin content of the deposited films from the Opt1 solution plated at various current densities.

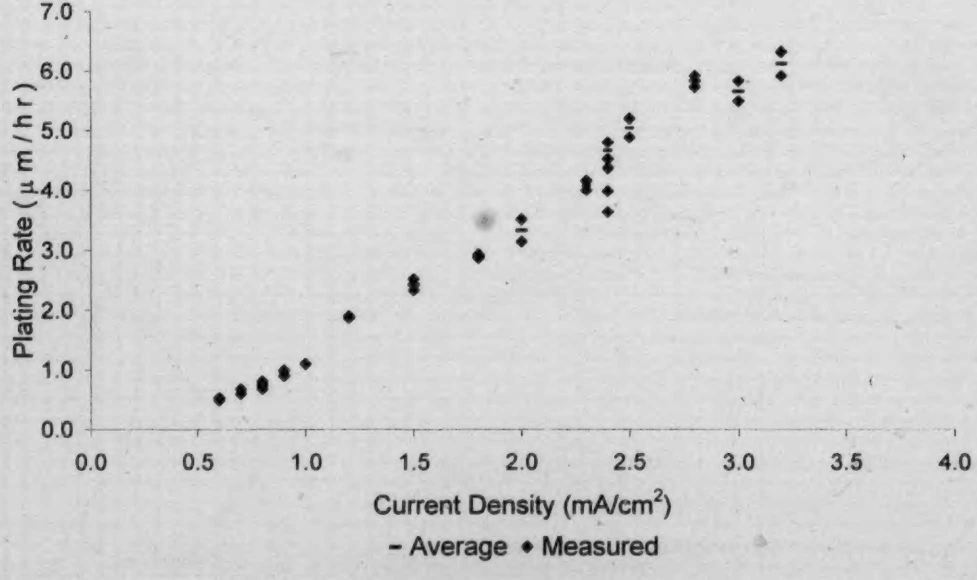

Figure 7-3: Plating rate of the deposited films from the Opt1 solution plated at various current densities.

Figure 7-2 was compared with the graph of composition versus current density for the standard solution (Figure 2-11). The plateau for Au_5Sn phase extends up to a current density of about 1.0 mA/cm^2 which is similar to that for the standard process, but it seems to be shifted upwards by about 5 at % Sn. The plateau for the AuSn phase appears for current densities from 1.8 to 2.5 mA/cm^2, which is a narrower range than that for the standard process (1.8 to 3.0 mA/cm^2). Further, this plateau seems to be shifted downwards by about 5 at % Sn.

Figure 7-3 shows that the plating rate increases with an increase in the current density to about 2.8 mA/cm^2, after which it levels off. After this current density the deposition rate does not increase with increasing current density. This current density likely corresponds to the limiting current density at which the maximum concentration gradient is reached. In other words, the concentration of the reactants at the electrode is zero and the rate of reaction is controlled by the rate of transport of the reactants to the electrode. The deposition rate in the current density range of 0.5 to 1.0 mA/cm^2 varies between 0.5 and 1.1 μm/hr, which corresponds to the obtainable range of deposition rates for the Au_5Sn phase. The deposition rate in the current density range of 1.8 to 2.5 mA/cm^2 varies between 3.0 and 5.0 μm/hr, which corresponds to the obtainable range of deposition rates for the AuSn phase.

For electrodeposition of each phase, the current densities can be chosen to minimize the variation in the composition while obtaining the highest obtainable deposition rate. From the available data, a current density of 2.3 mA/cm^2 appears to result in the smallest deposit compositional variation and the deposition rate is 4.0 μm/hr. However, to make a reliable decision on the current density, these experiments should be repeated to obtain more data points. Then, the repeatability, composition variability, and plating rates would be statistically significant.

Figure 7-4 shows the tin content of films deposited at 2.4 mA/cm^2 from the Opt1 solution as a function of ageing time. The tin content of the deposited film decreased from 43 to

33 at % Sn (based on average values) after 24 hours. Further, the tin content of the deposits decreased gradually to 25 at % Sn after 6 days. These results show that the useful shelf life of the solution is not 9 days as suggested by the turbidity results.

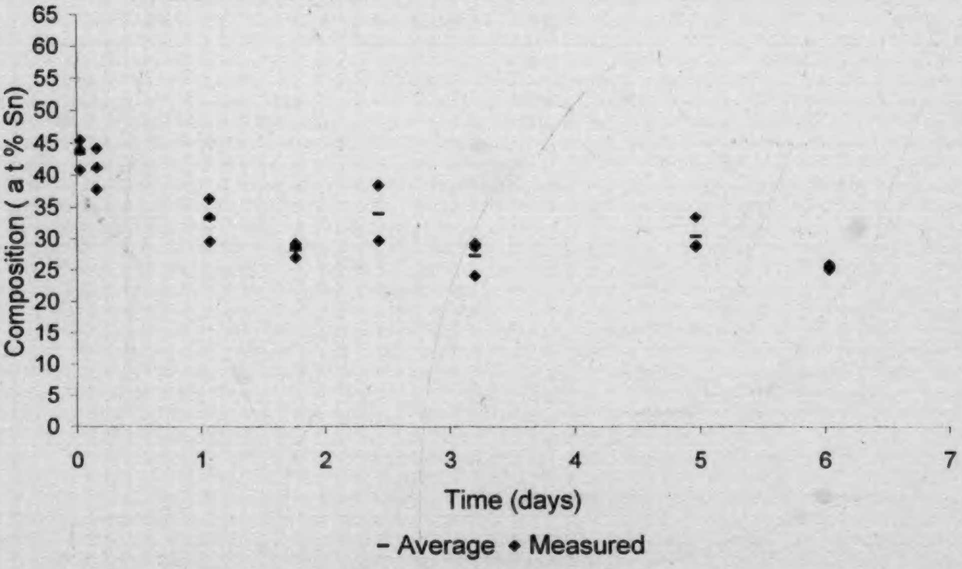

Figure 7-4: Tin content of films deposited at 2.4 mA/cm^2 from the Opt1 solution as a function of ageing time.

7.3.2. Opt3

The change in tin content and plating rate for the deposited films at various current densities are shown in Figure 7-5 and Figure 7-6 respectively. Similar to graphs presented for Opt1, the diamond shape points correspond to the values obtained from measuring three regions of the deposited films, and the dashed lines correspond to the average values of the measurements.

Figure 7-5 shows a composition plateau of 30 to 40 at % Sn in the current density range of 2.5 to 4 mA/cm^2. The obtained compositions are not exactly at the eutectic composition (30 at % Sn), and the range extends towards higher tin contents. Since gold is used as the seed layer for the gold-tin solder, its thickness can be adjusted to create an overall eutectic composition for the seed layer plus solder. Also, the gold-tin phase diagram shows a less steep liquidus line on the higher tin content side of the eutectic melting point, and this change in melting point (up to 370°C for 40 at % Sn) may be acceptable depending on the specific application.

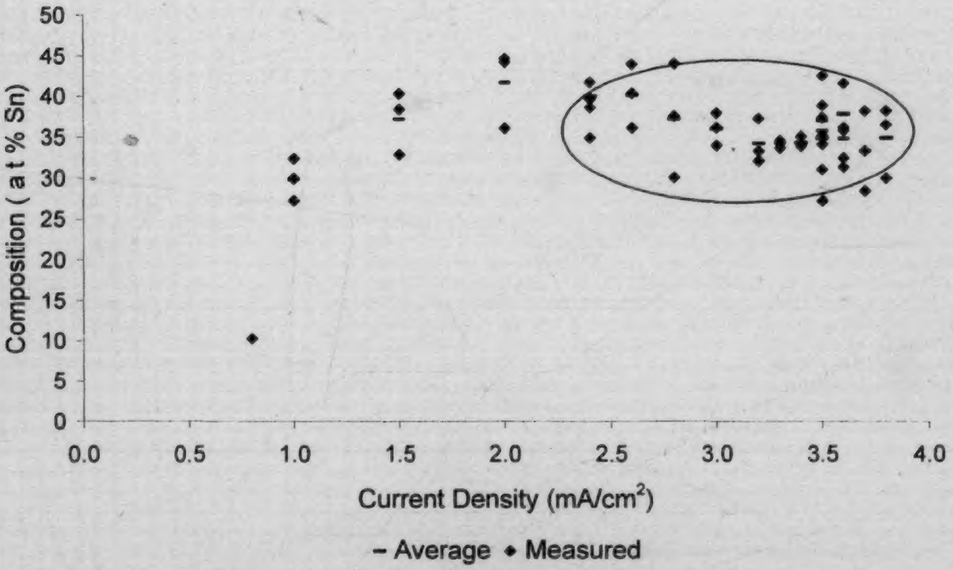

Figure 7-5: Tin content of the deposited films from the Opt3 solution at various current densities.

Figure 7-6 shows that the plating rate increases with an increase in the current density to about 2.5 mA/cm^2, after which it levels off. The plating rates in the current density range of 2.5 to 4 mA/cm^2 vary between 5 and 6.5 µm/hr.

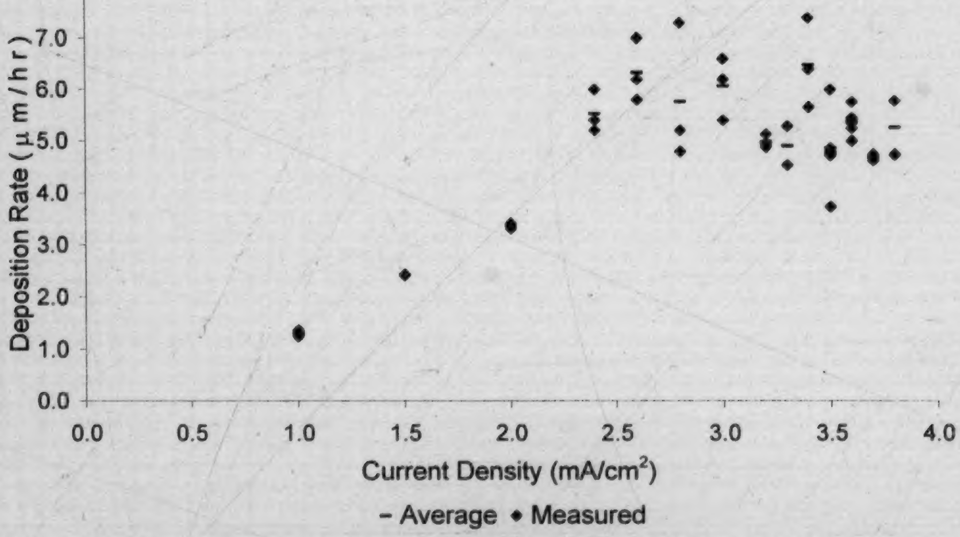

Figure 7-6: Plating rate of the deposited films from the Opt3 solution at various current densities.

The same argument presented for Opt1 holds here for choosing the current density to minimize the variation in the composition while obtaining the highest obtainable deposition rate. The repeatability and variations in composition and plating rates would be statistically more significant if the experiments were repeated and more points were obtained. From the available data, a current density of 2.6 mA/cm^2 appears to result in the smallest compositional variation within the sample and the deposition rate is 6.3 µm/hr. This current density is chosen at the lower end of the plateau, since increasing current density further does not improve the plating rate significantly and operation at this lower current density is more energy efficient.

Figure 7-7 shows the tin content of films deposited at 3.5 mA/cm^2 from the Opt3 solution as a function of ageing time. The tin content of the deposited film decreased by about 10 at % Sn after about 40 hours. Further, the tin content of the deposits decreases gradually to 17 at % Sn after 5 days. These results show that the useful shelf life of the solution is not 7.5 days as suggested by the turbidity results.

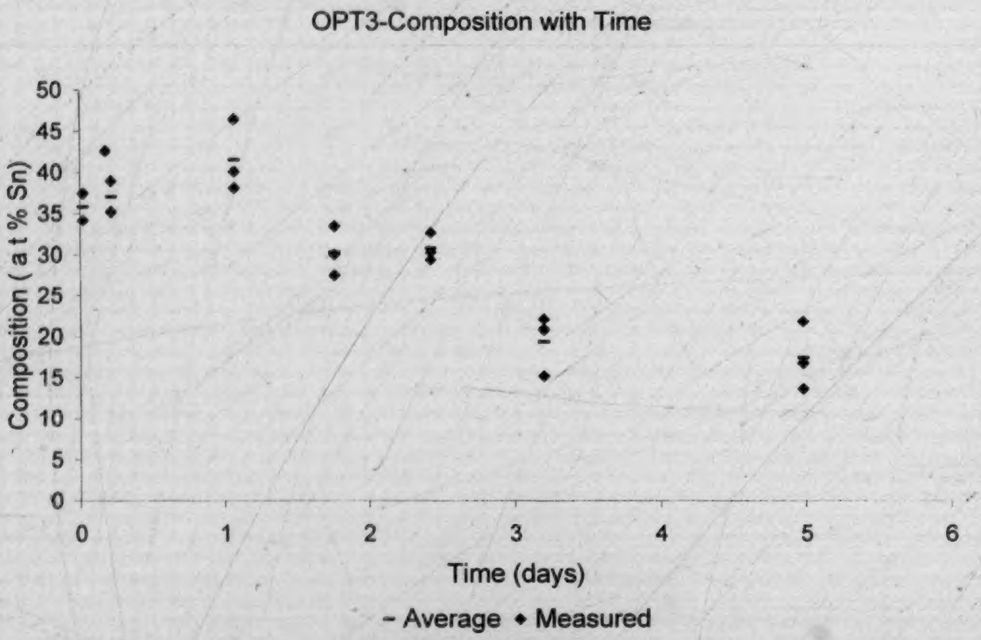

Figure 7-7: Tin content of films deposited at 2.4 mA/cm^2 from the Opt3 solution as a function of ageing time.

7.4. Conclusions

In this chapter three optimized processes were studied (Opt1-3, see Table 7-1). For the most part, the predicted response values for these processes were relatively close to the measured responses. However, poor predictability was observed for the points that combined the extreme levels of factors (Opt1 and Opt2).

Considering the measured shelf life and the attainable compositions and plating rates for Opt1 and Opt2, the Opt1 solution responses matched the requirements for the optimized process better. Thus, Opt1 was chosen as a possible alternative to the standard process to improve plating rates and shelf life. Further characterization experiments showed that the plating rate for Au_5Sn did not improve significantly (only from the standard rate of 0.7

μm/hr to 0.8 μm/hr) at a current density of 0.8 mA/cm^2. However, higher current densities (i.e., up to 1.0 mA/cm^2) can be used to improve the plating rate to 1.0 μm/hr. The plating rate for AuSn phase improved to 4.3 μm/hr, which is more than double the standard rate of 1.9 μm/hr. Although the turbidity value of Opt1 solution stays at low values for a longer time (9 days) compared to the standard solution turbidity (1 day), the useful shelf life of the solution is not improved. The composition of the plated deposit from Opt1 solution changes after one day of solution aging.

The measured response values for Opt3 showed that the factor setting for Opt3 can be used to improve the plating rate and the solution shelf life compared to the standard process. By electroplating the eutectic composition directly using only one current density simplifies the process. Further characterization experiments showed that the plating rate for the eutectic phase improved significantly. The plating rate improved to 5 to 6.5 μm/hr for the eutectic composition (depending on the current density, see Figure 7-6), which is at least four times the standard rate of less than 1.2 μm/hr for the eutectic composition (calculated from plating rates of 0.7 and 1.9 μm/hr for Au_5Sn and AuSn respectively). However, although the turbidity value of Opt3 solution stays at low values for a longer time (7.5 days) compared to the standard solution turbidity (1 day), the useful shelf life of the solution is not improved much. The composition of the plated deposits from Opt3 solution changes after two days of solution aging. This suggests a useful shelf life of two days, which is double the standard shelf life.

These results showed that the turbidity curves do not necessarily represent the useful shelf life of gold-tin electroplating solutions, although they correlated well with the shelf life results of the standard solution. Thus, the shelf lives of the optimized solutions are not improved markedly.

The alternative optimized solutions are preferred to the standard process. With the higher plating rates, more electrodeposition can be performed from one solution within the one day of useful shelf life. Thus, less time and chemicals are needed to produce the same amount of products. In addition, Opt3 is the more preferred solution compared to Opt1, because of its improved shelf life and the simplicity of its altered process.

The next chapter presents and summarizes the conclusions derived from this thesis work and provides recommendations for possible future work.

Chapter 8: Conclusions and Recommendations

8.1. Conclusions

The long term stability of the standard electroplating bath developed by Ivey's group was studied. The plated deposit composition as a function of aging time suggested a useful shelf life of one day for the standard solution. The tin content of the electroplated deposits decreased as the solution aged. The difference in the composition of differently stored samples showed that solution depletion, due to electrodeposition, affects the amount of compositional change in the deposits over time. The morphology study of the deposits, as a function of aging time ,showed that morphology deteriorates as the solution ages. Deposits from the aged standard solution were rougher and less dense compared to deposits from the fresh solution. The difference in storage methods also demonstrated that the amount of precipitates in the solution at the time of electrodeposition affects the composition and morphology of the deposit.

The turbidity behavior study of the standard solution showed that the turbidity was initially low, increased with time, and peaked out after about one day. The turbidity value dropped gradually to near zero the next day and stayed at very low values. The peak of the turbidity curve correlated with the useful shelf life of the solution.

Atomic absorption (AA) spectroscopy results showed that the concentration of tin in the standard solution remained constant as the solution aged. However, the concentration of gold in the standard solution decreased after about 24 hours. This behavior also correlated with the turbidity and composition curves and suggests a useful shelf life of one day.

The key factors affecting the stability and the plating rate of the gold-tin electroplating bath were identified using screening tests. Transmission electron microscopy (TEM) analysis was done to monitor gold precipitation during the solution mixing procedure. This TEM study showed that gold precipitates form as soon as ammonium citrate and $KAuCl_4$ are mixed. These nano-size particles remain within the solution throughout the mixing procedure. Thus, the final fresh solution contains nano-size gold particles. To improve the stability and prevent gold precipitation, attempts were made to eliminate ammonium citrate from the solution. These attempts were inconclusive, and it was decided to minimize the concentration of ammonium citrate in the solution.

The concentration of solution constituents was modified, which affected deposition behavior. The composition plateaus corresponding to Au_5Sn and AuSn for a standard solution were shifted as solution composition was modified. In some instances both plateaus were not attainable. Plating rates and deposit properties (morphology and stress) were affected by changing the solution concentration. Ammonium citrate proved to act a stress reliever for the electrodeposition process, as too much of a decrease in its concentration caused stress in the deposits. Changing the concentration of ammonium citrate had the most effect on the solution stability, while changing the gold and tin concentrations had the most effect on plating rates.

The concentration of ammonium citrate, potassium tetrachloroaurate, and tin (II) chloride were chosen as the three main factors affecting the stability and plating rate for use in the statistical design of experiments. A statistical design of the experiments for the gold tin electrodeposition process was performed and the Box-Behnken design type was used to study the process.

Composition, deposition rate, and shelf life data were obtained for each experimental run, and the regression table obtained from this data was presented. The response surface models including the surface, contour, and interaction plots were used to obtain a better understanding of the system behavior. The inverse relationship of shelf life and plating rate was readily apparent from these contour and surface plots. By adjusting the concentration of ammonium citrate and $KAuCl_4$, shelf life and plating rate could not be maximized simultaneously.

The multiple response optimization function of the commercial software was used to obtain improved and optimal process settings. Three optimal settings were chosen for further characterization. Optimization Opt1 was obtained to maximize the shelf life and plating rates of AuSn and Au_5Sn phases at current densities of 0.8 and 2.4 mA/cm^2 respectively. Optimization Opt2 was obtained to merely maximize the shelf life of the solution, and the obtainable compositions or plating rates were not considered. Finally, optimization Opt3 was obtained to simplify the deposition process and to electroplate the gold-tin eutectic composition in a single step with a long shelf life and a higher plating rate.

These optimized solutions were studied further, and the predicted response values were compared with the measured responses. Poor predictability was observed for the points that combined the extreme levels of factors (Opt1 and Opt2).

Solutions Opt1 and Opt3 were chosen as possible alternatives to the standard process to improve plating rates and shelf life.

Characterization experiments of Opt1 showed that although the plating rate for Au_5Sn was not improved significantly, it was more than doubled for the AuSn phase (improved to 4.3 µm/hr). The useful shelf life of the solution did not improve, since the composition of the plated deposit from Opt1 solution changed after one day of solution aging. However, the turbidity value of Opt1 solution stayed at low values for up to 9 days.

Further characterization experiments for Opt3 showed that the plating rate for the eutectic composition improved by at least four times the standard rate (improved to 5 to 6.5

μm/hr). The useful shelf life of the solution was almost doubled, since the composition of the plated deposits from Opt3 solution changed after two days of solution aging. Also, the turbidity value for the Opt3 solution stayed at low values for 7.5 days.

Although the turbidity curves were shown to represent the useful life of the standard solution, these curves do not necessarily represent the useful shelf life of gold-tin electroplating solutions once the composition of the constituents is changed.

The alternative optimized solutions (Opt1 and Opt3) are preferred to the standard process, although the shelf life was not significantly improved. Less time and materials are needed to produce the same amount of products using the higher plating rates attainable with these solutions. This is because more electrodeposition can be performed from one solution within the one (or two) day(s) of useful shelf life.

8.2. Recommendations and Comments

Some ideas for future research are proposed here. It should be noted that any change in the system should be studied thoroughly and systematically to be able to tell its effects. It is apparent from the literature that bath stability, plating rate, deposit morphology, and composition are interrelated, and addition of a secondary ingredient to the bath usually affects more than one of these. Also, in some systems the concentration of the secondary material could determine whether its existence is beneficial or harmful. In other words, the plating parameters may have to be optimized for any new, altered system. Otherwise, false conclusions regarding the harmfulness or irrelevancy of the change could be made.

An experimental process to study the effect of the concentrations of ascorbic acid and sodium sulfite on the stability and plating rate of the electrodeposition system needs to be performed. The obtained results can be further combined with the process model of this thesis work to provide a complete understanding of the solution behavior based on the concentration of its constituents.

It should be noted that the process model obtained in this thesis best represents the process space that was chosen for the Box-Behnken design. As poor predictability of the model at the corners of the design space was observed, poor predictability is also expected outside the design space (at much higher or lower concentrations of the key factors used in this design). However, further experimental runs can be added to the design at desired combinations of the factor levels. The analysis of the new obtained responses combined with the existing data would provide a better process model.

In general, the existing data and model of the process provide a basis for all future work in this area. Any future results can be used to add new dimensions to the model or improve the model further. For example, the stress developing in the deposited films can be measured quantitatively for all the experimental runs for the existing Box-Behnken design. Then, stress can be added as a new response and, after analysis, multi-response optimization can be performed to obtain longer shelf life and plating rates while minimizing the stress in the deposits.

Other techniques to monitor the stability of the solution need to be developed. Based on the results of this thesis, turbidity showed poor correlation with useful shelf life of the solution. Direct monitoring of the shelf life is very time consuming and not feasible for a large number of experiments. Thus a new, representative, and efficient technique needs to be developed.

One way to improve the reliability of the turbidity tests is to monitor the turbidity automatically. This technique would provide a better turbidity behavior curve as a function of the aging time. The automatic monitoring would provide the advantage of the sample being kept completely stationary, thereby avoiding any shaking or mixing. Also, the appearance of any turbidity peaks would be readily detected through automatic monitoring. Combining this turbidity technique with direct shelf life monitoring for various solutions of different compositions would provide a better understanding of the correlation between turbidity and shelf life.

The pH of the solution needs to be monitored as a function of the aging time. This experiment may provide useful information on the stability behavior of the solution, and it may prove to be an alternative method of monitoring shelf life. In other words, the change in the composition of the deposited films from an aged solution may correlate with pH changes in the solution.

One of the uncontrolled factors of the DOE in this thesis was the wait time needed for complete dissolution of sodium sulfite. All solutions were left over night to assure the complete dissolution, and the waiting times were approximately the same. However, since the required time varied, for each solution to turn clear, the ratio of the wait time to the required wait time was not the same for all runs. Studies need to be done to provide information on the effect of wait time on the solution stability. In other words, the dependence of the stability of the solution on the waiting time should be studied.

More experiments need to be performed to obtain more points for the plots of tin content and the plating rate of deposited films as functions of current density and aging time for Opt1 and Opt3 solutions. The repeatability, composition variations, and plating rates would be statistically more significant if the experiments were repeated and more points were obtained. These data can be used to choose a current density for operation that minimizes the variation in the composition while obtaining the highest attainable deposition rate.

Finally, a study on the effect of solution agitation at the time of electrodeposition on compositional variation through the sample is recommended. Mass transfer is improved during electroplating using agitation both by increasing the velocity of solution flow and by decreasing the thickness of the diffusion layer. Therefore, the species are available in a more uniform manner closer to the electrode, resulting in better compositional uniformity across the electrode.

REFERENCES

[Akhlaghi and Ivey 2003] Akhlaghi, S. and D. G. Ivey (2003). "Effect of Processing Parameters on the Electroplating of Au-Sn Solders." Plating and Surface Finishing **90**(7).

[Akihiro and Kazumi 2006] Akihiro, A. and K. Kazumi (2006). Electroless Gold Plating Liquid. Japan: WO2006006367.

[Akihiro, Yoshiyuki et al. 2006] Akihiro, A., H. Yoshiyuki, et al. (2006). Electroless Gold Plating Solution: EP1645658.

[Akihiro, Kazumi et al. 2006] Akihiro, A., K. Kazumi, et al. (2006). Electroless Gold Plating Solution: WO2006051637.

[American Society for Metals 2005] American Society for Metals (2005). Binary Phase Diagrams. Asm Handbooks Online.

[Amkor 2006] Amkor (2006). Flip Chip Packaging.**June 2006:** http://www.amkor.com/

[Bard and Faulkner 2001] Bard, A. J. and L. R. Faulkner (2001). Electrochemical Methods: Fundamentals and Applications.

[Box, Hunter et al. 2005] Box, G. E. P., J. S. Hunter, et al. (2005). Statistics for Experimenters: Design, Innovation, and Discovery, John Wiley & Sons Inc.

[Breviary Technical Ceramics 2006] Breviary Technical Ceramics (2006). Soft Soldering.**June 2006:** [http://www.keramverband.de/brevier_engl/8/2/4/8_2_4_1.htm

[Chin 1999] Chin, C. L. (1999). Analysis and Study of Stresses in the Structure of High Power Laser Chip Bonded on a Metallic Mount, Department of Electrical and Computer Engineering, University of California

[Copper Development Association UK 2006] Copper Development Association UK (2006). Soldering.**June 2006:** http://www.cda.org.uk/Megab2/costeff/pub98/sec4.htm

[Diamond 1919] Diamond, W. J. (1919). Practical Experimental Designs for Engineers and Scientists, Lifetime Learning Publications.

[Djurfors and Ivey 2001] Djurfors, B. and D. G. Ivey (2001). Film Growth Characterization of Pulse Electrodeposited Au/Sn Thin Films. The International Conference on Compound Semiconductor Manufacturing Technology, Las Vegas, NV, GaAs MANTecH Inc.

[Djurfors and Ivey 2002] Djurfors, B. and D. G. Ivey (2002). "Microstructural Characterization of Pulsed Electrodeposited Au/Sn Alloy Thin Films." Materials Science and Engineering **B90**(3): 309-320.

[Doesburg and Ivey 2001] Doesburg, J. and D. G. Ivey (2001). "Co-Deposition of Gold-Tin Alloys from a Non-Cyanide Solution." Plating and Surface Finishing **88**(4).

[Doesburg 2000] Doesburg, J. C. (2000). The Structure and Composition of an Electroplated Gold-Tin Solder Alloy Co-Deposited by Pulse Plating from Solutions Containing Ethylenediamine as Stabilizer. Material Engineering in Department of Chemical and Material Engineering, University of Alberta.

[illegible]iji, Masashi et al. 2006] Eiji, H., K. Masashi, et al. (2006). Method for Stablizing Electroless Gold Plating Liquid: JP2006077270.

[Elimelech, Gregory et al. 1998] Elimelech, M., J. Gregory, et al. (1998). Particle Deposition and Aggregation - Measurement, Modelling and Simulation, Elsevier.

[El-Rehim, Shaffei et al. 1996] El-Rehim, S. S., M. Shaffei, et al. (1996). "Effect of Additives on Plating Rate and Bath Stability of Electroless Deposition of Nickel-Phosphorus-Boron on Aluminum." Metal Finishing **94**(12): 29-30.

[Environment Protection Authority 2003] Environment Protection Authority (2003). Lead, Your Health and the Environment.**April 2005:** http://www.epa.nsw.gov.au/leadsafe/leadinf2.htm

[Fahong 2003] Fahong, J. (2003). Materials Requirements for Optoelectronic Packaging-Fiber Soldering, San Jose State University

[Flinn Scientific 2003] Flinn Scientific (2003). The Floating Tin Sponge.

[Forman and Minogue 2004, October] Forman, S. R. and G. Minogue (2004, October). "The Basics of Wafer-Level Ausn Soldering." Chip Scale Review **8**(7): 55-59.

[Gilleo 2002] Gilleo, K. (2002). Flip Chip Technology. Area Array Packaging Handbook, McGraw-Hill.

[Goldstein, Newbury et al. 2003] Goldstein, J., D. Newbury, et al. (2003). Scanning Electron Microscopy and X-Ray Microanalysis. New York Boston, Kluwer Academic/Plenum Publishers.

[Goodhew, Humphreys et al. 2001] Goodhew, P. J., J. Humphreys, et al. (2001). Electron Microscopy and Analysis. London and New York, Taylor & Francis.

[Graves 2005] Graves, B. (2005). Precision Plating of Electronic Components.**April 2005:** http://www.p2pays.org/ref/06/05175.htm

[Hanna, Hamid et al. 2004, Jan] Hanna, F., Z. A. Hamid, et al. (2004, Jan). "Controlling Factors Affecting the Stability and Rate of Electroless Copper Plating." Materials Letters **58**(1-2).

[He, Liu et al. 2005] He, A., Q. Liu, et al. (2005). "Investigation on the Stability of Au-Sn Electroplating Solution." Plating and Surface Finishing: 30-36.

[He, Liu et al. 2006] He, A., Q. Liu, et al. (2006). "Development of Stable, Non-Cyanide Solutions for Electroplating Au-Sn Alloy Films." Journal of Materials Science: Materials in Electronics **17**(1): 63-70.

[He, Djurfors et al. 2002] He, A., B. Djurfors, et al. (2002). "Pulse Plating of Gold-Tin Alloys for Microelectronic and Optoelectronic Applications." Plating and Surface Finishing **89**(11).

[Hempel, Herklotz et al. 1995] Hempel, W., G. Herklotz, et al. (1995). Bright Gold-Tin Alloy Electroplating Bath. DE: DE4406434.

[Hnilica 2006] Hnilica, T. (2006). Differences between Soft Solder and Hard Solder. **June 2006:** http://ajh-knives.com/soldering.html

[Hradil, Stavitsky et al. 2006] Hradil, G., R. Stavitsky, et al. (2006). Near Neutral Ph Tin Electroplating Solution. USA: US2006113195.

[Hradil, Hradil et al. 2005] Hradil, H., G. Hradil, et al. (2005). Electroplating Solution for Gold-Tin Eutectic Alloy. U.S.A.: WO2005110287.

[Hradil, Hradil et al. 2005] Hradil, H., G. Hradil, et al. (2005). Electroplating Solution for Gold-Tin Eutectic Alloy. US: US2005252783.

[Ivey and Sun 2001] Ivey, D. G, and W. Sun (2001). Codepositing of Gold-Tin Alloys. Canada: US6245208.

[Ivey, Djurfors et al. 2003] Ivey, D. G., B. M. Djurfors, et al. (2003). Electrodeposition Process and a Layered Composite Material Produced Thereby: US2003134142.

[Kashyap, Srivastava et al. 1986] Kashyap, R., S. K. Srivastava, et al. (1986). "The Role of Addition Agents in the Electrodeposition of Ni--Mn--Zn Alloys from a Sulphate Bath." Surface Technology **28**.

[Kato 2006] Kato, Y. (2006). Electroplating Device and Electroplating Method. Japan: JP2006083445.

[Knodler 1986] Knodler, A. (1986). Theory and Practice of Pulse Plating, American Electroplaters and Finishers Society.

[Kovarsky, Yu et al. 2006] Kovarsky, N. Y., C. Yu, et al. (2006). Method of Stabilizing Additive Concentrations in an Electroplating Bath for Interconnect Formation. USA: US2006108228.

[Le Nickel 1970] Le Nickel (1970). Improvements in or Relating to High-Rate Electrolytic Nickel-Plating Methods, and Installations. France: GB1213267.

[Liu, Song et al. 2005] Liu, X., K. Song, et al. (2005). "A Metallization Scheme for Junction-Down Bonding of High-Power Semiconductor Lasers." IEEE Transactions on Advanced Packaging **PP**(99): 1-9.

[Lowenheim 1974] Lowenheim, F. A. (1974). Modern Electroplating.

[Masaki, Masao et al. 2006] Masaki, S., N. Masao, et al. (2006). Non-Cyanide Electroless Gold Plating Solution and Process for Electroless Gold Plating: US2006062927.

[Masaru and Kazutaka 2005] Masaru, K. and S. Kazutaka (2005). Electroless Gold Plating Liquid: JP2005146410.

[Masato and Hiroyuki 2005] Masato, F. and Y. Hiroyuki (2005). Electroless Gold-Plating Liquid: JP2005105318.

[Mason, Gunst et al. 1989] Mason, R. L., R. F. Gunst, et al. (1989). Statistical Design and Analysis of Experiments, with Applications to Engineering and Science, John Wiley & Sons, Inc.

[Mathe 1992] Mathe, Z. (1992). "Electroless or Autocatalytic Gold Plating." Metal Finishing **90**(1): 33-34.

[Matsumoto and Inomata 1986] Matsumoto, S. and Y. Inomata (1986). Gold-Tin Alloy Plating Bath and Plating Method: JP61015992.

[McMillan and Considine 1999] McMillan, G. K. and D. M. Considine (1999). Process/Industrial Instruments and Controls Handbook, McGraw-Hill.

[Menini 2005] Menini, R. (2005). Use of Ultrasonic Agitation for Copper Electroplating: Application to High Aspect Ratio Blind Via Interconnections.**April 2005:** http://www.circuitree.com/CDA/Articles/Web_Only_Editorial/90e3e3c79bfe7010VgnVCM100000f932a8c0____

[Mohler 1984] Mohler, J. B. (1984). "Secondary Metals in Plating Baths." Metal Finishing **82**(3): 63-64.

[Montgomery and Runger 1994] Montgomery, D. C. and G. C. Runger (1994). Applied Statistics and Probability for Engineers, John Wiley & Sons, Inc.

[Morrissey 1994] Morrissey, R. J. (1994). Non-Cyanide Electroplating Solution for Gold or Alloys Thereof. US: US5277790.

[Morrissey 2004] Morrissey, R. J. (2004). Electroplating Solution for Alloys of Gold with Tin: US2004231999.

[Morrissey 2005] Morrissey, R. J. (2005). Electroplating Solution for Alloys of Gold with Tin, TECHNIC (US); MORRISSEY RONALD J (US): WO2005118917.

[Nakahara and McCoy 1980] Nakahara, S. and R. J. McCoy (1980). "Kirkendall Void Formation in Thin-Film Diffusion Couples." Applied Physics Letters 37(1): 42-44.

[National Institute of Standards and Technology (NIST) and International Sematech 2005] National Institute of Standards and Technology (NIST) and International Sematech (2005). E-Handbook of Statistical Methods: http://www.itl.nist.gov/div898/handbook/

[Ohring 2002] Ohring, O. (2002). Materials Science of Thin Films: Deposition and Structure, Academic Press.

[Okinaka 1990] Okinaka, Y. (1990). Chapter 15: Electroless Plating of Gold and Gold Alloys. Electroless Plating - Fundamentals and Applications. G. O. Mallory and J. B. Hajdu, William Andrew Publishing/Noyes.

[Perkin-Elmer] Perkin-Elmer 4000 Atomic Absorption Manuals.

[Ramachandran 1995] Ramachandran, V. S. (1995). Concrete Admixtures Handbook - Properties, Science, and Technology, William Andrew Publishing/Noyes.

[Ramanauskas, Gudaviciute et al. 2003] Ramanauskas, R., L. Gudaviciute, et al. (2003). Pulse Plating Effect on Microstructure and Corrosion Properties of Zn-Ni Alloy Coatings. Third Baltic Conference on Electrochemistry.

[Reid and Goldie 1974] Reid, F. H. and W. Goldie (1974). Gold Plating Technology, Electrochemical Publications Limited.

[Rezrazi, Doche et al. 2005] Rezrazi, M., M. L. Doche, et al. (2005). "Au-Ptfe Composite Coatings Elaborated under Ultrasonic Stirring." Surface and Coatings Technology **192**(1).

[Riley 2004] Riley, G. A. (2004). Too Much Gold Can Be a Bad Thing.**June 2006:** http://www.flipchips.com/tutorial37.html

[Rosato, Rosato et al. 2000] Rosato, D. V., D. V. Rosato, et al. (2000). Injection Molding Handbook, Springer - Verlag.

[Sadar 2002] Sadar, M. (2002). Turbidity Instrumentation - an Overview of Today's Available Technology. Reno, NV, Hach Company.

[Schlesinger and Paunovic 2000] Schlesinger, M. and M. Paunovic (2000). Modern Electroplating.

[Sel Rex Corp. 1971] Sel Rex Corp. (1971). Gold Alloy Electroplating Bath. USA: GB1221862.

[Shigeki and Kenji 2005] Shigeki, S. and Y. Kenji (2005). Substitution Type Electroless Gold Plating Liquid: JP2005307309.

[Shindo 2003] Shindo, Y. (2003). Gold Plating Solution and Gold Plating Method. United States Patent, Electroplating Engineers of Japan Limited: 6,511,589.

[Sinorama 2002] Sinorama (2002). Electroless Plating Processes.**April 2005:** http://www.sinorama.com/nickel02.htm

[Smith and Akhlaghi 2004] Smith, B. and S. Akhlaghi (2004). Alloy Electroplating: The Best Solution for Au-Sn Solder?**June 2006:** http://www.flipchips.com/tutorial46.html

[Stanley 1987] Stanley, G. G. (1987). The Extractive Metallurgy of Gold in South Africa, Johannesburg : South African Institute of Mining and Metallurgy.

[Stevens, Deuber et al. 1977] Stevens, P., J. M. Deuber, et al. (1977). Tin-Gold Electroplating Bath and Process. US, OXY METAL INDUSTRIES CORP: US4013523.

[Sun 1998] Sun, W. (1998). Electroplating of Gold-Tin Eutectic Solder. Material Engineering in Department of Chemical and Material Engineering, University of Alberta.

[Sun and Ivey 1998] Sun, W. and D. G. Ivey (1998). Electroplating of Gold-Tin Solder for Optoelectronic Applications. Electronic Packaging Materials Science X, San Francisco, California, U.S.A., Materials Research Society.

[Sun and Ivey 1999] Sun, W. and D. G. Ivey (1999). "Development of an Electroplating Solution for Codeposition Au-Sn Alloys." Materials Science Engineering **B65**: 111-112.

[Sun and Ivey 2001] Sun, W. and D. G. Ivey (2001). "Microstructural Study of Co-Electroplated Au/Sn Alloys." Journal of Material Science **36**: 757-766.

[TechSolve 2005] TechSolve (2005). Electroless Plating.**April 2005:** http://www.techsolve.org/

[Toshiaki, Yasuhiro et al. 2006] Toshiaki, S., K. Yasuhiro, et al. (2006). Gold Plating Liquid and Gold Plating Method: WO2006049021.

[Tsutomu, Tsuyoshi et al. 2005] Tsutomu, N., S. Tsuyoshi, et al. (2005). Copper Plating Bath and Plating Method: US2005072683.

[Uchida and Okada 2002] Uchida, E. and T. Okada (2002). Non-Cyanide-Type Gold-Tin Alloy Plating Bath: US2002063063.

[Wang 2006] Wang, F. H. (2006). Electroplating Additive and Its Preparation Method: CN1733977.

[Watanabe and ABE 1998] Watanabe, H. and S. ABE (1998). "Gold Wire Bondability of Electroless Gold Plating Using Disulfiteaurate Complex." JOURNAL OF APPLIED ELECTROCHEMISTRY **28**: 525+529.

[Williams and Carter 1996] Williams, D. B. and C. B. Carter (1996). Transmission Electron Microscopy - a Textbook for Materials Science - 4 Volumes, Plenum Press.

[Willoughby 2003] Willoughby, B. G. (2003). Air Monitoring in the Rubber and Plastics Industries, Rapra.

[Zhang 2001] Zhang, Y. (2001). Composition and Stability of Plating Baths for the Deposition of Gold-Tin Alloys-a Literature Review, Department of Chemical and Material Engineering, University of Alberta

[Zhang and Ivey 2004] Zhang, Y. and D. G. Ivey (2004). "Electroplating of Gold-Tin Alloys from a Sulfite-Citrate Bath." Plating and Surface Finishing **62**(4): 28-33.

[Zribi, Chromik et al. 1999] Zribi, A., R. R. Chromik, et al. (1999). Solder Metalization Interdiffusion in Microelectronic Interconnects. Electronic Components and Technology Conference.

Appendix A: Additives and Techniques Used to Improve Bath Stability and Plating Rate

Table A-1: Additives and techniques used to improve bath stability.

Reference	Plated Metal(s)	pH	Additives/Techniques	Other Conditions and Comments
[Zhang 2001]	Gold-Tin	< 7	Citrate (chelating agent), D-gluconate (stabilizer), pyrophosphate (tin chelating agent), tartaric acid (complexing agent, antioxidant), phosphonics, and EDTA (complexing agents)	Applies to cyanide baths.
[Kashyap, Srivastava et al. 1986]	Ni-Mn-Zn	< 7	Dextrin, glucose, or l-serine (decreased cathode polarization) β-alanine or glycine (increased cathode polarization)	Applies to Ni-Mn-Zn sulphate bath. Ammonium sulphate, thiourea, and ascorbic acid are other components of these baths. The Ni, Mn, and Zn metal contents in the deposits changed with the addition of different reagents.
[Zhang 2001]	Gold	< 7	Amines, citric acid, oxalic acid, or N-carboxymethyl-polyamines (i.e., EDTA)	Applies to both cyanide & non-cyanide baths. All additives are chelating agents.
[Reid and Goldie 1974]	Gold	< 7	Free sulfite and thiosulfate	Applies to gold- sulfite baths.
[El-Rehim, Shaffei et al. 1996]	Nickel (electroless)		Sulfonate, sulfate, or chloride anion groups	Naphthalene sulfonic acid did not improve the stability. The concentration of additives determined the amount of improvement in the stability.

Table A-1: Additives and techniques used to improve bath stability. (continued).

Reference	Plated Metal(s)	pH	Additives/Techniques	Other Conditions and Comments
[Hanna, Hamid et al. 2004, Jan]	Copper		Pyridine, cytosine, benzotriazole (BT), or 2-mercaptobenzothiozole (2MBT)	Tartarate or ethylenediaminetetraacetic (EDTA) copper baths were used. The additives modified the crystal structure of the copper deposits.
[Hanna, Hamid et al. 2004, Jan]	Copper		Mild air agitation	The bath stability increased by 20 times relative to a bath without aeration.
[Shindo 2003]	Gold	5 to 10	Trivalent gold compound, i.e. gold hydroxide salt and/or chloroaurate salt hydantoin compound of imidazolidinedione, 5,5-dimethylhydantoin, or hydantoic acid (chelating agent, 0.1 to 2.5 M/l)	This non-cyanide solution is claimed to have excellent stability due to the chosen chelating agent which is not reductive, and thereby autolysis caused by pyrolysis[1] or electrolysis does not occur. Conductive salts used include hydrochloric acid, sulfuric acid, nitric acid, or phosphoric acid. Buffers used include boric acid, succinic acid, phthalic acid, tartaric acid, citric acid, or phosphoric acid. Current density: 1-45 mA/cm^2 Temperature: 20-70°C
[Watanabe and ABE 1998]	Gold (electroless)		Potassium ferrocyanide, cupferron, or potassium nickel cyanide or 2,2-bipyridyl	Additives with concentrations of 10 to 100 parts per million (ppm) were used with the noncyanide baths. Originally, baths were unstable and self-decomposing after several hours.

---

[1] Pyrolysis: chemical change brought about by the action of heat.

Table A-1: Additives and techniques used to improve bath stability. (continued).

Reference	Plated Metal(s)	pH	Additives/Techniques	Other Conditions and Comments
[Schlesinger and Paunovic 2000]	Gold (electroless)		1,2-diaminoethane and KBr combined with: hypophosphite, formaldehyde, hydrazine, borohydride, or DMAB (reducing agent)	Baths were sensitive to contamination with small amounts of nickel ions.
[Schlesinger and Paunovic 2000]	Gold (electroless)		Ethylenediamine or EDTA (stabilizing agent) formaldehyde or hydrazine (reducing agent) arsenic compound	This sulfite-based bath is reported to yield hard gold deposits.
[Schlesinger and Paunovic 2000]	Gold (electroless)		Thiourea (reducing agent), methyl thiourea	Au(I)-sulfite-ethylenediamine complex was used as the source of gold. The performance of the bath was found to be pH dependent. Good deposits were obtained from a bath containing both thiourea and methyl thiourea at the concentration ratio of three.
[Schlesinger and Paunovic 2000]	Gold (electroless)		Triethanolamine, nitrilo-triacetic acid, or sodium thiosulfate	The sulfite-based bath was considered.
[Schlesinger and Paunovic 2000]	Gold (electroless)		Heterocyclic mercapto compounds, i.e. 2-mercaptobenzothiazole (MBT), 2-mercaptobenzoimidazole (MBI), or 6-ethoxy-2-mercaptobenzothiazole (EMBT)	Trace amounts of the additives were added. The bath contained ascorbic acid. Stability improved from 3 to 35 hours. Also, increasing the sulfite concentration increased the stability.

Table A-1: Additives and techniques used to improve bath stability. (continued).

Reference	Plated Metal(s)	pH	Additives/Techniques	Other Conditions and Comments
[Sun and Ivey 1999] & [Matsumoto and Inomata 1986]	Gold-Tin (electrolytic)	3 To 7	Peptone and $NiCl_2$	$KAuCl_4$ and $SnCl_2$ were used as source of gold and tin ions. Bath also contained triammonium citrate and L-ascorbic acid. Current density range of 1-4 mA/cm^2 was used for plating. No specific data was given on the stability of the solution.
[Akihiro and Kazumi 2006]	Gold (electroless)	~ 7	Pyrosulfurous acid, thiosulfuric acid, sulfurous acid, aminocarboxylic acid, pyrosulfurous acid or its alkali metal salts, alkaline earth metal salts, or ammonium salts	The non-cyanide plating liquid is claimed to have low toxicity and improves solder adhesion.
[Masaki, Masao et al. 2006]	Gold (electroless)	< 7	X-(CH_2)n-SH (complexing agent)(1.7 to 8.3 g/l) i.e. sodium mercaptoethanesulfonate, sodium mercaptopropanesulfonate, or aminoethanethiol.	(n is 2 or 3 and X SO_3H or NH_2) Gold sulfite salt or a chloroaurate salt are used as a source of gold (0.75 to 1.25 g/l). Citrate salts are added to the solution as conductive salts, i.e., monopotassium citrate and tripotassium citrate. A pH adjuster such as potassium hydroxide may be added. The pH and temperature are preferred to be in the range of 3 to 6 and 40 to 90°C respectively. It is claimed that the complex formed exhibits a deposition potential close to that of $KAu(CN)_2$ and is very stable.

Table A-1: Additives and techniques used to improve bath stability. (continued).

Reference	Plated Metal(s)	pH	Additives/Techniques	Other Conditions and Comments
[Masaki, Masao et al. 2006]	Gold (electrolytic)	> 7	X-(CH_2)n-SH (complexing agent)(1.7 to 8.3 g/l)	(n is 2 or 3 and X SO_3H or NH_2) An electrolytic gold plating solution is to be used in the alkaline region condition of the pH value of 7 or higher. However, this alkaline region condition is not compatible with the mask layer in electronic applications.
[Eiji, Masashi et al. 2006]	Gold (electroless)		Detecting the oxidation-reduction potential of the plating liquid and cyanide ions replenished	Used when instability is due to the reduction of the concentration in free cyanide ions in the plating liquid. An ORP (oxidation-reduction potential) meter is used to measure the oxidation-reduction potential. The replenishment period and quantity of cyanide ions are decided based on the stability.
[Akihiro, Kazumi et al. 2006]	Gold (electroless)	~ 7	Hydrogensulfite compound, i.e. Sodium hydrogensulfite, potassium hydrogensulfite, ammonium hydrogensulfite thiosulfate compound, amino-carboxylic acid	Water-soluble gold compound is used in this non-cyanide bath. Good adhesion to a solder and a coating film is claimed.
[Kovarsky, Yu et al. 2006]	All		Maintaining a relatively constant additive concentration in the plating cell.	During the plating process, the plating solution is continuously circulated through a chemical management unit. An absorbent material is positioned in this unit. Depending on the concentration of the additive in the plating solution, the additive is absorbed or released from the absorbent material.

Table A-1: Additives and techniques used to improve bath stability. (continued).

Reference	Plated Metal(s)	pH	Additives/Techniques	Other Conditions and Comments
[Masato and Hiroyuki 2005]	Gold (electroless)		Aminocarboxylic acid, or water-soluble amine (complexing agent) hydrazine, hydroquinone, pyrogallol or their derivatives (reducing agent) arsenic, thallium, lead, or benzotriazole compounds (base metal elution inhibitor)	This bath also includes gold sulfite, glycolic acid, diglycolic acid or their salts. It is claimed that the bath has excellent stability and a high plating rate.
[Toshiaki, Yasuhiro et al. 2006]	Gold (electrolytic)		Iodine and/or iodide ions polyhydric alcohol having 4 or more carbon atoms, i.e. diethylene glycol, triethylene glycol	This gold plating bath is claimed to be stable and low in toxicity, while achieving performance comparable to cyanide-based gold plating baths. The amount of the polyhydric alcohol is claimed to be 10-90% by weight.
[Sun and Ivey 1999] & [Sun 1998]	Gold-Tin (electrolytic)	6.5	Na_2SO_3 (20–100 g/l), $Na_2S_2O_3$ (20–100 g/l) or $Na_2H_2EDTA{\cdot}2H_2O$ (5–40 g/l)	Based on the screening tests, sodium sulphite was selected as the gold stabilizer. The addition of the other stablizers caused gold precipitation.
[Hradil, Stavitsky et al. 2006]	Tin	5.5 to 8	Propoxalated or ethoxylated polyalchohols (surfactants) (25 - 200 g/l) gluconic acid, heptagluconic acid or pyrophosphate (Complexing agents) (25 - 200 g/l)	These additives are claimed to provide a semi-bright deposit at high current efficiencies. The amount of complexing agent required is proportional to the metal concentration. i.e., at a tin concentration of 15 g/l, the preferred gluconic acid concentration is claimed to be 50 - 120 g/l. Buffers: sodium hydroxide, potassium hydroxide, ammonium hydroxide.

Table A-1: Additives and techniques used to improve bath stability. (continued).

Reference	Plated Metal(s)	pH	Additives/Techniques	Other Conditions and Comments
[Akihiro, Yoshiyuki et al. 2006]	Gold (electroless)	4 to 10	Sulfurous acid compound (stabilizer), i.e., sulfurous acid and alkali metal, alkaline earth metal, ammonium. pyrosulfurous acid compound, i.e., pyrosulfurous acid, alkali metal, alkaline earth metal, ammonium aminocarboxylic acid compound (complexing agent) i.e., ethylenediaminetetraacetic acid, hydroxyethylethylenediaminetriacetic acid, dihydroxyethylethylenediaminediacetic acid, propanediaminetetraacetic acid, diethylenetriamine pentaacetic acid, triethylenetetraminehexaacetic acid, glycine, glycylglycine, glycylglycylglycine, dihydroxyethylglycine, iminodiacetic acid, hydroxyethyliminodiacetic acid, nitrilotriacetic acid, nitrilotripropionic acid, and alkali metal, alkaline earth metal, ammonium salts.	All are used in the concentration of 0.1 - 200 g/l, preferably 1 - 100 g/l. There are no particular restrictions on the gold compound that can be used as long as it is cyanide-free and water soluble (preferably gold sulfite, gold thiosulfate, gold thiocyanate, chloroauric acid (0.1 - 100 g/l, preferable 0.5 - 20 g/l of gold). Possible buffers include phosphoric acid compound, i.e., phosphoric acid, pyrophosphoric acid or alkali metal, alkaline earth metal, and ammonium salts of these, alkali metal dihydrogenphosphates, alkaline earth metal dihydrogenphosphates, ammonium dihydrogenphosphates, di-alkali metal hydrogenphosphates, di-alkaline earth metal hydrogenphosphates, and diammonium hydrogenphosphates (1 - 100 g/l). The gold film is claimed to have good solder adhesion. A pH of 5 to 9 is preferred. Temperature: 10 to 95 °C (preferably 50 to 85 °C).
[Kato 2006]	All		Dosing additives continuously	The desired additives are dosed into the plating solution to compensate for the drop in their concentration.

Table A-1: Additives and techniques used to improve bath stability. (continued).

Reference	Plated Metal(s)	pH	Additives/Techniques	Other Conditions and Comments
[Doesburg and Ivey 2001]	Gold-Tin (electrolytic)	< 7	Ethylenediamine (EDA) (0-0.135 M)	The stability is claimed to increase from 16 days to 28 days based on solution appearance. Rougher deposits are obtained with increase in ethylenediamine concentration. The addition of the additive increased polarization and decreased the range of current densities available for plating.
[Hradil, Hradil et al. 2005; Hradil, Hradil et al. 2005]	Gold-Tin	2 to 10	Oxalic acid, citric acid, ascorbic acid, gluconic acid, malonic acid, tartaric acid and/or iminodiacetic acid or their salts (complexing agents). Anionic surfactants based on phosphate esters (alloy stabilization agent) (0.01 to 10 ml/l) with the general formulas: 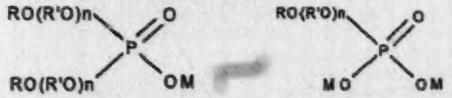 RO(R'O)n O P RO(R'O)n OM RO(R'O)n O P MO OM wherein R is an alkyl or alkyl aryl group, n is 7 - 10 moles of ethylene and/or propylene oxide, M is hydrogen, sodium, potassium or other counter ion, and R' is an ethyl and/or propyl group. i.e. ethoxylated phenol ester.	It is claimed that eutectic composition can be deposited over a usable range of current densities from this solution. The source of gold ions may be mono- or tri-valent potassium or ammonium gold cyanide (stable) or sulfite gold (short life span). The source of tin ions may be any soluble stannous or stannic ions, i.e., sulfate, chloride, methane sulfonate, oxalate. The relative amount of gold and tin ions in the solution determines the composition of the deposit. Temperature: 20 - 70 °C. (Higher temperature results in higher gold content in the deposit.)

Table A-1: Additives and techniques used to improve bath stability. (continued).

Reference	Plated Metal(s)	pH	Additives/Techniques	Other Conditions and Comments
[Wang 2006]	Tin		Mixture of lauryl phenol polyoxydivinyl ether, polyoxyethylene aniline ether, N, N-diethylm toluidine, hydracrylic acid, acetylglycine acid, naphthalene sulfonic acids, polyoxyethylene polyoxyprophylene propylene, and hydroquinone, and deionized water	The mixing order and process is important. It is claimed that addition of proper amounts of these additives eliminate compressive stress, control crystal process, form a perfect crystallization structure, and control particle size, thickness of plating layer, and tin expansibility. It is claimed that this process eliminates whisker growth.
[Hempel, Herklotz et al. 1995]	Gold-Tin	3 to 14	Potassium hydroxide (0-30 g/l, preferably 0-20 g/l), potassium salt of gluconic, glucaric and/or glucuronic acid (30-150 g/l, preferably 50-100 g/l), piperazine (0.1-10 g/l, preferably 1-6 g/l), and arsenic compound (0.1-150 mg/l, preferably 1-100 mg/l)	The source of gold and tin ions are 0.1-100 (preferably 1-40) g/l of potassium dicyanoaurate and 1-200 (preferably 1-100) g/l of soluble Sn(IV) compound respectively. It is claimed that this bath is stable and precipitation does not occur even after longer operation periods. Temperature: 20-70 °C current densities 1-100 mA/cm^2

Table A-1: Additives and techniques used to improve bath stability. (continued).

Reference	Plated Metal(s)	pH	Additives/Techniques	Other Conditions and Comments
[Morrissey 2004]	Gold-Tin	3 to 5	2,2'-dipyridyl (0.1 - 1 g/l) thallium, lead, or arsenic (to obtain deposits of highly uniform appearance).	Gold is contained in the form of a soluble cyanide complex, and tin is in the form of a complex of stannous ion with a suitable organic ligand. Stannous ion is known to be complexed by various organic ligands. In the electrolytes of this invention, citrates, oxalates, and iminodiacetates were all investigated and found to be suitable. For this invention, citrate is the ligand of choice, both for stability and for compatibility with the electrolyte system. Buffer: citric acid, formic acid, lactic acid, malic acid, succinic acid, gluconic acid, glycolic acid, or combinations of them (75-300 g/l). It is claimed that this invention provides deposits over really large arrays of wafers and printed circuit boards.
[Schlesinger and Paunovic 2000]	Tin	< 7	Phenol- or cresol-sulfonic acid, gelatin, β-naphthol, peptone, catechol (antioxidant), hydroquinone (antioxidant) alkylphenol, imidazoline heterocylic aldeydes, etholylated β-naphtholsulphonic acid polyalkylene oxides, or resorcinol	Additives are claimed to brighten, reduce grain size, reduce dendritic growth, increase current density range, promote leveling, and reduce stress and pitting. The role of each specific named additive is not stated separately.

Table A-2: Additives and techniques used to improve plating rate.

Reference	Plated Metal(s)	pH	Additives/Techniques	Other Conditions and Comments
[El-Rehim, Shaffei et al. 1996]	Nickel (electroless)		Sulfonate, sulfate anion groups (increased the plating rate) chloride anion group (decreased the plating rate)	Chloride decreased the rate due to its attack of the substrate. The concentration of each additive affected the amount of improvement in the plating rate.
[Hanna, Hamid et al. 2004, Jan]	Copper		Pyridine, cytosine, benzotriazole (BT), and 2-mercaptobenzothiozole (2MBT)	Copper tartarate or ethylenediaminetetraacetic (EDTA) baths were considered. Plating rate improved from 1.1 to 1.8 mg/(cm^2 h) in the tartarate bath at 30 °C and from 5.4 to 10.5 mg/(cm^2 h) in the EDTA bath at 50°C.
[Reid and Goldie 1974]	Gold		Increasing the concentration of the bath ions by increasing the amount of conducting salts	Increasing the amount of conducting salts will permit the use of higher current densities resulting in better current distribution in the higher current density regions.
[Schlesinger and Paunovic 2000]	Tin		Mechanical, cathode rod, and filtration types of agitation	Applies to major acid electroplating tin chemistries.
[Reid and Goldie 1974]	Gold		Vigorous agitation: mechanical, air, nitrogen, and solution circulation	The electrolytic migration of the gold anions towards the anodes can be overcome by vigorous agitation. The agitation effect is maximized if all methods combined simultaneously.
[Reid and Goldie 1974]	Gold		Ultrasonic stirring	Investigations have shown an increase in brightness, micro-hardness, and current efficiency and density.

Table A-2: Additives and techniques used to improve plating rate. (continued).

Reference	Plated Metal(s)	pH	Additives/Techniques	Other Conditions and Comments
[Rezrazi, Doche et al. 2005]	Gold-Nickel		Ultrasonic stirring	The low transmission power of an ultrasound generator (which has a range of 100-800 kHz) has been applied to the system in addition to the previous mechanically stirred (500 kHz) system.
[Reid and Goldie 1974]	All baths		Proper fixturing, good anode-cathode spacing and anode shielding	Optimum current distribution can be obtained. As a result, higher overall current densities and plating rates can be achieved.
[Akhlaghi and Ivey 2003]	Gold-tin	<7	Raising the temperature	Increasing the temperature from 25 to 50°C, increased the plating rate by 2.3 times. Temperature increase beyond 35°C decreased the tin content in the film by 2.3 at% tin/ °C. This is due to the oxidation of tin ions in the deposit.
[Akhlaghi and Ivey 2003]	Gold-tin	<7	Mechanical agitation by moving the cathode Using an overhead stirrer	Agitation higher than 150 rpm reduces the tin content in the solution by 10 at % tin for every addition of 50 rpm. Higher agitation replaces the metal ions or complexes at the cathode surface, and favours the plating of the more noble metal (gold).
[Okinaka 1990]	Gold (electroless)		Depolarizers such as Pb^{-} or Ti^{+}	It is claimed that the plating rate is improved substantially.
[Okinaka 1990]	Gold (electroless)		Thallous sulfate, Ga, In, Ge, Sn, Sb, and Bi	Applies to cyanide based baths.
[Schlesinger and Paunovic 2000]	Gold		Thiosulfate	Gold-sulfite baths including ascorbic acid were considered. This deposition rate was increased greatly. Thiosulfate was added as a second complexing agent.

Table A-2: Additives and techniques used to improve plating rate. (continued).

Reference	Plated Metal(s)	pH	Additives/Techniques	Other Conditions and Comments
[Schlesinger and Paunovic 2000]	Gold		Ethylenediamine (0.005 M), thallous ion, or Tl+ (1 ppm)	Baths containing sulfite-thiousulfate and ascorbic acid were considered.
[Sun and Ivey 1999]	Gold		Phosphates, carbonates, acetates and citrates	Additives are used at conducting agents.
[Masaki, Masao et al. 2006]	Gold (electroless)		Thallium (Tl)	Added as a grain refiner, it is found to improve the deposition rate of gold. It was added in the form of thallium sulfate or thallium acetate in the amounts of 0.1 to 100 ppm.
[Shigeki and Kenji 2005]	Gold (electroless)	< 7	Heterocyclic aromatic compound having two or more nitrogen atoms in the molecule (oxidation inhibitor)	The bath is used to form a gold film on an electroless nickel plating film, which also contains a water soluble gold compound and a conductive salt. It is claimed that the plating rate is high.
[Le Nickel 1970]	Nickel	2.8 to 4.8	Continuously recycling, regenerating, and filtering the bath.	Nickel salts and organic additive(s) are added during the recycling and before the filtration. Also, pH is monitored and adjusted continuously.

Table A-2: Additives and techniques used to improve plating rate. (continued).

Reference	Plated Metal(s)	pH	Additives/Techniques	Other Conditions and Comments
[Masaru and Kazutaka 2005]	Gold (electroless)	3 to 7.5	Copper compounds (deposition accelerator), i.e., copper cyanide, copper sulfate, copper pyrophosphate, copper thiocyanate, disodium copper ethylenediaminetetraacetate tetrahydrate, and copper chloride. Copper complex salt, i.e. $K_3Cu(CN)_4$ or Cu-EDTA copper cyanide complex: CuCN + KCN or CuSCN + KSCN or KCN + CuSO4 + $EDTA_2Na$. (0.1 - 500 mg/l of copper).	Method used in cyanide based bath. The gold potassium cyanide concentration for a high plating rate is 0.5 g/l to 20 g/l. This bath also contains 0.05 to 1.5 mol/l ascorbic acid or its derivative (i.e., sodium ascorbate and potassium ascorbate, ammonium ascorbate salts, ascorbic acid-6-sulfate, 6-deoxy-L-ascorbic acid, and D-arabo-ascorbic acid). If the supplied copper ions are applied directly to the bath, precipitation occurs in the form of copper sulfate, copper oxide, etc. Thus, a complexing agent is added to suppress the precipitation of copper ions and stabilizes them as a copper complex in the solution. Temperature: 20 - 95°C.
[Tsutomu, Tsuyoshi et al. 2005]	Copper	< 4	Sulfur-containing saturated organic compound (promotes the electrocoating rate), i.e., bis(3-sulfopropyl)disulfide (SPS) and mercaptopropane sulfonic acid (MPS) (0.1-200 mg/l)	This bath also contains copper ions, an organic acid or an inorganic acid, chloride ions, high molecular weight surfactant which controls the electrodeposition reaction.

Appendix B: Turbidity Curves

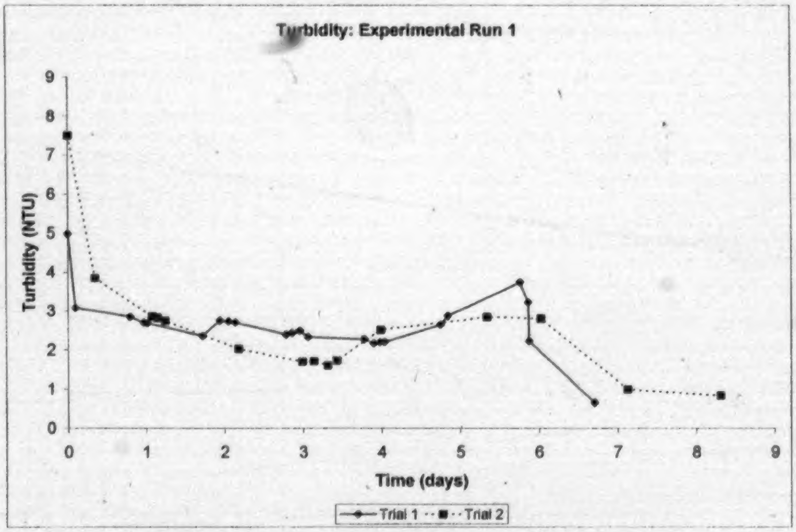

Figure B-1: Turbidity curve for experimental run 1.

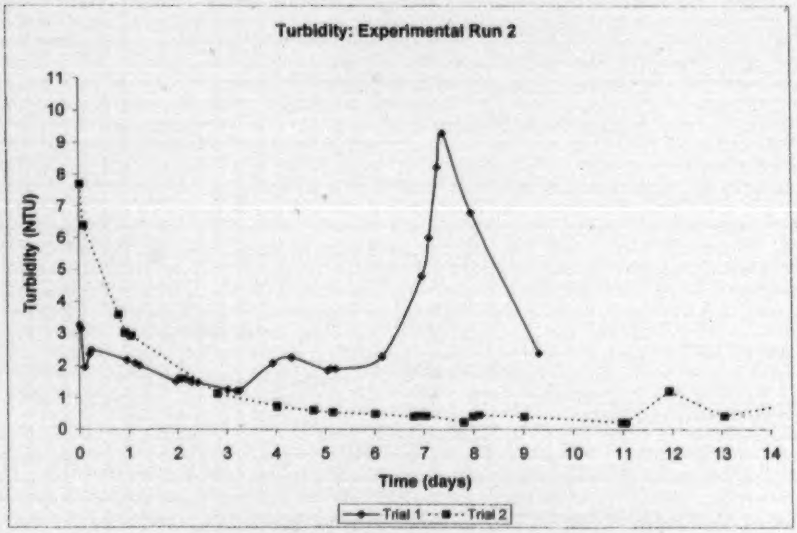

Figure B-2: Turbidity curve for experimental run2.

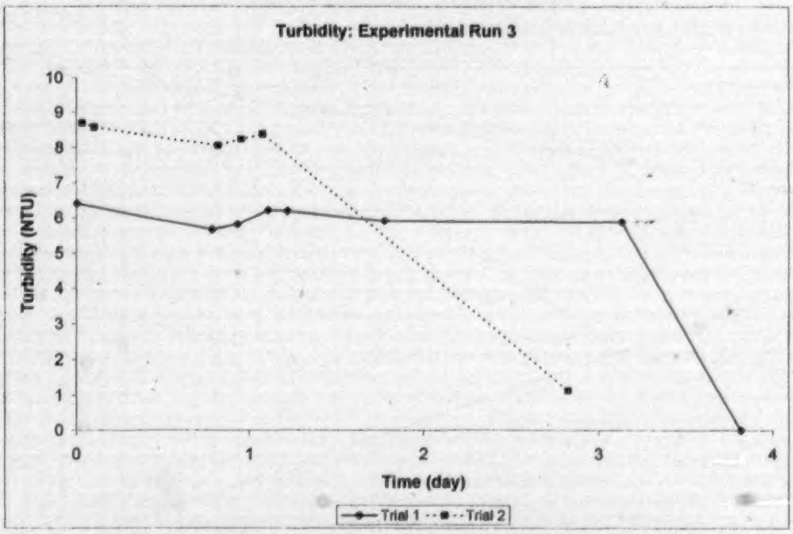

Figure B-3: Turbidity curve for experimental run 3.

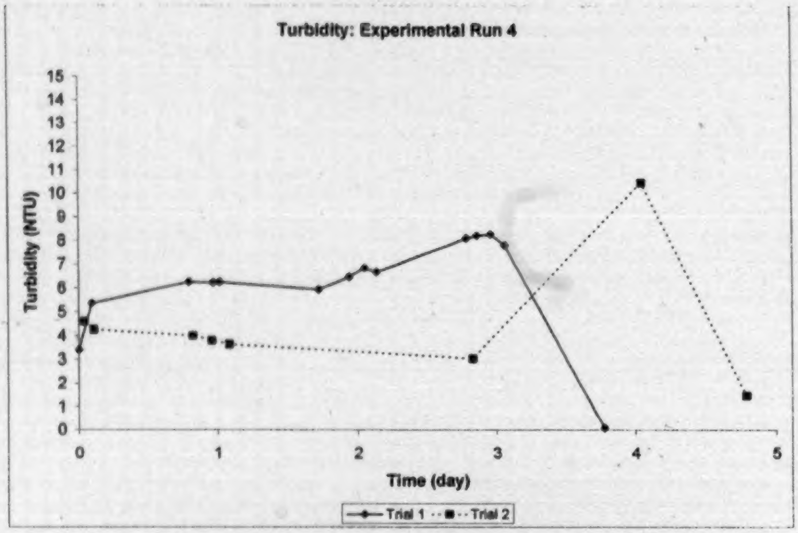

Figure B-4: Turbidity curve for experimental run 4.

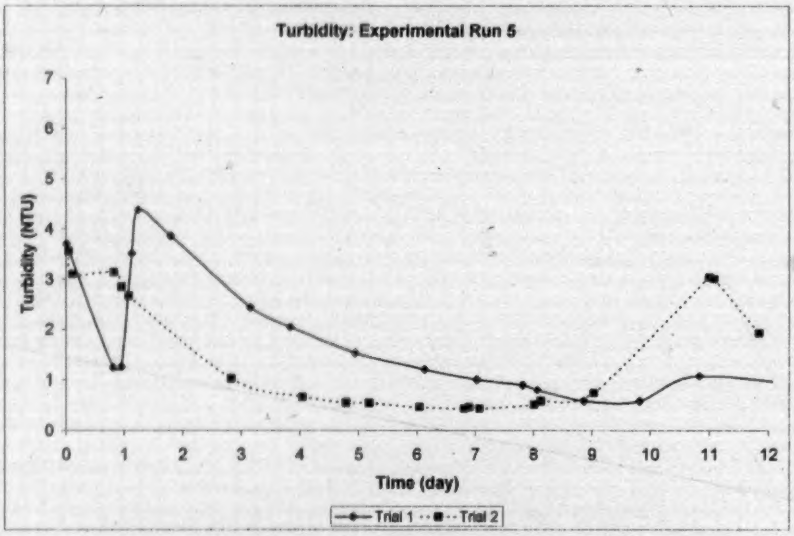

Figure B-5: Turbidity curve for experimental run 5.

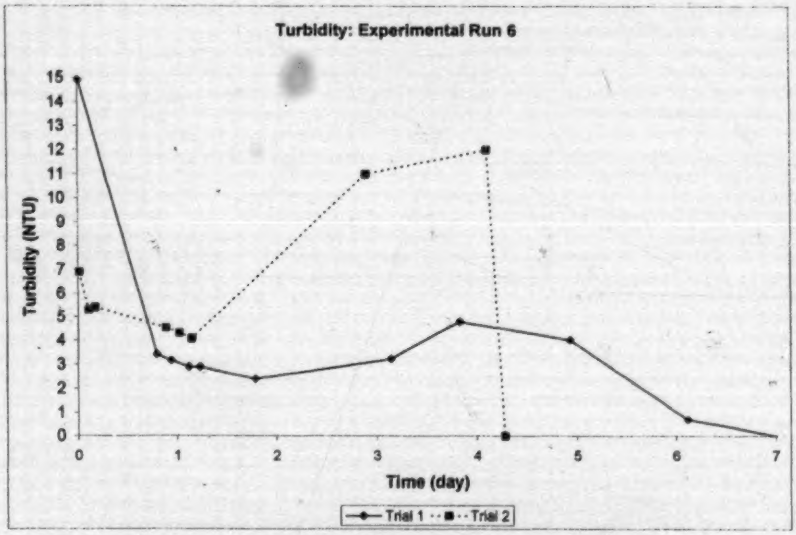

Figure B-6: Turbidity curve for experimental run 6.

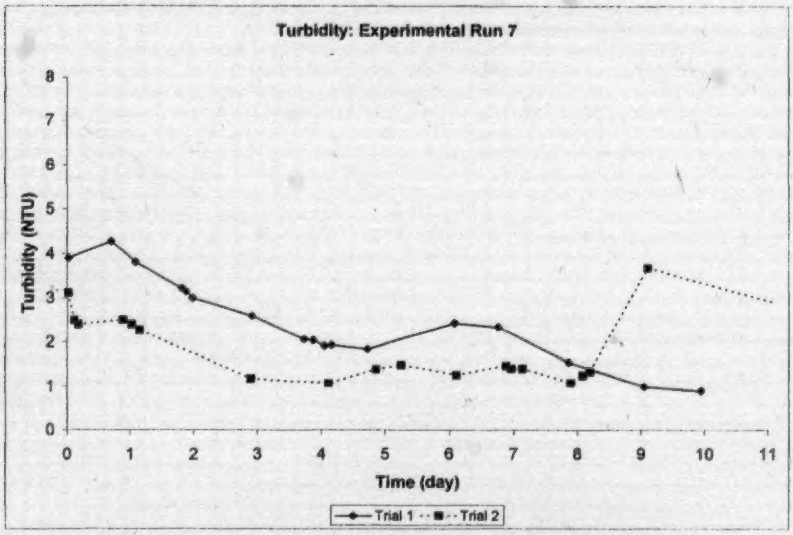

Figure B-7: Turbidity curve for experimental run 7.

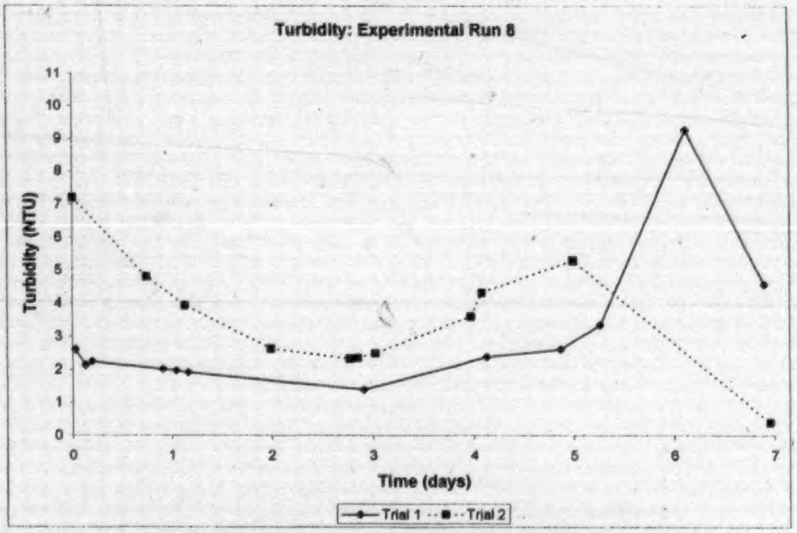

Figure B-8: Turbidity curve for experimental run 8.

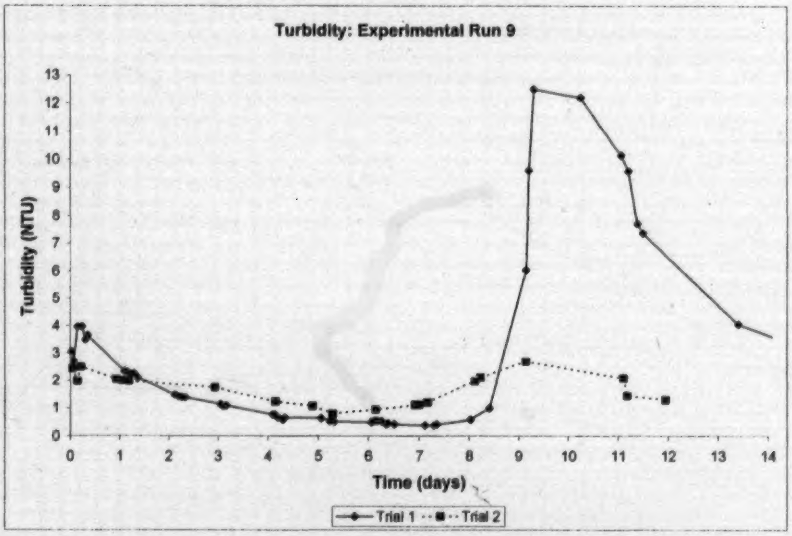

Figure B-9: Turbidity curve for experimental run 9.

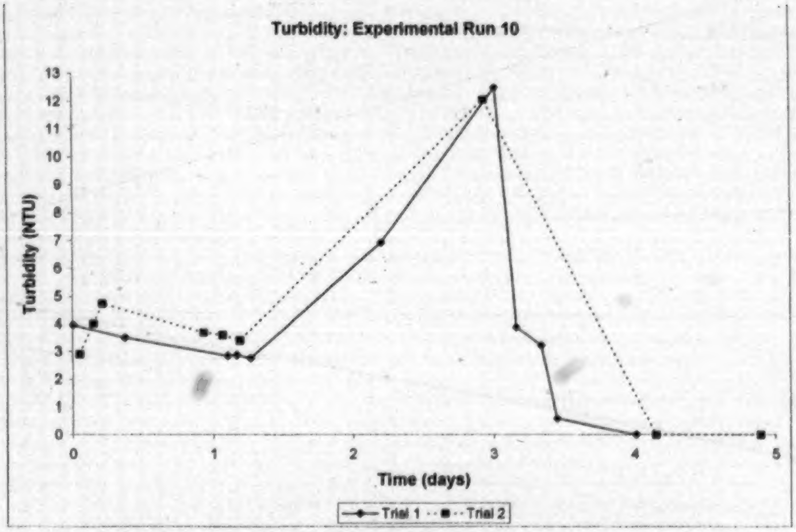

Figure B-10: Turbidity curve for experimental run 10.

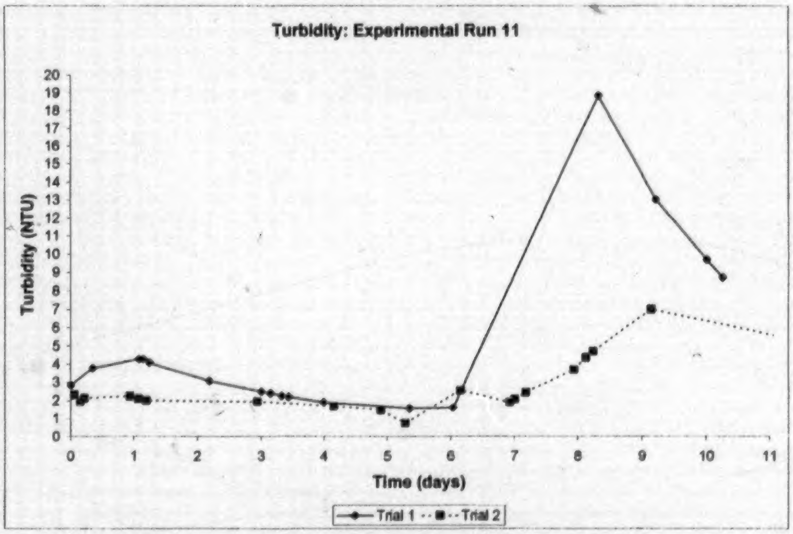

Figure B-11: Turbidity curve for experimental run 11.

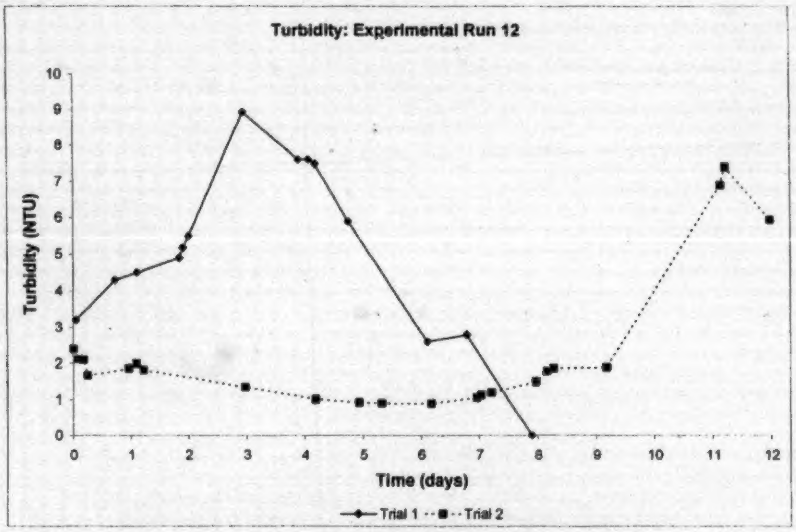

Figure B-12: Turbidity curve for experimental run 12.

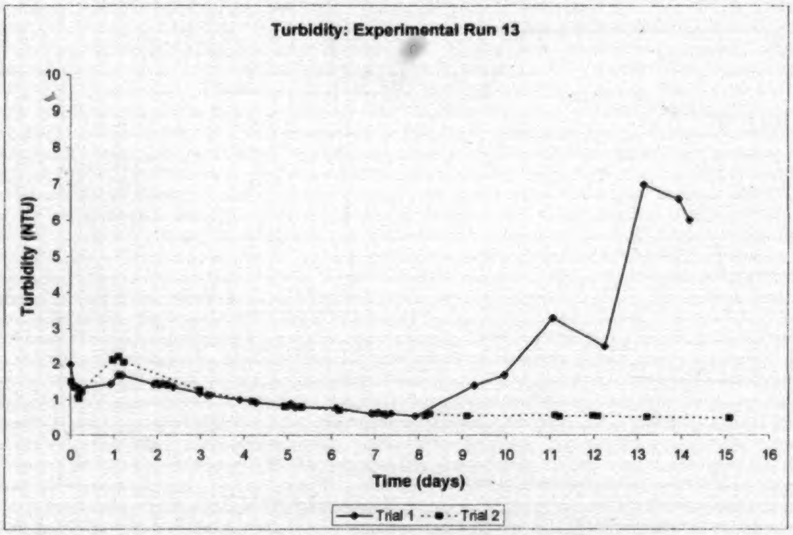

Figure B-13: Turbidity curve for experimental run 13.

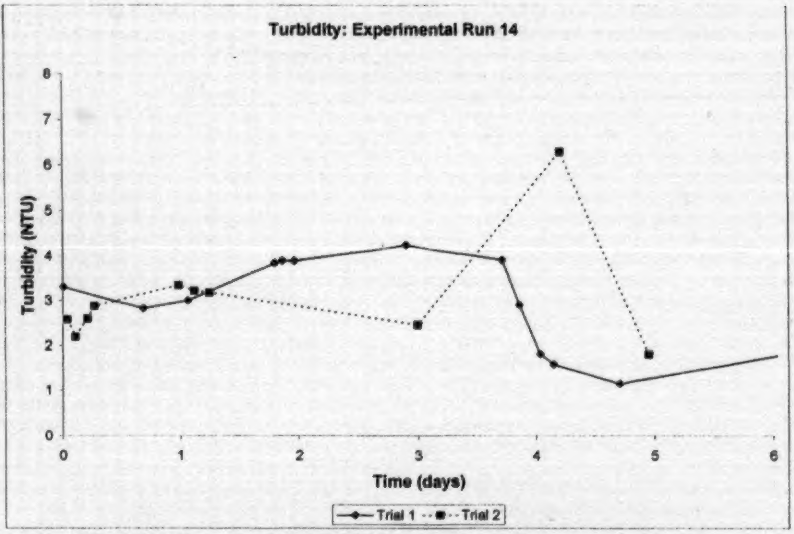

Figure B-14: Turbidity curve for experimental run 14.

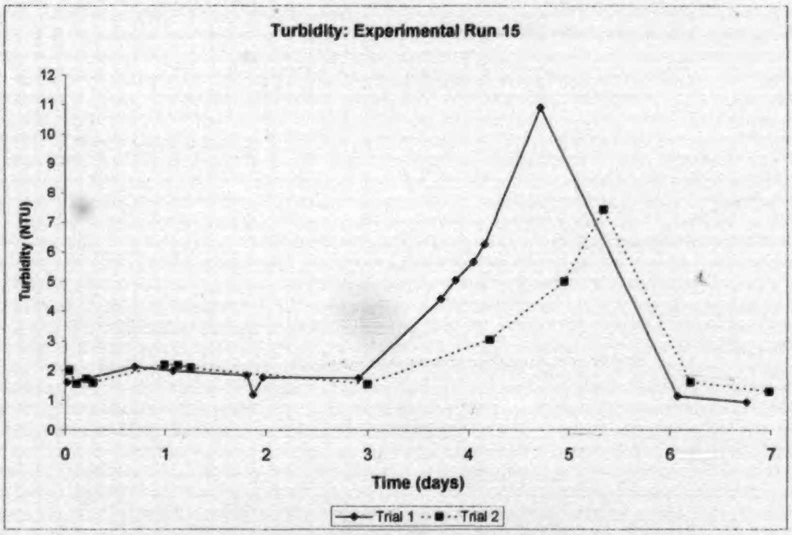

Figure B-15: Turbidity curve for experimental run 15.

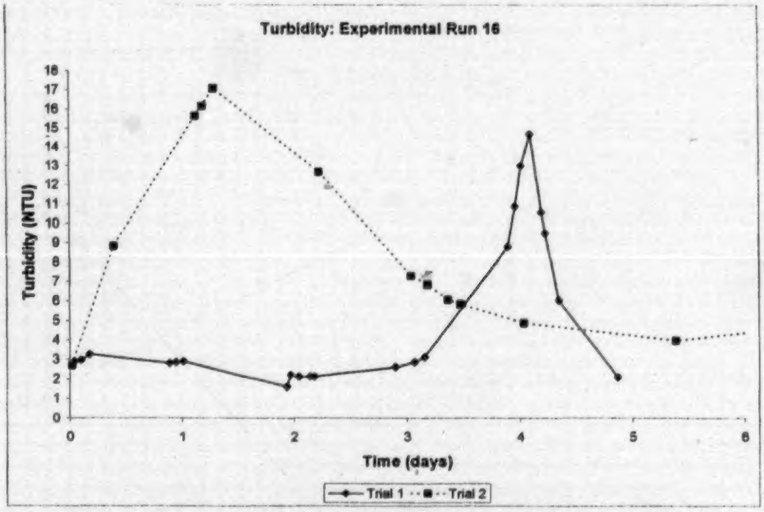

Figure B-16: Turbidity curve for experimental run 16.

Appendix C: Design Sheets

The following tables show the design sheets for all responses completed in the DOE PRO XL software. In composition design sheets, Y1, Y2, and Y3 correspond to the values obtained from three selected areas using EDS analysis. In plating rate design sheets, Y1, Y2, and Y3 correspond to the values obtained from thickness measurements at different locations of the "v" shape mark on the deposited films using profilometry. In the shelf life design sheet, Y1 and Y2 correspond to the values obtained from the two turbidity trials. The Ybar column corresponds to the mean of the Y values and is calculated automatically by the software. The S column, which is also calculated automatically by the software, corresponds to standard deviation of the Y values and is calculated by equation:

$$S = \sqrt{\frac{\sum_{1}^{n}(Yn - Ybar)^2}{(n-1)}}, \qquad \textbf{(Equation C-1)}$$

where n is the number of replications.

Table C-1: Design sheet for composition at 0.8 mA/cm^2.

Ammonium Citrate	$KAuCl_4$	$SnCl_2.2H_2O$	Sn at % @ 0.8 mA/cm^2				
			Y1	Y2	Y3	Y bar	S
30	5	10	54.4	40.3	46.3	47.0	7.1
30	15	10	13.4	18.2	15.0	15.5	2.4
70	5	10	46.7	36.6	37.7	40.3	5.5
70	15	10	12.6	10.2	13.1	12.0	1.5
30	10	5	34.5	32.4	37.8	34.9	2.7
30	10	15	40.0	52.2	49.1	47.1	6.3
70	10	5	13.6	15.5	15.5	14.9	1.1
70	10	15	17.6	14.8	15.4	15.9	1.5
50	5	5	47.3	45.1	39.0	43.8	4.3
50	5	15	43.9	39.4	42.6	42.0	2.3
50	15	5	15.9	15.3	16.0	15.7	0.4
50	15	15	15.5	12.9	19.3	15.9	3.2
50	10	10	14.3	14.5	15.5	14.8	0.6
50	10	10	12.5	10.9	13.3	12.2	1.2
30	10	10	19.6	22.0	22.5	21.4	1.6
50	10	5	19.2	15.6	14.5	16.4	2.5

Table C-2: Design sheet for composition at 2.4 mA/cm^2.

Ammonium Citrate	$KAuCl_4$	$SnCl_2.2H_2O$	Sn at % @ 2.4 mA/cm^2				
			Y1	Y2	Y3	Y bar	S
30	5	10	50.5	48.4	58.4	52.4	5.3
30	15	10	52.1	47.5	47.4	49.0	2.7
70	5	10	50.9	52.8	49.3	51.0	1.8
70	15	10	33.8	41.0	43.6	39.5	5.1
30	10	5	46.8	43.5	45.6	45.3	1.7
30	10	15	45.2	49.3	46.4	47.0	2.1
70	10	5	45.6	35.2	43.6	41.5	5.5
70	10	15	44.3	46.8	45.9	45.7	1.3
50	5	5	40.5	43.0	37.6	40.4	2.7
50	5	15	55.7	50.8	53.7	53.4	2.5
50	15	5	37.4	40.5	42.5	40.1	2.6
50	15	15	46.2	41.7	46.7	44.9	2.8
50	10	10	45.0	42.1	40.6	42.6	2.2
50	10	10	41.0	37.7	37.1	38.6	2.1
30	10	10	46.7	45.2	47.5	46.5	1.2
50	10	5	46.0	45.8	42.9	44.9	1.7

Table C-3: Design sheet for composition at 3.5 mA/cm^2.

			Sn at% @ 3.5 mA/cm^2				
Ammonium Citrate	**$KAuCl_4$**	**$SnCl_2.2H_2O$**	**Y1**	**Y2**	**Y3**	**Y bar**	**S**
30	5	10	53.1	50.2	58.6	54.0	4.3
30	15	10	51.0	48.7	47.8	49.2	1.7
70	5	10	46.5	37.4	45.6	43.2	5.0
70	15	10	39.3	44.6	46.0	43.3	3.5
30	10	5	40.8	38.7	38.5	39.3	1.3
30	10	15	45.1	54.6	56.3	52.0	6.0
70	10	5	41.7	24.8	33.4	33.3	8.5
70	10	15	43.7	50.5	43.1	45.8	4.1
50	5	5	47.7	47.6	49.3	48.2	1.0
50	5	15	44.4	46.0	52.8	47.7	4.5
50	15	5	28.0	30.3	33.9	30.7	3.0
50	15	15	51.8	46.3	51.0	49.7	3.0
50	10	10	52.0	50.6	38.1	46.9	7.7
50	10	10	59.9	51.8	41.1	50.9	9.4
30	10	10	52.8	49.1	49.2	50.4	2.1
50	10	5	41.8	36.3	32.8	37.0	4.5

Table C-4: Design sheet for plating rate at 0.8 mA/cm^2.

			Rate @ 0.8 mA/cm^2				
Ammonium Citrate	**$KAuCl_4$**	**$SnCl_2.2H_2O$**	**Y1**	**Y2**	**Y3**	**Y bar**	**S**
30	5	10	0.7	0.7		0.7	0.0
30	15	10	0.8	0.9	0.8	0.8	0.1
70	5	10	1.2	1.1		1.2	0.1
70	15	10	1.1	1.0	1.0	1.0	0.1
30	10	5	1.3	1.3	1.5	1.4	0.1
30	10	15	0.7	0.7	0.9	0.8	0.1
70	10	5	1.1	0.9		1.0	0.1
70	10	15	0.7	0.6		0.7	0.1
50	5	5	1.3	1.3		1.3	0.0
50	5	15	1.1	1.2		1.2	0.1
50	15	5	1.0	0.9	0.9	0.9	0.1
50	15	15	0.7	0.9	0.8	0.8	0.1
50	10	10	0.6	0.6		0.6	0.0
50	10	10	0.5	0.5		0.5	0.0
30	10	10	0.5	0.6	0.4	0.5	0.1
50	10	5	0.9	1.0		1.0	0.1

Table C-5: Design sheet for plating rate at 2.4 mA/cm^2.

			Rate @ 2.4 mA/cm^2				
Ammonium Citrate	KAuCl$_4$	SnCl$_2$.2H$_2$O	Y1	Y2	Y3	Y bar	S
30	5	10	3.2	3.5		3.4	0.2
30	15	10	3.3	3.1	3.0	3.1	0.2
70	5	10	2.6	3.1		2.9	0.4
70	15	10	3.8	4.4	4.1	4.1	0.3
30	10	5	4.2	4.2	4.0	4.1	0.1
30	10	15	3.0	2.9	3.0	3.0	0.1
70	10	5	4.2	5.0		4.6	0.6
70	10	15	3.3	3.5		3.4	0.1
50	5	5	2.1	2.0		2.1	0.1
50	5	15	3.3	2.8		3.1	0.4
50	15	5	2.9	3.3	3.2	3.1	0.3
50	15	15	4.4	4.5	4.4	4.4	0.1
50	10	10	3.3	2.9		3.1	0.3
50	10	10	3.9	3.6		3.8	0.2
30	10	10	3.7	3.8	3.7	3.7	0.1
50	10	5	4.0	3.1		3.6	0.6

Table C-6: Design sheet for plating rate at 3.5 mA/cm^2.

			Rate @ 3.5 mA/cm^2				
Ammonium Citrate	KAuCl$_4$	SnCl$_2$.2H$_2$O	Y1	Y2	Y3	Y bar	S
30	5	10	4.9	5.4		5.2	0.4
30	15	10	4.6	5.1		4.9	0.4
70	5	10	4.6	4.3		4.5	0.2
70	15	10	6.2	6.6	6.7	6.5	0.3
30	10	5	5.0	5.0	4.6	4.9	0.2
30	10	15	4.1	4.2	4.1	4.1	0.1
70	10	5	4.5	5.3		4.9	0.6
70	10	15	4.2	4.0		4.1	0.1
50	5	5	3.4	3.8		3.6	0.3
50	5	15	4.1	3.6		3.9	0.4
50	15	5	5.0	5.1	5.1	5.1	0.1
50	15	15	0	0	0	0.0	0.0
50	10	10	6.2	7.6		6.9	1.0
50	10	10	5.9	6.9		6.4	0.7
30	10	10	7.2	5.4		6.3	1.3
50	10	5	5.8	5.2	5.6	5.5	0.3

Table C-7: Design sheet for shelf life.

			Shelf Life			
Ammonium Citrate	$KAuCl_4$	$SnCl_2.2H_2O$	Y1	Y2	Y bar	S
30	5	10	3.0	11.0	7.0	5.7
30	15	10	5.5	6.0	5.8	0.4
70	5	10	4.5	5.0	4.8	0.4
70	15	10	2.5	4.0	3.3	1.1
30	10	5	10.5	11.0	10.8	0.4
30	10	15	4.5	4.0	4.3	0.4
70	10	5	8.0	8.0	8.0	0.0
70	10	15	3.0	2.5	2.8	0.4
50	5	5	13.0	15.0	14.0	1.4
50	5	15	3.5	4.0	3.8	0.4
50	15	5	6.0	11.0	8.5	3.5
50	15	15	3.0	2.5	2.8	0.4
50	10	10	6.0	5.0	5.5	0.7
50	10	10	3.5	1.0	2.3	1.8
30	10	10	7.5	9.0	8.3	1.1
50	10	5	9.0	11.0	10.0	1.4